2026 | Faculty of Medicine and Life Sciences

UHASSELT
KNOWLEDGE IN ACTION

Maastricht University

Doctoral dissertation submitted to obtain the degree of
Doctor of Biomedical Sciences, to be defended by

Raúl Ramos Pupo

DOCTORAL DISSERTATION

Novel vaccination and antiviral approaches for the prevention and treatment of COVID-19

Promoter: Prof. Dr. Piet Stinissen | Hasselt University

Co-promoter: Prof. Dr. Niels Hellings | Hasselt University

2026 | Faculty of Medicine and Life Sciences

Doctoral dissertation submitted to obtain the degree of
Doctor of Biomedical Sciences, to be defended by

Raúl Ramos Pupo

DOCTORAL DISSERTATION

Novel vaccination and antiviral approaches for the prevention and treatment of COVID-19

Promoter: Prof. Dr. Piet Stinissen | Hasselt University

Co-promoter: Prof. Dr. Niels Hellings | Hasselt University

D/2026/Raúl Ramos Pupo, uitgever

Declaration of integrity

The PhD researcher and the UHasselt supervisor hereby formally declare that the research conducted for the purpose of this PhD thesis was executed in accordance with the principles of good scientific conduct, as stipulated in the UHasselt Integrity charter, the UHasselt charter supervisor – PhD Researcher, the UHasselt Integrity Policy, and the UHasselt guidelines for the use of (generative) AI in research.

Access and embargo

No embargo. The author asserts that this PhD thesis is made Open Access immediately upon submission. The full text is publicly available without restrictions.

"When you look at yourself from a universal standpoint, something inside always reminds or informs you that there are bigger and better things to worry about."

Albert Einstein

Author's declaration

I hereby declare that the work presented in this doctoral thesis is either my own original work or the result of collaborative preclinical research in which I was actively involved. Statements detailing the specific contributions are provided at the beginning of Chapters 2 and 3.

The research presented in this doctoral thesis was conducted through collaboration between Hasselt University (Belgium), Havana Medical University (Cuba), and other Cuban research institutions.

The Doctoral Committee at Hasselt University monitored the progress of the doctoral research and provided continuous evaluation and scientific guidance throughout the doctoral trajectory. Supervision has been provided by promoter Prof. Dr. Piet Stinissen and co-promoter Prof. Dr. Niels Hellings, both appointed by Hasselt University, as well as by the external tutor Prof. Dr. Oliver Pérez, appointed by Havana Medical University.

Raúl Ramos Pupo, MD
Hasselt, Belgium
May 2026

Doctoral jury

Prof. dr. I. Lambrichts, Hasselt University, *Chairman*

Prof. dr. P. Stinissen, Hasselt University, *Promoter*

Prof. dr. N. Hellings, Hasselt University, *Co-promoter*

Prof. dr. J. Bogie, Hasselt University, *Committee*

Prof. dr. K. Dallmeier, Catholic University of Leuven, *External member*

Prof. dr. O. Perez, Havana Medical University, *External tutor*

Prof. dr. D. Steensels, Hasselt University, *External member*

Table of contents

List of tables

List of figures

List of abbreviations

Abbreviation	Definition
ACE2	Angiotensin-Converting Enzyme 2
ADAR	Adenosine Deaminases Acting on RNA
Alum	Aluminum salt adjuvant
ANOVA	Analysis of Variance
APC	Antigen-Presenting Cell
APOBEC	Apolipoprotein B mRNA Editing Enzyme, Catalytic Polypeptide-Like
ARDS	Acute Respiratory Distress Syndrome
AR	Attack Rate
BALF	Bronchoalveolar Lavage Fluid
BCR	B-Cell Receptor
B_{RM}	Tissue-Resident Memory B cell
CaDPA	Calcium Dipicolinic Acid
CFR	Case Fatality Ratio
CFSE	Carboxyfluorescein Succinimidyl Ester
CLpro	Chymotrypsin-Like Protease (3CLpro; Mpro)
COVID-19	Coronavirus Disease 2019
Ct	Cycle Threshold
CTB	Cholera Toxin B subunit
DC	Dendritic Cell
DMV	Double-Membrane Vesicle
DNA	Deoxyribonucleic Acid
dsRNA	Double-Stranded Ribonucleic Acid
EFSA	European Food Safety Authority
ELISA	Enzyme-Linked Immunosorbent Assay
EMA	European Medicines Agency
ER	Endoplasmic Reticulum
ERGIC	Endoplasmic Reticulum–Golgi Intermediate Compartment
ExoN	Exoribonuclease
FACS	Fluorescence-Activated Cell Sorting
FDA	Food and Drug Administration
FiO_2	Fraction of Inspired Oxygen
FITC	Fluorescein Isothiocyanate
GALT	Gut-Associated Lymphoid Tissue
GSK-3	Glycogen Synthase Kinase 3
GSK-3β	Glycogen Synthase Kinase 3 Beta
Hbl	Hemolysin Binding and Lytic
HIV	Human Immunodeficiency Virus
HR1	Heptad Repeat 1
HR2	Heptad Repeat 2

ICU	Intensive Care Unit
IFIT	Interferon-Induced Proteins with Tetratricopeptide Repeats
IFN	Interferon
IFR	Infection Fatality Ratio
IgA	Immunoglobulin A
IgD	Immunoglobulin D
IgG	Immunoglobulin G
IL	Interleukin
IM	Intramuscularly
IN	Intranasally
IRF3	Interferon Regulatory Factor 3
ISG	Interferon-Stimulated Gene
kb	Kilobase
LAG-3	Lymphocyte Activation Gene 3
LAIV	Live Attenuated Influenza Vaccine
LNP	Lipid Nanoparticle
LTB	Heat-Labile Enterotoxin B Subunit
M	Membrane Protein
MALT	Mucosa-Associated Lymphoid Tissue
MAPK	Mitogen-Activated Protein Kinase
MAVS	Mitochondrial Antiviral Signaling Protein
MDA5	Melanoma Differentiation-Associated Protein 5
MERS-CoV	Middle East Respiratory Syndrome Coronavirus
MHC-I	Major Histocompatibility Complex Class I
mmHg	Millimeters of Mercury
mRNA	Messenger Ribonucleic Acid
Mpro	Main Protease
MTase	Methyltransferase
mTOR	Mammalian Target of Rapamycin
N	Nucleocapsid Protein
NALT	Nasal-Associated Lymphoid Tissue
NF-κB	Nuclear Factor kappa-light-chain-enhancer of activated B cells
Nhe	Non-Hemolytic Enterotoxin
NK	Natural Killer Cell
Nsp	Non-Structural Protein
NTD	N-Terminal Domain
ORF	Open Reading Frame
PAMP	Pathogen-Associated Molecular Pattern
PaO_2	Partial Pressure of Oxygen
PASC	Post-Acute Sequelae of SARS-CoV-2 Infection
RT-qPCR	Reverse Transcription quantitative Polymerase Chain Reaction
PD-1	Programmed Cell Death Protein 1
PE	Phycoerythrin
PHEIC	Public Health Emergency of International Concern
PI3K	Phosphatidylinositol 3-Kinase

PKB	Protein Kinase B
PLpro	Papain-Like Protease
PRF	Programmed Ribosomal Frameshifting
PRR	Pattern Recognition Receptor
RaTG13	*Rhinolophus affinis* Tongguan 2013 (strain of bat coronavirus)
RBD	Receptor-Binding Domain
RdRp	RNA-Dependent RNA Polymerase
RIG-I	Retinoic Acid-Inducible Gene I
RNA	Ribonucleic Acid
RSV	Respiratory Syncytial Virus
RTC	Replication–Transcription Complex
R_0	Basic Reproduction Number
R_t	Effective Reproduction Number
RT	Room Temperature
S	Spike Protein
S1	Spike Subunit 1
S2	Spike Subunit 2
SAR	Secondary Attack Rate
SARS-CoV	Severe Acute Respiratory Syndrome Coronavirus
SASP	Small Acid-Soluble Protein
SD	Standard Deviation
sgRNA	Subgenomic RNA
sIgA	Secretory Immunoglobulin A
SpO_2	Peripheral Oxygen Saturation
STAT	Signal Transducer and Activator of Transcription
Th	T helper cell
TIM-3	T-cell Immunoglobulin and Mucin-domain containing-3
TLR	Toll-Like Receptor
TMPRSS2	Transmembrane Protease Serine 2
T_{RM}	Tissue-Resident Memory T cell
TRS	Transcription-Regulating Sequence
TTFC	Tetanus Toxin Fragment C
UTR	Untranslated Region
VHH	Variable Heavy domain of Heavy-chain antibodies
VITT	Vaccine-Induced Thrombosis with Thrombocytopenia
VOC	Variant of Concern
VOI	Variant of Interest
VUM	Variant Under Monitoring
WHO	World Health Organization
WNT	Wingless and Int-1

Chapter 1

General introduction and aims

1. General introduction and aims

1.1 History of COVID-19

Coronavirus Disease 2019 (COVID-19) is the infectious illness caused by the novel Severe Acute Respiratory Syndrome Coronavirus 2 (SARS-CoV-2), a member of the *Coronaviridae* family. First identified in late 2019 in Wuhan, China, COVID-19 rapidly evolved into a global health emergency, profoundly impacting public health systems, economies, and societies worldwide. Initially presenting as a respiratory infection, the disease predominantly affects the lungs but is now recognized as a multisystem disorder, capable of causing cardiovascular, neurological, gastrointestinal, and renal complications characterized by systemic immune dysregulation and immunopathology [1-4].

The unprecedented scale and speed of SARS-CoV-2 transmission, combined with its ability to cause both asymptomatic and severe disease, have posed immense challenges for disease control and prevention. COVID-19 has not only tested global healthcare capacity but also accelerated scientific innovation, leading to rapid advances in diagnostics, therapeutics, and vaccine development [5-8].

1.1.1 Origin and early cases

Coronaviruses belong to the family *Coronaviridae* and the genus *Betacoronavirus*. Before 2019, two notable coronaviruses had caused global outbreaks: SARS-CoV (Severe Acute Respiratory Syndrome Coronavirus) in 2002–2003 and MERS-CoV (Middle East Respiratory Syndrome Coronavirus) in 2012. Both were zoonotic viruses transmitted from animals to humans, likely through intermediate hosts [9-11].

In December 2019, an outbreak of pneumonia of unknown origin was reported in Wuhan, Hubei Province, China. Epidemiological investigations linked many early cases to the Huanan Seafood Wholesale Market, where live wild animals were sold [12, 13]. Genome sequencing revealed a novel coronavirus with approximately 79% similarity to SARS-CoV and 96% to bat coronavirus RaTG13, indicating a probable origin. The exact intermediate host remains unclear, though pangolins were initially considered as a possible candidate [14-16].

1.1.2 Early transmission

Based on retrospective studies, the earliest confirmed case occurred on November 17, 2019. By December 31, 2019, China reported a cluster of cases to the World Health Organization (WHO). On January 7, 2020, the novel virus was officially identified and named SARS-CoV-2. The first death was reported on January 11, 2020, and the first cases outside China appeared shortly after, with Thailand confirming on January 13, 2020 [17, 18].

1.1.3 International spread

Rapid international travel facilitated the spread to multiple continents. The first U.S. case was confirmed on January 21, 2020, and Europe reported cases soon thereafter. On January 30, 2020, the WHO declared the outbreak a Public Health Emergency of International Concern (PHEIC). Community transmission became evident by February 2020 [19-21].

1.1.4 Pandemic status

On March 11, 2020, the WHO declared COVID-19 a global pandemic. By then, over 118,000 cases and 4,000 deaths were reported across more than 110 countries. Governments worldwide implemented unprecedented interventions, including lockdowns, social distancing, travel bans, and mask mandates [22-24].

1.1.5 Current status

As of 5 May 2023, the WHO officially ended the COVID-19 outbreak's status as a PHEIC. While the emergency declaration has ended, COVID-19 continues to circulate globally, causing illness, hospitalizations, and deaths, though at much lower and more manageable levels compared to peak periods [25, 26]. As of August 2025, over 780 million confirmed cases of COVID-19 have been reported worldwide, and more than seven million confirmed deaths have been attributed directly to the virus. In many countries, there have also been indirect deaths or excess mortality beyond those officially counted. COVID-19 is now being managed much more like a long-term endemic respiratory disease rather than an acute emergency, with ongoing surveillance, vaccination, treatment, and public health measures adapted to local risk [27-29].

1.2 SARS-CoV-2

1.2.1 Viral structure

SARS-CoV-2 is a betacoronavirus in the family *Coronaviridae*, subgenus *Sarbecovirus*. It has an enveloped, positive-sense, single-stranded RNA genome of ~29.9 kb containing 14 open reading frames (ORFs) and encoding 29 proteins that determine the virus's functional characteristics, grouped into non-structural, structural, and accessory proteins (**Table 1.1**). Cellular ribosomes directly translate ORF1a and ORF1ab into two polyproteins (pp1a and pp1ab), found in the first two-thirds of the viral genome from the 5′ end. Two viral proteases, papain-like protease (PLpro) and main protease (Mpro or CLpro), then process the polyproteins to generate 16 non-structural proteins (NSP1–NSP16). Interesting, a -1 programmed ribosomal frameshifting (-1PRF) between ORF1a and ORF1b causes the ribosome to stall and slip backward by one nucleotide (the "-1" shift) before continuing translation in a new reading frame. This shift allows the virus to translate two different polyproteins from the same stretch of RNA: the pp1a when no shift occurs and the pp1ab when the -1PRF shift happens. Importantly, the virus must maintain a precise ratio of these proteins, roughly 2 to 3 times more pp1a than pp1ab, to replicate successfully. Finally, in the last third, the sequences for the four structural proteins: Spike (S), Envelope (E), Membrane (M), and Nucleocapsid (N); and the eight accessory proteins: ORF3a, ORF3b, ORF6, ORF7a, ORF7b, ORF8b, ORF9b, and ORF10, are located (**Figure 1.1**) [30-32].

Table 1.1. SARS-CoV-2 proteins [33-35]

Name	Genome position, nt & aa length	Protein type	Function
NSP1 (leader protein)	266–805 (540 nt); 180 aa	Non-structural; host shutoff factor	Binds to the 40S ribosomal subunit and occludes the mRNA entry channel, causing host translation shutdown while allowing preferential translation of viral RNAs. Promotes host mRNA degradation and suppresses innate antiviral responses.
NSP2	806–2719 (1914 nt); 638 aa	Non-structural; host-interaction factor	Interacts with host endosomal and translational regulatory proteins; modulates intracellular signaling pathways that favor viral replication.
NSP3 (PLpro)	2720–8554 (5835 nt); 1945 aa	Non-structural; protease/regulator	Contains papain-like protease activity for polyprotein cleavage. Exhibits deubiquitinase and deISGylase functions that antagonize innate immunity and contribute to replication organelle formation.
NSP4	8555–10054 (1500 nt); 500 aa	Non-structural; membrane protein	Works with NSP3 and NSP6 to remodel ER membranes into double-membrane vesicles that house the replication–transcription complex.
NSP5 (Mpro/3CLpro)	10055–10972 (918 nt); 306 aa	Non-structural; protease	Cysteine protease is responsible for the majority of viral polyprotein cleavages required to generate mature non-structural proteins.
NSP6	10973–11842 (870 nt); 290 aa	Non-structural; membrane protein	A transmembrane protein that modulates autophagy and contributes to the formation of replication organelles.
NSP7	11843–12091 (249 nt); 83 aa	Non-structural; polymerase cofactor	Forms a complex with NSP8 and NSP12 to stabilize and enhance RNA polymerase processivity.
NSP8	12092–12685 (594 nt); 198 aa	Non-structural; polymerase cofactor	Acts as a primase-like and processivity factor supporting RdRp activity and RNA template stabilization.
NSP9	12686–13024 (339 nt); 113 aa	Non-structural; RNA-binding protein	Single-stranded RNA-binding protein that assists RNA handling within the replication complex.
NSP10	13025–13441 (417 nt); 139 aa	Non-structural; enzymatic cofactor	An allosteric cofactor that activates NSP14 and NSP16 for RNA proofreading and cap methylation.
NSP11	13442–13480 (39 nt); 13 aa	Non-structural; short peptide	Short peptide with unclear function; region incorporated into NSP12 in the frameshift context.
NSP12 (RdRp)	13442–16237 (2796 nt); 932 aa	Non-structural; polymerase	Catalytic core of viral RNA synthesis responsible for genome replication and subgenomic transcription.
NSP13 (Helicase)	16238–18040 (1803 nt); 601 aa	Non-structural; helicase	NTP-dependent helicase that unwinds RNA structures to facilitate replication and transcription.

NSP14 (ExoN/N7-MTase)	18041–19621 (1581 nt); 527 aa	Non-structural; proofreading/capping	Provides 3′→5′ exonuclease proofreading and N7-methyltransferase activity for RNA cap formation.
NSP15 (NendoU)	19622–20659 (1038 nt); 346 aa	Non-structural; endoribonuclease	Uridylate-specific endoribonuclease that limits dsRNA accumulation to evade host sensing.
NSP16 (2'-O-MTase)	20660–21553 (894 nt); 298 aa	Non-structural; capping enzyme	Catalyzes 2′-O methylation of the RNA cap to mimic host mRNA and evade IFIT restriction.
Spike (S)	21563–25384 (3822 nt); 1273 aa	Structural; fusion glycoprotein	Trimeric fusion glycoprotein mediating ACE2 binding and membrane fusion; main antigenic determinant.
ORF3a	25393–26220 (828 nt); 275 aa	Accessory; viroporin	Viroporin forms ion channels, altering vesicular trafficking and modulating host inflammatory responses.
ORF3b	25814-25879 (66 nt); 22 aa	Accessory; IFN antagonist; overlapping ORF	Short overlapping protein reported to antagonize type I interferon responses; annotation-dependent.
Envelope (E)	26245–26472 (228 nt); 75 aa	Structural; membrane protein	Small viroporin involved in virion assembly, budding, and pathogenicity.
Membrane (M)	26523–27191 (669 nt); 222 aa	Structural; membrane protein	Central organizer of virion assembly that determines envelope shape and coordinates structural proteins.
ORF6	27202–27387 (186 nt); 61 aa	Accessory; immune antagonist	An interferon antagonist that blocks the nuclear import of STAT factors and antiviral gene expression.
ORF7a	27394–27759 (366 nt); 121 aa	Accessory; membrane protein	Membrane protein implicated in host interaction, immune modulation, and apoptosis.
ORF7b	27756–27887 (132 nt); 43 aa	Accessory; membrane protein	Small membrane-associated protein incorporated into virions; function not fully defined.
ORF8	27894–28259 (366 nt); 121 aa	Accessory; immune modulator	An immune evasion protein that downregulates MHC-I and interferes with antigen presentation.
Nucleocapsid (N)	28274–29533 (1260 nt); 419 aa	Structural; RNA-binding protein	RNA-binding protein that packages the genome, supports replication, and modulates the host response.
ORF9b	28284–28574 (291 nt); 97 aa	Accessory; overlapping ORF	Mitochondria-targeting protein that disrupts MAVS/TOM70 signaling to suppress innate immunity.
ORF9c	28734–28952 (219 nt); 73 aa	Accessory; overlapping ORF	Putative membrane-associated protein with limited evidence for host–virus interaction roles.
ORF10	29558–29674 (117 nt); 38 aa	Accessory	Very small putative protein with weak evidence for functional expression.

This table is based on Wuhan-Hu-1 (accession NC_045512.2).

1.2.2 Mechanisms of infection

Cell entry is initiated by the receptor-binding domain (RBD) localized in subunit 1 of S (S1), which binds to the host cell receptor angiotensin-converting enzyme 2 (ACE2). Host proteases, such as transmembrane serine protease 2 (TMPRSS2), prime the spike protein for membrane fusion [36-38]. The unique polybasic S1/S2 cleavage site in SARS-CoV-2 enhances entry efficiency and tissue tropism compared with the previous SARS-CoV-1. Subunit 2 of S (S2) undergoes conformational changes to mediate fusion of viral and host membranes, releasing viral RNA into the cytoplasm. The genomic RNA acts directly as mRNA, translated into the polyproteins pp1a and pp1ab, which are cleaved into NSPs, and subsequently assemble into the replication–transcription complex (RTC) on double-membrane vesicles derived from the ER. The RTC accomplishes genomic and subgenomic RNA synthesis that drives full-length negative-strand templates for genome replication and production of structural and accessory proteins before virion assembly, buds into secretory vesicles, and egresses via exocytosis (**Figure 1.2**) [38-40].

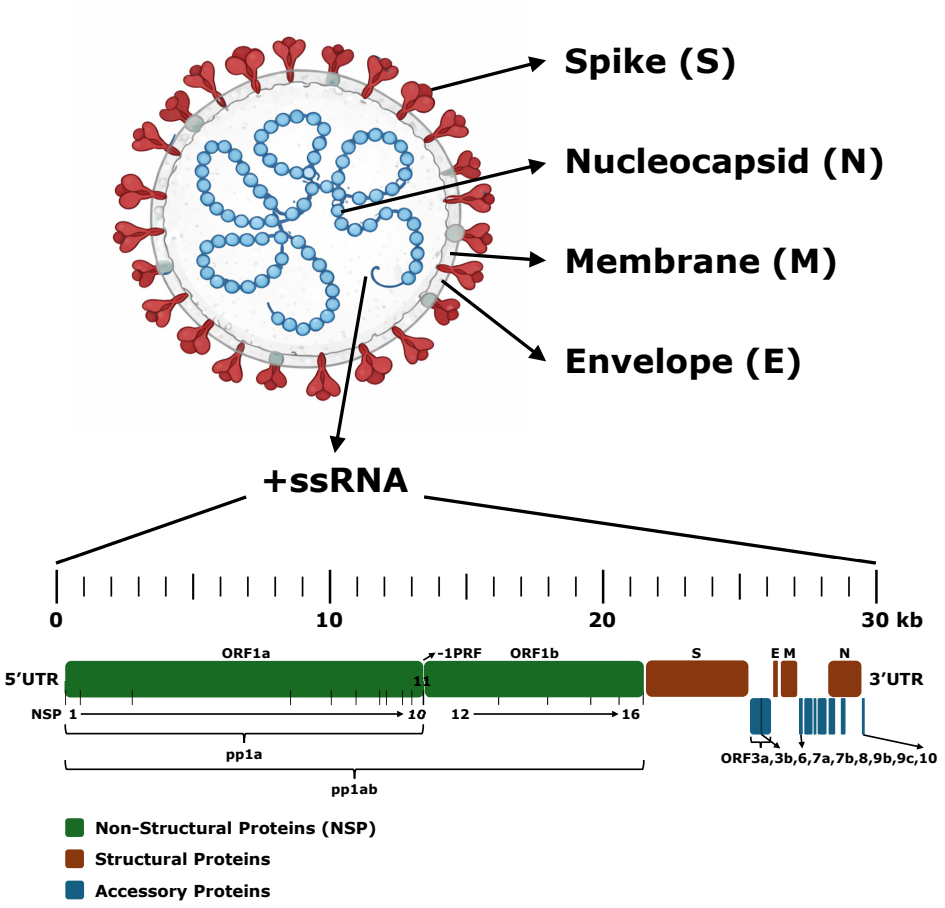

Figure 1.1. SARS-CoV-2 viral structure and genome organization. Diagram of the SARS-CoV-2 viral structure and its genome organization. Four proteins form the virus's structure: Spike (S), Nucleocapsid (N), Membrane (M), and Envelope (E). The SARS-CoV-2 genome is a complex positive-strand RNA molecule approximately 29.9 kb in length. It is organized into a 5' untranslated region (UTR), 14 open reading frames (ORFs) grouped into non-structural, structural, and accessory proteins, followed by a 3' UTR. ORF1a and ORF1ab, located in the first two-thirds of the viral genome, encode two polyproteins (pp1a and pp1ab), which in turn generate 16 non-structural proteins (NSP1–16). A -1 programmed ribosomal frameshifting (-1PRF) between ORF1a and ORF1b leads the virus to translate the two different polyproteins from the same stretch of RNA: pp1a (NSP1-11) when no shift occurs and pp1ab (NSP1-16, except NSP11, whose sequence is effectively replaced by the start of NSP12) when the -1PRF shift happens. Finally, in the last third, the four structural proteins: Spike (S), Envelope (E), Membrane (M), and Nucleocapsid (N); and the eight accessory proteins: ORF3a, ORF3b, ORF6, ORF7a, ORF7b, ORF8b, ORF9b, and ORF10 are encoded. This diagram is based on Wuhan-Hu-1 (accession NC_045512.2).

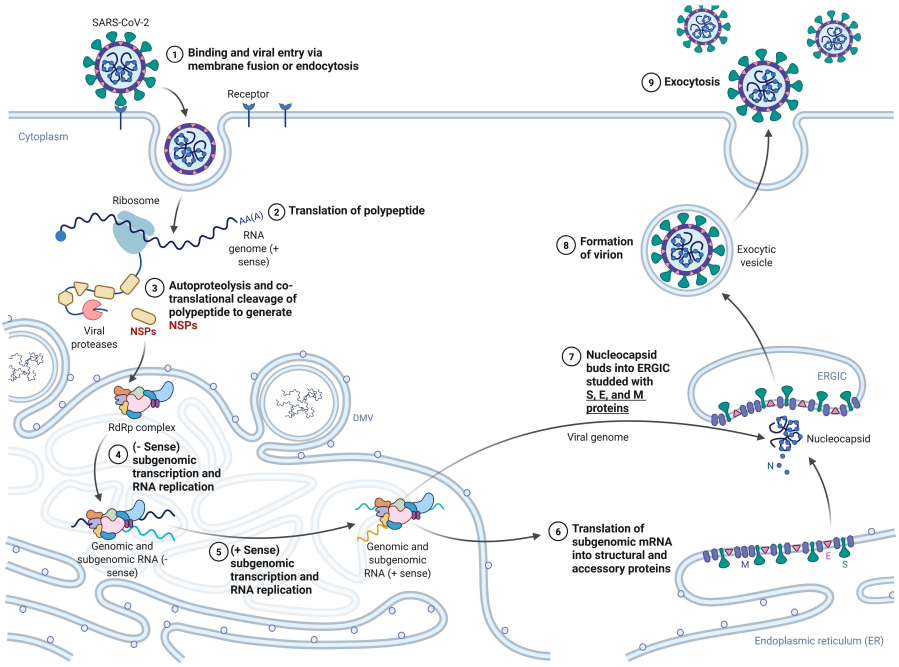

Figure 1.2. Replication cycle of SARS-CoV-2 in host cells. Diagram of the replication cycle. SARS-CoV-2 initiates infection by binding the spike (S) glycoprotein to angiotensin-converting enzyme 2 (ACE2), followed by protease-mediated membrane fusion or endocytosis, and the release of the positive-sense single-stranded RNA genome into the cytoplasm. The genomic RNA is directly translated into the polyproteins pp1a and pp1ab, which are proteolytically cleaved by the viral proteases PLpro and Mpro to generate nonstructural proteins (NSPs) that assemble into the replication–transcription complex (RTC). The RTC associates with endoplasmic reticulum (ER)-derived double-membrane vesicles (DMVs), where negative-sense RNA intermediates are synthesized and used for genomic replication and discontinuous transcription of subgenomic RNAs. Subgenomic mRNAs encode structural proteins (S, E, M, and N), which are translated and inserted into the ER membrane. The nucleocapsid (N) protein encapsidates newly synthesized genomic RNA, and viral assembly occurs in the ER–Golgi intermediate compartment (ERGIC). Mature virions are transported in secretory vesicles and released from the cell via exocytosis.

1.2.3 Immune evasion

SARS-CoV-2 employs a diverse arsenal of immune evasion strategies that collectively blunt host antiviral defenses and promote viral persistence.

1.2.3.1 Suppression of interferon responses

Type I and III interferons (IFNs) constitute the first line of defense against viral infections by restricting viral replication and inducing interferon-stimulated genes

(ISGs). Unlike many respiratory viruses, SARS-CoV-2 triggers relatively weak IFN responses during early infection [41]. Several viral proteins directly antagonize IFN pathways: NSP1 degrades host mRNA and blocks translation initiation, reducing IFN and cytokine expression [42]; ORF6 blocks nuclear import of STAT1/STAT2, impairing IFN signaling [42]; and NSP13, NSP14, and NSP16 contribute to viral RNA capping, masking it from recognition by RIG-I (Retinoic Acid-Inducible Gene I)-like receptors [39]. Collectively, these mechanisms blunt early antiviral responses, permitting unchecked viral replication in the initial stages of infection.

1.2.3.2 Avoidance of pattern recognition

SARS-CoV-2 further reduces innate detection by sequestering its RNA within double-membrane vesicles, thereby shielding it from cytosolic sensors such as MDA5 (Melanoma Differentiation-Associated Protein 5) and RIG-I [43]. Accessory proteins contribute additional antagonism; for example, ORF9b interacts with the mitochondrial antiviral signaling protein (MAVS), disrupting downstream NF-κB (Nuclear Factor kappa-enhancer of activated B cells) and IRF3 (Interferon Regulatory Factor 3) activation [44]. Such strategies delay innate recognition and the induction of proinflammatory and antiviral pathways.

1.2.3.3 Impairment of antigen presentation and lymphocyte dysfunction

SARS-CoV-2 interferes with the adaptive immune response by limiting antigen presentation. ORF8 has been shown to downregulate major histocompatibility complex class I (MHC-I) molecules on the surface of infected cells, reducing $CD8^+$ T-cell recognition [45]. Similarly, ORF6 impairs antigen presentation indirectly by blocking the nuclear import of transcription factors required for MHC expression [46]. These mechanisms weaken cytotoxic T lymphocyte–mediated clearance of the virus, thereby facilitating its persistence in infected cells. Moreover, in severe COVID-19, lymphopenia is common, characterized by apoptosis and redistribution to infected tissues, whereas residual T cells often display features of exhaustion, including increased expression of inhibitory receptors such as PD-1 (Programmed Cell Death Protein 1), TIM-3 (T-cell Immunoglobulin and Mucin-domain containing-3), and LAG-3 (Lymphocyte Activation Gene 3) [47, 48]. Accordingly, chronic antigen stimulation, combined with high levels of inflammatory cytokines, is postulated to promote T-cell exhaustion, limiting effective adaptive responses.

1.2.3.4 Antibody escape: glycan shielding and mutational escape

The spike glycoprotein of SARS-CoV-2 is extensively glycosylated, forming a glycan shield that masks critical epitopes from neutralizing antibodies [49]. This structural feature reduces antibody accessibility, particularly in the RBD and N-terminal domain (NTD), thereby enhancing viral persistence. Additionally, accumulation of mutations in the spike is a central driver of antibody escape. Variants of concern (VOCs) such as Beta (B.1.351), Delta (B.1.617.2), and Omicron (B.1.1.529 and its sublineages) carry substitutions at key residues (e.g., E484, K417, N501, L452, F486) that diminish neutralization by convalescent plasma, vaccine-induced antibodies, and monoclonal antibodies [50]. Omicron subvariants, in particular, harbor over 30 spike mutations, conferring broad escape from prior immunity while retaining efficient ACE2 binding [51]. Consequently, the rapid spike evolution has rendered many anti-spike monoclonal antibodies ineffective, resulting, for example, in successive Omicron lineages accumulating mutations that abolished the activity of nearly all early-generation therapies of this type [52]. Therefore, updating current therapies and developing novel therapeutics are essential, as exemplified by the recent discovery of a panel of single-domain antibodies (Variable Heavy domain of Heavy-chain antibodies, VHHs) targeting S2 that broadly neutralize SARS-CoV-1 and SARS-CoV-2 with unusually high potency [53].

1.2.3.5 Complement and innate humoral evasion

Beyond adaptive immune responses, SARS-CoV-2 interferes with key components of innate immunity, particularly the complement system. Both the S and N proteins have been reported to modulate complement activation pathways, thereby reducing complement-mediated opsonization of viral particles and limiting complement-dependent clearance of infected cells [45]. This dampening of complement activity limits early viral clearance, thus contributing to infection persistence. In addition, SARS-CoV-2 exploits host cell surface factors such as heparan sulfate as attachment cofactors to facilitate viral entry. By engaging these ubiquitous glycosaminoglycans, the virus enhances its binding efficiency to target cells and partially bypasses innate restriction mechanisms that would otherwise limit infection at early stages [54].

1.2.3.6 Immune evasion in persistent infection

In immunocompromised hosts, SARS-CoV-2 can persist for months, during which intra-host viral evolution occurs under selective pressure from convalescent plasma, monoclonal antibodies, or partial immunity. These cases frequently demonstrate sequential acquisition of immune-escape mutations that parallel those observed in circulating variants [55]. Such chronic infections may serve as reservoirs for the emergence of novel variants with enhanced immune evasion properties.

1.2.4 Viral evolution: mutation, proofreading, and recombination

The large genome size underpins both functional complexity and evolutionary potential [56]. SARS-CoV-2 reflects a dynamic interplay between mutation, proofreading, and recombination. Mutations supply raw genetic diversity, proofreading balances genome stability with adaptability, and recombination accelerates innovation by reshuffling genetic material [57-59].

1.2.4.1 Origin of mutations

Mutations arise primarily during replication by the RdRp (RNA-dependent RNA polymerase, NSP12). Although the replication complex is relatively accurate compared to other RNA viruses, stochastic nucleotide misincorporations occur. Additional mutational forces include host-mediated RNA editing enzymes such as APOBEC (Apolipoprotein B mRNA Editing Enzyme, Catalytic Polypeptide-Like) and ADAR (Adenosine Deaminases Acting on RNA), which induce characteristic mutational signatures [60].

1.2.4.2 Spectrum of mutations

SARS-CoV-2 mutations are biased toward C→U and G→U transitions, reflecting host editing processes [61]. Many mutations are synonymous or deleterious, but some confer adaptive advantages. Mutations in the spike protein are particularly significant due to their role in receptor binding, immune recognition, and vaccine efficacy. For example, the D614G substitution enhanced viral infectivity and rapidly became globally dominant in 2020 [62]. Later, mutations such as N501Y, E484K, and L452R contributed to increased transmissibility and immune escape in Alpha, Beta, and Delta variants, respectively [63].

1.2.4.3 Impact on viral fitness

Accumulated mutations affect transmissibility, pathogenicity, and antigenicity. Beneficial mutations may confer higher replication efficiency, improved binding to ACE2, or reduced susceptibility to neutralizing antibodies. This explains the recurrent emergence of VOCs with convergent mutations in the RBD [52, 64].

1.2.4.4 Coronavirus proofreading system, evolutionary consequences, and implications for antiviral therapy

A unique feature of coronaviruses is their proofreading mechanism, mediated by the 3'–5' exoribonuclease activity of NSP14, in complex with its cofactor NSP10. This activity corrects misincorporated nucleotides during replication, reducing the error rate by ~15- to 20-fold compared to other RNA viruses [65-67]. Consequently, it enables coronaviruses to maintain large genomes without catastrophic mutational meltdown. At the same time, a tightly regulated balance between replication accuracy and genetic variability preserves viral adaptability. Importantly, proofreading does not eliminate evolution: mutations that enhance viral fitness still accumulate, albeit at a slower pace than in viruses like influenza or HIV (Human Immunodeficiency Virus) [58, 68, 69]. Regarding antiviral therapy, proofreading influences the efficacy of nucleoside analog antivirals. For example, remdesivir can evade proofreading and inhibit replication, whereas other analogs are excised by NSP14, limiting their effectiveness [70]. Targeting NSP14 proofreading is therefore considered a potential therapeutic strategy.

1.2.4.5 Mechanism of recombination in SARS-CoV-2 and its evolutionary role

Coronaviruses undergo recombination via template switching during replication. The RdRp frequently pauses and reinitiates on homologous or heterologous templates, producing mosaic genomes. This is facilitated by the long genome and the presence of transcription-regulating sequences (TRSs), which promote strand switching [71, 72]. For SARS-CoV-2, recombination has been increasingly documented during the pandemic, particularly as multiple variants co-circulate. Recombinant lineages such as XD (Delta–Omicron hybrid), XE (Omicron BA.1–BA.2 hybrid), and XBB (BA.2.10.1–BA.2.75 recombinant) have been identified [73, 74]. Some recombinants exhibit altered transmissibility and immune evasion,

underscoring recombination as a driver of variant emergence. All in all, recombination accelerates viral adaptation by combining beneficial mutations from different lineages into a single genome. This mechanism not only increases diversity but may also help SARS-CoV-2 evade population immunity more efficiently than mutation alone [50, 75, 76].

1.2.5 New Variants of Concern (VOCs): from Wuhan-Hu-1 to Omicron and beyond

From the original Wuhan-Hu-1 sequence to the complex, post-Omicron landscape, SARS-CoV-2 evolution has been marked by episodic selective sweeps (D614G, Alpha, Delta, Omicron), ongoing antigenic drift, and recombination-driven innovation. The virus has repeatedly converged on similar functional solutions (enhanced ACE2 engagement, improved proteolytic activation, and mutations that reduce neutralization) while public-health responses (vaccination, therapeutics, surveillance) and population immunity continually reshape the evolutionary trajectory (**Table 1.2**) [77, 78].

1.2.5.1 The reference virus — Wuhan-Hu-1

The first publicly shared complete genome of the novel coronavirus (designated Wuhan-Hu-1) was released in January 2020 following the identification of an unexplained pneumonia cluster in Wuhan, China. That sequence established the positive-sense RNA framework used for global comparisons and lineage assignment. Early phylogenetic analyses showed tight clustering of initial human isolates and placed the virus within the *Sarbecovirus* subgenus [79].

1.2.5.2 The first global sweep: D614G (early 2020)

Within months of global spread, an early spike substitution (D614G) became dominant worldwide. Multiple laboratory and epidemiological studies found that this substitution increased infectivity and upper-respiratory viral loads without clear evidence of increased intrinsic disease severity, and the G614 genotype rapidly fixed in many regions due to a competitive fitness advantage [62, 80, 81]. This early selective sweep demonstrated that even single substitutions in the spike protein can have major epidemiological effects.

1.2.5.3 The Alpha–Beta–Gamma era: adaptive steps in 2020–2021

By late 2020, several SARS-CoV-2 lineages with multiple spike mutations were designated VOC due to either increased transmissibility or evidence of immune escape [63, 82]. Alpha (B.1.1.7), first detected in the United Kingdom in autumn 2020, carried key mutations such as N501Y and the H69/V70 deletion that enhanced ACE2 affinity and viral spread, allowing it to rapidly become dominant in many regions [83]. In parallel, Beta (B.1.351) and Gamma (P.1), identified in South Africa and Brazil, respectively, harbored RBD substitutions including E484K, K417N/T, and N501Y that reduced neutralization by convalescent and vaccine sera, marking the beginning of significant antigenic concerns [76]. This period highlighted two concurrent evolutionary trajectories of the virus: selection for higher transmissibility (Alpha) and selection for immune escape (Beta and Gamma).

1.2.5.4 Delta: transmission and clinical impact (mid-2021)

Delta (B.1.617.2), first widely reported from India in late 2020/early 2021, exhibited a pronounced increase in transmissibility and viral RNA load, and was associated with a higher risk of hospitalization in some studies. Delta's spike mutations (including L452R and P681R) likely enhanced ACE2 interaction and S1/S2 processing, facilitating rapid global replacement of earlier VOCs in mid-2021. Delta underscored how a lineage combining transmissibility and partial immune evasion could dominate rapidly [84-86].

1.2.5.5 Omicron: a major antigenic shift from late 2021

In November 2021, genomic surveillance in southern Africa detected a highly divergent lineage, Omicron (B.1.1.529), characterized by an unusually large number of spike mutations (>30) concentrated in the RBD and NTD. Omicron produced a rapid, global wave of infections beginning in late 2021 and was designated a VOC by the WHO within days of detection [87]. Its constellation of substitutions greatly reduced neutralization by prior-strain infection or early vaccine formulations, leading to immune escape and, thus, a high frequency of breakthrough infections [88, 89]. All in all, Omicron demonstrated very high transmissibility but, in many settings, lower per-infection severity relative to Delta, an effect attributed partly to population immunity and partly to virological

differences in tropism/replication kinetics [90, 91]. Moreover, its multiple sublineages are a consequence of rapid diversification (e.g., BA.1, BA.2, BA.4/5, and their descendants), which repeatedly replace one another. Subsequent antigenic drift has increased its ability to escape the immune system [87, 92].

1.2.5.6 Recombinants and hybrid lineages (2022–2024)

As the incidence and co-circulation of divergent Omicron sublineages increased, recombination events produced hybrid genomes that combined segments from distinct parental lineages. Notable recombinants included XE (Omicron BA.1–BA.2), XD (Delta–Omicron BA.2) [93-95], and XBB (second-generation BA.2 variants BJ.1 and BM.1.1.1) [96, 97]. XBB and its descendants (e.g., XBB.1.5) exhibited marked immune escape relative to preceding Omicron lineages and, through additional substitutions, improved fitness in late 2022–2023 [88, 98, 99]. Recombination accelerated the appearance of constellations that would have taken longer to assemble by stepwise mutation.

1.2.5.7 Later waves: BA.2.86, JN.1, and ongoing drift BA.3.2, XFG, and NB.1.8.1 (2023–2025)

Surveillance through 2023–2024 documented continued antigenic evolution and the emergence of multiple sublineages that shaped regional and global epidemiology. BA.2.86 (Pirola) attracted early concern due to its highly divergent spike protein and a marked antigenic distance from prior Omicron variants, prompting the WHO to monitor it as a VOI/VUM (Variant of Interest/Variant Under Monitoring) while studies evaluated its immune escape and clinical implications [100-103]. Throughout 2024, JN.1 and numerous descendants (including the SLiP, FLiRT, and KP.2 clusters) became globally predominant, illustrating continued antigenic drift within the Omicron lineage and a shift in the circulating genetic background [104-106]. Other highly divergent offshoots, such as BA.3.2, demonstrated substantial immune escape but limited spread due to reduced replication fitness [107, 108]. By 2025, newer VUMs, including XFG and NB.1.8.1, had accumulated additional spike substitutions associated with moderate antibody evasion and steady international growth. Nevertheless, WHO assessments continue to classify the overall public health risk of these lineages as low, as current vaccines remain effective in preventing severe disease outcomes despite ongoing antigenic evolution [107, 109, 110].

Table 1.2. SARS-CoV-2 variants of concern (VOCs) [75-108]

Variant designation	*Pango lineage*	Region first detected	Key spike mutations	Transmissibility	Immune escape and vaccine impact	Disease severity
Wuhan-Hu-1 (Wild type)	—	Wuhan, China (Dec 2019)	Baseline genome	Baseline reference	Baseline neutralization sensitivity	Reference strain
Alpha	B.1.1.7	UK, Sept 2020	N501Y, Δ69-70, P681H, Δ144, A570D	≈30–50% higher than Wuhan-Hu-1	Mild reduction in neutralization; vaccines are effective for severe disease	Slightly increased hospitalization risk in some studies
Beta	B.1.351	South Africa, mid-2020	K417N, E484K, N501Y, others	Higher transmissibility (less than Alpha in some settings)	Marked immune escape; reduced neutralization; diminished vaccine efficacy for mild infection	Possible ↑ severity; data mixed
Gamma	P.1	Brazil (Manaus), late 2020	K417T, E484K, N501Y, others	Higher transmissibility vs prior local variants	Significant immune escape; vaccine breakthrough documented	Increased hospitalization in some regions
Delta	B.1.617.2	India, late 2020	L452R, P681R, T478K	Much higher transmissibility; rapid global dominance	Moderate immune escape; reduced antibody activity; boosters improved protection	Higher hospitalization and severity vs Alpha
Omicron (BA.1-BA.5, etc.)	B.1.1.529 + sublineages	Southern Africa, Nov 2021	More than 30 spike protein mutations; K417N, E484A, N501Y, deletions	Much higher transmissibility; rapid global spread	Strong immune escape; vaccine breakthroughs common; boosters protective for severe outcomes	Generally lower intrinsic severity vs Delta; impact varies by immunity

JN.1 (VOI)	JN.1 (BA.2.86 descendant)	Global, Aug 2023	Derived from BA.2.86 + S:L455S	Growth advantage vs older Omicron sublineages	Partial immune escape; vaccines still protective against severe disease	Severity similar to other Omicron sublineages
Emerging VUMs (e.g., KP.3.1.1, XEC, NB.1.8.1)	Multiple (post-Omicron)	Global, 2024–2025	E.g., S:F456L, S:Q493E on JN.1 background	Early signals of growth advantage	Likely further erosion of neutralization; vaccine protection for severe disease preserved	No confirmed increase in intrinsic severity to date

1.3 Clinical picture of COVID-19

1.3.1 Incubation period and disease onset

The incubation period for COVID-19 typically ranges from 2 to 14 days after exposure, with a median of approximately 5 to 6 days. Symptom onset varies depending on the viral variant, vaccination status, and host factors. Early phases often resemble other viral respiratory infections, complicating clinical differentiation from influenza or other coronaviruses [111, 112].

1.3.2 Spectrum of clinical manifestations

COVID-19 demonstrates an extraordinary clinical spectrum, from asymptomatic infection to severe multi-organ failure. Population-based studies suggest that 20–40% of infections may be asymptomatic, though estimates vary across cohorts and variants [113]. The majority of symptomatic patients experience mild upper respiratory tract illness, characterized by fever, fatigue, myalgia, cough (often dry), sore throat, headache, anosmia or ageusia, particularly with pre-Omicron variants. Gastrointestinal symptoms (diarrhea, nausea, abdominal pain) are also reported in up to 20% of cases [114, 115]. Patients with moderate COVID-19 typically present with clinical or radiological evidence of lower respiratory tract involvement, such as pneumonia, but without hypoxemia (SpO_2 ≥94% on room air) [116]. Severe COVID-19 is defined by features of acute respiratory failure, including severe dyspnea with a respiratory rate >30 breaths/min, hypoxemia (SpO_2 <94%, PaO_2/FiO_2 <300 mmHg), and bilateral pulmonary infiltrates on chest imaging. Progression may occur rapidly after day 7–10 of illness, coinciding

with dysregulated host immune responses rather than direct viral replication [117, 118]. Approximately 5–10% of symptomatic cases develop critical illness, often requiring intensive care. Complications include: Acute Respiratory Distress Syndrome (ARDS), septic shock, multi-organ dysfunction, involving cardiac, renal, hepatic, and neurological systems. Mortality is the highest in this group, especially among the elderly and those with comorbidities [119-121].

Although initially characterized as a respiratory illness, COVID-19 was later recognized as a multisystem disease, characterized by dysregulated immunity that triggers endothelial dysfunction and thromboinflammation. It may include a broad spectrum of cardiovascular (e.g., myocarditis, arrhythmias, heart failure, and thromboembolic events), neurological (e.g., encephalopathy, seizures, cerebrovascular events, anosmia, and ageusia), renal (e.g., acute kidney injury), gastrointestinal (e.g., diarrhea, hepatocellular injury, cholestatic patterns), and dermatological manifestations (e.g., chilblain-like lesions, urticaria, and vasculitic eruptions) [122-124].

1.3.3 Recovery and post-acute sequelae

Recovery from COVID-19 is highly variable, depending on disease severity, host factors, and comorbidities. While individuals with mild illness often recover within two to three weeks, those with moderate or severe disease may require extended convalescence due to prolonged respiratory symptoms, fatigue, or reduced exercise tolerance. In severe and critical cases, recovery is complicated by residual lung injury, fibrosis, thromboembolic events, and secondary infections, sometimes necessitating long-term rehabilitation. Beyond acute illness, a significant subset of patients develop post-acute sequelae of SARS-CoV-2 infection (PASC), commonly referred to as long COVID, characterized by persistent fatigue, dyspnea, chest pain, cognitive impairment, dysautonomia, and neuropsychiatric symptoms lasting weeks to months [3, 125-127].

1.4 Epidemiological aspects

1.4.1 Transmissibility

SARS-CoV-2 can be transmitted directly from person to person and indirectly through contaminated objects. The first occurs mainly through respiratory

droplets, which typically spread up to two meters via coughing, sneezing, or even talking. Additionally, airborne transmission by free-floating aerosols (<5 μm, initially underestimated) was estimated to remain contagious in the air for up to 3 hours. The second, after manipulation of contaminated objects and contact with mucous membranes such as the eyes, nose, or mouth [128-130].

The initial underestimation of aerosol transmission severely compromised early epidemiological forecasting and subsequent vaccine mitigation strategies. Unlike heavy coughing, which produces a mix of large droplets and aerosols, simply breathing, talking, or singing generates microscopic droplets (e.g., in asymptomatic infections). These particles ride on ambient air currents, much like cigarette smoke. When exhaled, a person can fill a stagnant indoor space with virus-laden aerosols, exposing everyone in the room over time. Thus, the standard transmission models of predictable, linear contact networks shifted to highly overdispersed, proximity-independent indoor outbreaks. Immunologically, these fine aerosols pose a distinct challenge by directly penetrating mucosal surfaces, where intramuscularly induced systemic IgG provides an inadequate shield against viral replication and shedding [131-134].

Epidemiological studies have demonstrated that SARS-CoV-2 can infect a range of animal species, including domestic pets such as dogs and cats, as well as certain farm animals, mainly through close contact with infected humans. However, current evidence indicates that they are epidemiological dead-end hosts, meaning that while infection can occur, they do not play a significant role in sustaining transmission chains in human populations, with mink being the only farmed animals consistently linked to severe illness and zoonotic transmission to humans. [135-137].

Research has explored the possibility of alternative transmission pathways, including bloodborne, vertical (mother-to-child), and sexual transmission. Current evidence suggests that SARS-CoV-2 is not primarily transmitted through blood, and there have been no documented cases of transfusion-transmitted COVID-19. Viral RNA has occasionally been detected in blood samples from infected individuals, but these findings reflect transient viremia rather than infectious virus capable of transmission [138, 139]. Regarding vertical transmission, a limited number of studies have reported the detection of viral RNA, antibodies, or antigens

in placental tissue or in newborns soon after birth, suggesting that in utero or peripartum transmission may occur rarely. However, the overall risk remains very low, and most neonatal infections are thought to result from postnatal exposure to respiratory secretions from infected caregivers [140, 141]. Evidence for sexual transmission is also limited. While viral RNA has been detected in semen and vaginal fluids in some studies, infectious virus has not been isolated, and epidemiological data do not support sexual contact as a significant mode of spread. Therefore, the risk of transmission through sexual activity is considered negligible compared to respiratory routes. Nonetheless, close physical contact inherently increases the likelihood of respiratory transmission [142, 143].

1.4.2 Key indicators

Key epidemiological indicators are essential tools for understanding, monitoring, and controlling the spread of infectious diseases such as COVID-19. They provide critical insights into how rapidly a disease is spreading, its severity, and the effectiveness of public health measures in reducing transmission and mortality. By quantifying various aspects of disease dynamics, these indicators guide decision-making for governments, health organizations, and researchers, allowing timely interventions and resource allocation.

Among the most important indicators are the basic reproduction number (R_0) and the effective reproduction number (R_t), which measure the contagiousness of the disease and its real-time spread or decline. The attack rate (AR) and secondary attack rate (SAR) assess the prevalence of the infection within populations or households, while the case fatality ratio (CFR) and infection fatality ratio (IFR) measure the severity of the disease and the proportion of deaths among infected individuals [144-146].

1.4.2.1 Basic and effective reproduction numbers

The transmission capacity, typically estimated using R_0, represents the average number of new cases generated by an infected individual over the course of their infection and serves as a valuable indicator of the direction of an epidemic. An R_0 value less than 1 indicates a low extension capacity and relative control over time of an infectious disease, while values greater than 1 reflect an outbreak stage and the need for measures to limit its dissemination. However, not all contacts will

become infected (due to protective measures and natural and artificial immunity); thus, the Rt, describing the average number of secondary cases per infectious case in a population at time t comprising both susceptible and non-susceptible hosts, will be lower than the R_0. The initial estimates of these parameters for COVID-19 were well above one until strict lockdowns and behavioral changes (such as the use of facemasks and social distancing) contained the rapid spread during the pandemic's early stages, and later, widespread vaccination and prior infection reduced susceptibility. R_0 remained above one throughout the pandemic for all major variants, and Rt was below one only temporarily after strong public health measures or peak immunity [147-149].

1.4.2.2 Attack rates

The AR refers to the proportion of a population that becomes infected with COVID-19 over a specific period, indicating the extent to which the infection is widespread within a defined group or area. During the early stages of the pandemic and the emergence of new VOCs, the AR was high in densely populated regions and long-term care facilities, where exposure risk was greatest. On the other hand, SAR measures the proportion of susceptible individuals who become infected after exposure to a confirmed case, indicating how easily the virus spreads among near contacts. Among households, SAR was reported to range from 15% to 30%, with higher rates observed with more transmissible variants, such as Delta and Omicron. They reflect the overall transmissibility and the effectiveness of control measures, allowing for the evaluation of the impact of quarantine, contact tracing, masking, isolation, and vaccination on interrupting transmission chains [150-152].

1.4.2.3 Case and infection fatality ratios

The CFR represents the proportion of confirmed COVID-19 cases that result in death. Early in the pandemic, when testing was limited mainly to severe cases, the CFR appeared higher, ranging from 2 to 5%. As testing expanded and more mild or asymptomatic infections were identified, the CFR became more accurate. The IFR estimates the proportion of all infected individuals (including undiagnosed and asymptomatic cases) who die from the disease, providing a more precise measure of the disease's actual lethality in the population. It is usually lower than the CFR because it includes undetected infections. The global IFR has generally

ranged from 0.3 to 1.0%, varying by age, health status, and access to medical care [153-155].

1.4.3 Risk factors

Several key risk factors influence both the likelihood of contracting COVID-19 and its severity. Age is one of the strongest determinants, with older adults (especially those over 60) facing higher risks of hospitalization and death. Pre-existing medical conditions such as cardiovascular disease, high blood pressure, diabetes, obesity, chronic respiratory illness, kidney or liver disease, and cancer significantly increase vulnerability. Individuals suffering from primary or secondary immunodeficiency, including those undergoing chemotherapy, transplant recipients, or HIV patients, are also at higher risk of severe illness. Lifestyle and environmental factors, such as smoking, malnutrition, exposure to air pollution, and living or working in crowded settings, contribute to increased transmission. Furthermore, socio-economic disparities, including limited access to healthcare and occupational exposure among frontline workers, have led to unequal impacts across populations [156-159].

1.4.4 Public health measures

Public health measures have been central to reducing transmission and controlling outbreaks. Early interventions emphasized non-pharmaceutical measures such as social distancing, use of face masks, hand hygiene, and restrictions on gatherings. Lockdowns and travel bans, though disruptive, were implemented globally to reduce community transmission and prevent healthcare systems from becoming overwhelmed. Surveillance through widespread testing and contact tracing enabled the identification and isolation of cases, thereby breaking transmission chains. Additionally, broader public health strategies were emphasized through education, community engagement, and international collaboration [160, 161].

1.4.4.1 Pandemic approach in Cuba

Cuba has a long history of epidemic control and had a robust primary healthcare infrastructure when the pandemic started. The National Action Plan for Epidemics was activated and engaged many sectors (tourism, education, trade, civil defense, etc.) to respond, implementing early surveillance at ports, airports, and marinas, including temperature screening and protocols for returning residents. Soon, the

borders were closed, and strict restrictions were applied when they were reopened to incoming travelers, who had to follow quarantine and undergo RT-qPCR testing. Stringent measures were implemented internally, including face mask mandates, restrictions on gatherings, closures or limitations of public spaces, and active surveillance of contacts and suspected cases. In unison, a local biotechnological research and development approach succeeded in two local vaccine platforms: Abdala (and the mucosal vaccine candidate *Mambisa*, both developed in the Center for Genetic Engineering and Biotechnology) and Sovereign (*Soberana*, including 3 vaccines: *Soberana* 01, *Soberana* 02, and the booster *Soberana* Plus; all developed in the Finlay Vaccine Institute and the Center of Molecular Immunology) vaccines (5 in total), thus avoiding the major international ones. Then, a massive immunization campaign enabled a significant national containment of the disease. Cuba, however, faced substantial constraints due to an escalating economic crisis, including limited health resources and infrastructure issues. Finally, during the recovery process, a phase-based approach was used to ease restrictions. Thus, communities, municipalities, and provinces transitioned through three phases of recovery based on the status of epidemiological indicators [162-165].

1.4.4.2 Pandemic approach in Belgium

In Belgium, following the initial cases, authorities swiftly implemented restrictive measures, including the closure of schools, non-essential shops, and restaurants, as well as border closures, lockdowns, and the cancellation of events. They also mandated working from home when possible. The first strict measures were implemented in March 2020, followed by further lockdowns and increased restrictions as the number of cases continued to rise. There were multiple epidemic waves. Following the first instance, a relaxation occurred during the summer, followed by a resurgence in autumn, leading to a second major lockdown that lasted well into 2021. Measures were periodically adjusted based on case numbers, hospital admissions, the number of critical patients, and other relevant factors. However, they often sparked debates over legal bases and civil liberties [166-168].

Non-pharmaceutical interventions, such as social distancing, mask use, gathering limits, testing, contact tracing, and isolation, were essential. When international

vaccines became available in late 2020 and early 2021, they turned out to be a key determinant in controlling the spread. Initially, four COVID-19 vaccines (Comirnaty from Pfizer/BioNTech, Spikevax from Moderna, Vaxzevria from Oxford/AstraZeneca, and Janssen from Johnson & Johnson) were used in the primary vaccination campaign, all of which were approved by the European Medicines Agency (EMA) [169-171].

1.4.5 Immunoprophylaxis

Vaccination campaigns have been one of the most effective tools for long-term control of COVID-19. The rapid development and deployment of vaccines, utilizing novel technologies such as mRNA platforms, marked a significant milestone in global health, significantly reducing the risk of severe illness, hospitalization, and death. Booster doses were introduced to address waning immunity and adapt to VOCs. However, challenges remain in achieving equitable vaccine distribution, especially in low- and middle-income countries, where supply, infrastructure, and vaccine hesitancy hinder coverage.

1.5 Vaccine development

1.5.1 SARS-CoV-2 epitopes of interest

For SARS-CoV-2, several epitopes have been identified as key targets for immune recognition and vaccine development. The most important are located on the S protein, particularly within the RBD, which binds to the ACE2 receptor on human cells and is the main target of neutralizing antibodies. Antibody-binding epitopes in the RBD and NTD are crucial for blocking viral entry and are the focus of most mRNA and protein-based vaccines [176-178].

Beyond the S protein, other relevant epitopes are found across multiple viral proteins, including the N, M, and E proteins, which play a vital role in eliciting helper and cytotoxic T-cell responses. These responses support the clearance of infected cells and provide longer-lasting immunity. Importantly, these structural epitopes tend to be more conserved, meaning they remain effective against new variants [179-181].

1.5.2 SARS-CoV-2 vaccine platforms

The primary vaccine strategies have focused on inducing neutralizing antibodies against the S protein, particularly its RBD, and on stimulating robust T-cell immunity to ensure long-lasting protection. In the unprecedented race to develop COVID-19 vaccines, both novel and conventional platforms have been extensively explored [178, 179].

1.5.2.1 mRNA vaccines

mRNA vaccines, such as those from Pfizer-BioNTech and Moderna, deliver genetic instructions that encode the S protein, allowing host cells to produce the antigen and thereby trigger an immune response without the risk of infection. These vaccines are highly effective and can be rapidly adapted to new VOCs. However, as a novel technology that utilizes genetic material, mRNA-lipid nanoparticle (mRNA-LNP) complexes pose distinct pharmacokinetic and toxicological challenges. Although genomic integration is biologically impossible because mRNA operates entirely outside the cell nucleus, these complexes do not remain confined to the injection site. A portion enters the systemic circulation, accumulating in off-target tissues, such as the liver and the vascular endothelium. This systemic distribution can trigger unintended off-target cellular translation of the foreign antigen, potentially precipitating a localized T-cell-mediated autoimmune inflammation, such as in transient myocarditis. Furthermore, synthetic ionizable lipids and stabilizers, such as polyethylene glycol (PEG), used to shield the fragile genetic cargo, possess inherent pro-inflammatory properties. These components can induce cellular stress, trigger pre-existing anti-PEG hypersensitivity, or cause accelerated blood clearance upon repeated dosing. Beyond these biological hurdles, current formulations require costly production infrastructure and a strict ultra-cold distribution chain [180-182].

1.5.2.2 Viral vector vaccines

Viral vector vaccines, including those developed by Oxford/AstraZeneca and Johnson & Johnson, use harmless adenoviruses to deliver the S genes into cells, which in turn generate the immunogen and induce a robust response. They are less expensive and less complex to distribute than mRNA vaccines, requiring only a standard cold chain; however, they may have reduced efficacy for some VOCs,

and pre-existing immunity to the viral vector may limit their effectiveness. Additionally, they induce slower antigen kinetics than direct cytoplasmic mRNA translation, resulting in lower total spike production per cell and moderate neutralizing antibody levels compared with mRNA platforms. The first dose also generates strong anti-vector antibodies that can neutralize the vector on subsequent doses, thereby diminishing booster performance. Moreover, a side effect known as vaccine-induced thrombosis with thrombocytopenia (VITT) has been reported [183, 184].

1.5.2.3 Subunit vaccines

The principle underlying the development of subunit vaccines was based on the observation that one does not need to administer the entire pathogen to elicit a strong immune response, but merely an immunogenic fragment. Therefore, they do not contain any microorganisms, representing a long-established platform with an excellent safety profile and stability. Examples for COVID-19 include Novavax and Cuban vaccines (section 1.4.4.1), which comprise purified recombinant S protein or RBD, adjuvanted to enhance immune activation. Importantly, they are stored and transported under standard refrigeration conditions [163, 179, 185, 186].

1.5.2.4 Inactivated whole-virus vaccines

Inactivated whole-virus vaccines utilize chemically or heat-inactivated SARS-CoV-2 particles, allowing the immune system to recognize the full spectrum of viral antigens without the risk of infection. Thus, they mimic natural exposure and induce a broad humoral immune response, leading to the production of neutralizing antibodies against multiple viral components. However, because the virus is no longer replicating, these vaccines tend to elicit weaker cellular immunity compared to genetic vaccine platforms. Despite this limitation, inactivated vaccines, such as those developed by Sinopharm and Sinovac, have played a major role in global COVID-19 vaccination efforts, particularly in low- and middle-income countries, due to their proven safety record, uncomplicated storage and transportation requirements, and well-established manufacturing processes [187, 188].

1.5.2.5 DNA vaccines

This innovative platform utilizes genetically engineered DNA to stimulate an immune response. A plasmid encoding the S protein gene is administered, and once it enters human cells, it is transcribed into mRNA, which is then translated into the antigen. One of the main challenges is delivery: mRNA vaccines need to cross only one membrane to reach their site of action (the cytoplasm), whereas DNA ones must get into the nucleus. Due to this difference, the lipid nanoparticles that effectively deliver mRNA are less effective for DNA. Thus, they are considered to have lower immunogenicity than mRNA or viral vector vaccines. The first approved DNA COVID-19 vaccine is ZyCoV-D, developed in India by Zydus Cadila. It was authorized for emergency use in 2021, becoming the world's first approved DNA vaccine for humans [189-191].

1.6 Adjuvants

A primary challenge in vaccinology has been that, as antigens became simpler and more purified to reduce reactogenicity, their immunostimulatory capacity decreased in parallel. To address the former, adjuvants appeared as substances included in vaccines to enhance the magnitude, breadth, and duration of the immune response, playing a critical role in vaccine success, especially in subunit and pathogen-inactivated vaccines, which, on their own, elicit weaker immunity [192, 193].

1.6.1 Classification, history, and mechanisms

Adjuvants can be categorized as immunostimulants and delivery systems. Immunostimulants are danger signal molecules that trigger the maturation and activation of antigen-presenting cells (APCs) by targeting Toll-like receptors (TLRs) and other pattern recognition receptors (PRRs), thereby promoting the production of antigenic and co-stimulatory signals. These signals, in turn, enhance adaptive immune responses. On the other hand, delivery systems are carrier materials that facilitate antigen presentation by prolonging the bioavailability of loaded antigens and targeting them to APCs [193, 194].

In the early 1920s, Gaston Ramon pioneered the fundamental concept of adding a secondary substance to boost the immune response, being credited by scientific

consensus with the original concept and discovery of adjuvanticity. At about the same time, in 1926, the first practical chemical adjuvant was developed when Alexander Glenny found that mixing aluminum salts with antigens and injecting the mixture into guinea pigs induced higher antibody levels than administering antigens alone [195]. Interestingly, until 1994, only aluminum adjuvants were licensed, and since then, no more than eleven additional adjuvants were certified for use in human vaccines (**Table 1.3**), despite the multiple efforts evaluating different classes of compounds during decades, such as mineral salts, microbial products, emulsions, saponins, synthetic small molecule agonists, polymers, nanoparticles, and liposomes [193, 196].

The mechanisms by which adjuvants enhance immune responses have not been completely characterized. It was not until the 1997 discovery of how innate immunity instructs adaptive immunity that scientists began to unravel this scientific enigma. For an antigen to be immunogenic, it must be accompanied by pathogen-associated molecular patterns (PAMPs) that can trigger PRRs in APCs, thus generating costimulatory signals required for activation of adaptive immunity [193, 196, 197].

Table 1.3. Licensed adjuvants in vaccines

Adjuvant	Composition	First introduction year and vaccine
Aluminum salts (Alum) [195, 198]	Aluminum hydroxide, aluminum phosphate, or potassium aluminum sulfate.	1926 - Pertussis
Proteoliposome (OMV platform) [199]	Outer membrane vesicles (OMV) derived from *Neisseria meningitidis* serogroup B outer membrane.	1989 - Meningococcal disease (VA-MENGOC-BC)
Virosomes [200]	Liposome-like vesicles combining natural phospholipids (lecithin, cephalin) and influenza viral envelope glycoproteins (haemagglutinin, neuraminidase). Also called immunopotentiating reconstituted influenza virosomes (IRIVs).	1994 - Hepatitis A (Epaxal)
MF59 (Micro Fluidized 59 by Chiron Corporation) [201, 202]	Oil-in-water emulsion composed of squalene, the nonionic surfactants Tween 80 and Span 85, and a citrate buffer in water.	1997 – Influenza (Fluad)
rCTB (recombinant cholera toxin B subunit)	Cholera toxin B subunit (non-toxic subunit) is produced synthetically using genetic engineering. The only adjuvant incorporated in a licensed mucosal vaccine.	2001 – Cholera and traveler's diarrhea (Dukoral)
AS04 (Adjuvant System 04 by GlaxoSmithKline (GSK)) [203]	Combines aluminum salt (aluminum phosphate) with monophosphoryl lipid A (MPL).	2005 – Hepatitis B (Fendrix)
RC529 (proprietary code name by Corixa Corporation) [204, 205]	Synthetic lipid A mimetic, specifically an aminoalkyl glucosaminide 4-phosphate.	2006 – Hepatitis B (Supervax)
AS03 (Adjuvant System 03 by GlaxoSmithKline (GSK)) [206, 207]	Oil-in-water emulsion containing squalene, alpha-tocopherol (vitamin E), and Tween 80.	2008 – Influenza H5N1 (Prepandrix)
Montanide ISA51 (Incomplete Seppic Adjuvant 51) [208, 209]	Water-in-oil emulsion made from a mixture of mineral oil and mannitol monooleate-type surfactants, with equal parts of the oil and water phases.	2008 – Non-small cell lung cancer (CIMAvax-EGF)
AF03 (Adjuvant Formulation 03 by Sanofi Pasteur) [210, 211]	Oil-in-water emulsion composed of squalene, polyoxyethylene cetostearyl ether, mannitol, and Tween 80.	2010 – Influenza H1N1 (Humenza)
$AS01_B$ (Adjuvant System 01_B by GlaxoSmithKline (GSK)) [212, 213]	MPL and *Quillaja saponaria* Molina fraction 21 (QS-21), a natural compound extracted from the Chilean soapbark tree, combined in a liposomal formulation.	2017 – Herpes zoster (Shingrix)
CpG 1018 (unmethylated cytosine phosphoguanine 1018 by Dynavax Technologies) [214, 215]	Synthetic bacterial DNA immunostimulatory sequence (ISS) agonist of Toll-like receptor-9 (TLR9).	2018 – Hepatitis B (HEPLISAV-B)
Matrix-M (proprietary brand name by Novavax) [216, 217]	Derived from *Quillaja* saponins, which are extracted from the bark of the *Quillaja saponaria* Molina tree.	2022 – COVID-19 (Nuvaxovid)

1.6.2 Adjuvants for COVID-19 vaccines

The landscape of adjuvants for COVID-19 vaccines encompasses both conventional options, such as aluminum salts, MF59, and CpG 1018, as well as novel options, including Matrix-M and Advax.

1.6.2.1 Conventional approaches

Conventional adjuvant approaches used in COVID-19 vaccines rely on established, well-characterized adjuvant systems designed to enhance antigen immunogenicity, particularly for subunit and inactivated vaccine platforms. Aluminum salts, the oldest licensed adjuvant, were widely used, for instance, in Cuban subunit vaccines and in the inactivated whole-virus vaccine from Sinopharm, where they enhanced neutralizing antibody responses despite relatively modest T-cell activation [163, 164, 187].

Oil-in-water emulsions, including MF59, AS03, and AS01, were incorporated into several protein-subunit COVID-19 vaccine candidates that underwent different clinical trials but did not ultimately receive authorization [218-221].

CpG 1018, a TLR9 agonist and more modern adjuvant, combined with alum in the subunit Taiwanese vaccine Medigen MVC-COV1901, was authorized for emergency use in 2021. This formulation induces a strong, specific humoral response and a Th1-biased immunity [222, 223].

1.6.2.2 Novel approaches

Matrix-M was licensed in 2022 as a novel adjuvant in the COVID-19 vaccine Nuvaxovid developed by Novavax. It is a saponin-based adjuvant extracted from the bark of the *Quillaja saponaria* Molina tree. The fractionated saponins are formulated with phosphatidylcholine and cholesterol into 40-nm cage-like Matrix particles. Matrix-M contains two distinct active nanoparticles: Matrix-A particles (Fraction-A saponins) and Matrix-C particles (Fraction-C saponins) in a weight ratio of 85:15, respectively. Clinical studies have shown that Matrix-M–adjuvanted vaccines (including also the R21/Matrix-M malaria vaccine) induce a robust adaptive immune response, characterized by high levels of protective antibodies with broad epitope specificity, as well as antigen-specific T cells. The T-cell

response includes T helper (Th)-1 biased $CD4^+$ T cells, circulating follicular Th cells, and $CD8^+$ T cells [216, 217, 214, 225].

Advax is a next-generation polysaccharide-based vaccine adjuvant derived from delta inulin, designed to enhance both humoral and cellular immune responses while maintaining an excellent safety and tolerability profile. It primarily acts by enhancing antigen presentation and promoting the efficient activation of dendritic cells, without inducing excessive reactogenicity. This makes it particularly suitable for vaccines intended for vulnerable populations such as infants, the elderly, and individuals with chronic disease. In COVID-19 vaccine development, Advax has been incorporated into several experimental vaccine formulations, with the SpikoGen protein-subunit vaccine from Vaxine (in collaboration with CinnaGen) being the most notable, which was authorized for emergency use in 2021 in the Middle East. This vaccine incorporates a combination of Advax and CpG 55.2 (a synthetic human TLR9 agonist) as an adjuvant and has been shown to induce robust neutralizing antibodies, a Th1-skewed response, and long-lasting cellular immunity [226-228].

1.6.2.3 Lipid nanoparticles in mRNA vaccines

Lipid nanoparticles (LNPs) employed in COVID-19 mRNA vaccines constitute a self-adjuvanted delivery system that integrates antigen transport and innate immune activation within a single platform, eliminating the need for separate conventional adjuvants. Beyond protecting the mRNA from degradation and enabling efficient cytosolic delivery, LNPs, together with innate sensing of the mRNA cargo, trigger early local innate immune activation characterized by the production of inflammatory cytokines and chemokines. This "danger signal" recruits and activates APCs, thereby supporting effective priming of adaptive immunity, including robust T-cell responses and high-affinity antibody production. Although regulatory frameworks classify LNPs as novel excipients rather than formal adjuvants, their intrinsic immunostimulatory properties contribute critically to the high immunogenicity and clinical effectiveness of mRNA vaccine platforms [229, 230].

1.7 Mucosal immunoprophylaxis

Mucous membranes serve as the primary entry sites for most pathogens. Because these surfaces contain specialized immune structures called mucosa-associated lymphoid tissue (MALT), such as gut-associated lymphoid tissue (GALT) and nasal-associated lymphoid tissue (NALT), mucosal vaccines can induce secretory IgA (sIgA) antibodies and tissue-resident memory T cells (T_{RM}), which act as a frontline defense. Unlike systemic vaccines, which mainly generate serum IgG and circulating T cells, mucosal vaccines can block pathogens before they infect or replicate, reducing transmission and providing sterilizing immunity. This makes mucosal approaches especially relevant for respiratory infections such as COVID-19, where preventing replication at the airway mucosa (rather than severe disease alone) is critical for population-level control. However, most licensed vaccines are administered systemically [231-233].

1.7.1 Licensed mucosal vaccines

Only a total of 13 mucosal viral and bacterial vaccines have been approved by the FDA (Food and Drug Administration) or the WHO, and only three of these are administered intranasally. All three are live attenuated influenza vaccines (LAIVs), including FluMist (the only one licensed by the FDA), Nasovac, and the AstraZeneca pandemic H5N1 LAIV. Importantly, only one of these mucosal vaccines (Dukoral, a cholera oral vaccine) contains an adjuvant in its formulation: the recombinant cholera subunit B (rCTB). Consequently, to date, no adjuvants have been licensed for use in intranasal vaccines (**Table 1.4**) [223-241].

Table 1.4. Licensed mucosal vaccines

Vaccine	Type	Mucosal Route	Target
FluMist (MedImmune, acquired by AstraZeneca) [234, 235]	Live attenuated virus, no adjuvant	Intranasal, spray into the nose (FDA approved)	Influenza virus subtypes A and type B (quadrivalent)
Nasovac (Serum Institute of India) [236]	Live attenuated virus, no adjuvant	Intranasal, spray into the nose (WHO prequalified)	Influenza virus subtypes A and type B (trivalent, version S or quadrivalent version S4)
Pandemic LAIV (AstraZeneca) [237]	Live attenuated virus, no adjuvant	Intranasal spray into the nose (WHO prequalified)	Influenza H5N1

Rotarix (GSK Biologics, Belgium) [238, 239]	Live attenuated virus, no adjuvant	Oral (WHO prequalified)	Rotavirus gastroenteritis caused by G1 and non-G1 serotypes (G3, G4, and G9)
RotaTeq (Merck & Co., Inc., USA) [239, 240]	Live attenuated virus, no adjuvant	Oral (FDA approved and WHO prequalified)	Pentavalent rotavirus vaccine to protect against G1, G2, G3, G4, and G9 serotypes
ROTAVAC (Bharat Biotech, India) [239, 241]	Live attenuated virus, no adjuvant	Oral (WHO prequalified)	Severe rotavirus gastroenteritis. Monovalent and pentavalent (5D)
ROTASIIL (Serum Institute of India) [239, 242]	Live attenuated virus, no adjuvant	Oral (WHO prequalified)	Pentavalent rotavirus vaccine, strains from human-bovine rearrangements with the G1, G2, G3, G4 and G9 serotypes
Vivotif (Bavarian Nordic Inc, USA) [243]	Live attenuated bacteria, no adjuvant	Oral (FDA approved and WHO prequalified)	Salmonella typhi bacteria (specifically the Ty21a strain)
OPV (multiple manufacturers) [244]	Live attenuated virus, no adjuvant	Oral (WHO prequalified)	Different formulations of OPV exist, protecting against one, two, or all three types (serotypes 1, 2, and 3) of poliovirus
Vaxchora (Bavarian Nordic Inc, USA) [245, 246]	Live attenuated bacteria, no adjuvant	Oral (FDA approved)	*Vibrio cholerae* serogroup O1 bacteria
Dukoral (Valneva Sweden AB) [247, 248]	Inactivated bacteria adjuvanted with rCTB	Oral (WHO prequalified)	*Vibrio cholerae* serogroup O1 bacteria covering both major serotypes (Inaba and Ogawa) and biotypes (classical and El Tor), and the heat-labile toxin (LT) (cross-protection) produced by enterotoxigenic *Escherichia coli* (ETEC)
Shanchol (GCBC Vaccines Pvt. Ltd, India) / Euvichol (EuBiologics Co., Ltd, Republic of Korea) [249, 250]	Inactivated bacteria, no adjuvant	Oral (WHO prequalified)	Inactivated *Vibrio cholerae* O1 (classical & El Tor biotypes, Inaba & Ogawa serotypes) and O139 strain
Adenovirus 4 & 7 vaccine (Barr Laboratories, Inc, USA) [251, 252]	Live unattenuated virus, no adjuvant	Oral (FDA approved)	Febrile acute respiratory disease (ARD) caused by adenovirus types 4 and 7 (intended solely for use in U.S. military populations aged 17 through 50)

1.7.2 Mucosal vaccines for COVID-19

Five mucosal vaccines are currently approved at a national level for the prevention of COVID-19. However, none of them have been authorized by a drug regulatory agency designated as stringent or listed by the WHO:

- Razi-Cov Pars is an intranasal protein subunit vaccine developed by Iran's Razi Vaccine and Serum Research Institute, which received authorization for use in Iran in October 2021, being the first globally. Importantly, it is formulated with a novel plant-derived oil-in-water emulsion adjuvant system called RAS-01 (Razi Adjuvant System-01), composed of sesame, olive, and soybean oils, and the non-ionic surfactant Tween 80 [253, 254].
- A nasal spray form of the Sputnik V (Salnavac) vaccine was authorized in April 2022 in Russia. It uses the same adenovirus viral vector platform as the original intramuscular Sputnik V, which involves two different recombinant human adenoviruses (Ad26 and Ad5) without an added adjuvant in its formulation [255, 256].
- Convidecia Air (Ad5-nCoV, intranasal version of the intramuscular Convidecia) is a non-replicating viral vector, non-adjuvanted and needle-free COVID-19 vaccine developed by CanSino Biologics, China (authorized in September 2022). It uses harmless human adenovirus type 5 as a vector to deliver the genetic instructions for the SARS-CoV-2 spike protein into human cells. Immunization occurs through a nebulizer (Aerogen’s proprietary aerosol drug delivery technology), which delivers a mist into the airways, inducing robust immunity [257, 258].
- iNCOVACC (BBV154) is an intranasal, non-replicating chimpanzee adenovirus-vectored vaccine (ChAd36) encoding a prefusion-stabilized S protein with two proline substitutions in S2 and developed through a partnership between Washington University in St. Louis (USA), which designed the vector constructs, and Bharat Biotech International Limited (India), which handled product development and manufacturing in India (and approved there in November 2022) [259, 260].
- Pneucolin (dNS1-RBD) is an intranasal vaccine that uses a live-attenuated influenza virus vector expressing the RBD of the S protein. Specifically, a cold-adapted H1N1 influenza virus strain that has been genetically modified. It was approved for emergency use authorization in adults in China in December 2022 [261, 262].

1.7.3 *Bacillus subtilis* spores as a promising mucosal adjuvant

Developing safe and potent mucosal adjuvants for intranasal vaccines is crucial in immunoepidemiology. Respiratory pathogens, such as influenza, RSV (Respiratory Syncytial Virus), and SARS-CoV-2, enter the body through the upper airway, where systemic vaccines provide limited protection. Unlike live attenuated intranasal vaccines, which are effective but unsuitable for immunocompromised individuals and difficult to adapt rapidly to virus evolution, non-replicating protein, inactivated, or mRNA vaccines require an adjuvant to overcome the airway's tolerogenic environment, rapid mucociliary clearance, and weak innate immune activation. Effective mucosal adjuvants would promote local, specific IgA secretion and T_{RM}, providing sterilizing immunity that reduces both infection and transmission. Because no intranasal adjuvant is yet licensed for human use (and in total, only one mucosal adjuvant has been WHO prequalified, rCTB in the oral Dukoral vaccine), discovering safe activators of mucosal immune pathways remains a key priority for enabling next-generation, needle-free mucosal vaccines. In this context, *B. subtilis* spores stand out as a promising candidate [219, 231, 232, 247, 263-266].

1.7.3.1 *B. subtilis*, sporulation, and spore structure

B. subtilis is a Gram-positive, rod-shaped, soil-dwelling bacterium widely used as a model organism for studying bacterial physiology, genetics, and cellular differentiation. One of its hallmark features is its ability to undergo sporulation, a tightly regulated developmental process triggered by nutrient limitation or environmental stress. This process begins with the activation of the master regulator Spo0A, which initiates asymmetric cell division, resulting in the production of a larger mother cell and a smaller forespore. The mother cell engulfs the forespore, surrounds it with protective layers, including the cortex and proteinaceous spore coat, and eventually lyses to release the mature spore (**Figure 1.3**). Sporulation enables the formation of metabolically dormant, highly resistant endospores that can survive heat, desiccation, radiation, and chemical insults for extended periods, representing an opportunity in terms of stability, storage, and transportation requirements for pharmacological products containing them. These endospores can remain dormant until favorable conditions return, at which point they germinate and revert to a vegetative cell [265, 267-269].

B. subtilis spores possess a complex structure with multiple protective layers:

- **Coat:** Composed of over 70 proteins organized into an inner coat, an outer coat, and a crust, this layer protects against chemicals and lysozyme.
- **Cortex:** Mainly made of peptidoglycan, the cortex maintains spore resistance and dormancy. Its loose structure enhances resilience, and modifications like O-acetylation reduce sensitivity to lysozyme.
- **Core:** Enclosed by the inner forespore membrane, the core contains essential enzymes, DNA, ribosomes, tRNA, and CaDPA (dipicolinic acid complexed with calcium). This composition dehydrates the core, enhancing heat resistance. Small acid-soluble proteins (SASPs) provide additional protection to DNA against UV radiation, desiccation, and high temperatures [265, 267-269].

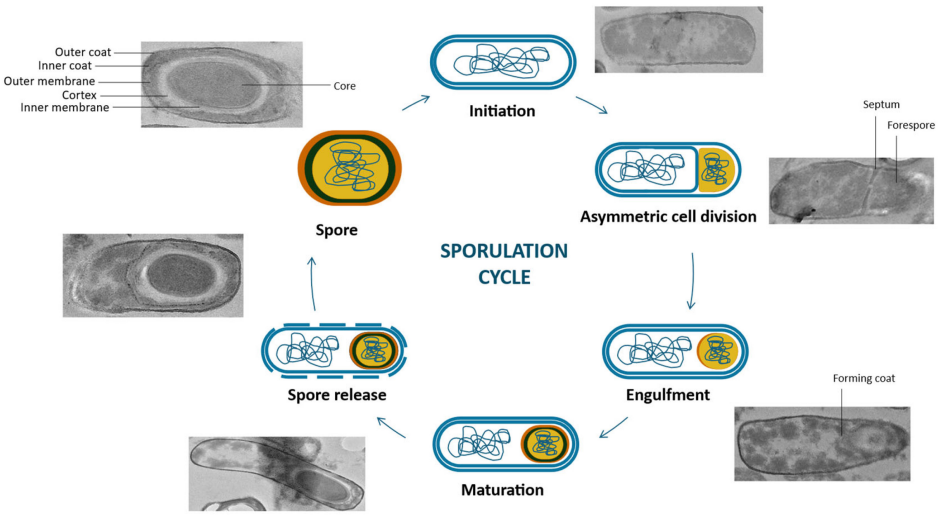

Figure 1.3. The sporulation cycle of *B. subtilis*. Schematic and transmission electron micrographs. In this process, nutrient deprivation triggers activation of Spo0A, initiating sporulation. The cell undergoes asymmetric division, resulting in the formation of a forespore and a mother cell. The mother cell engulfs the forespore, which develops a peptidoglycan cortex, while a protective spore coat forms around it. The mature spore accumulates dipicolinic acid and calcium, enhancing its resilience. The mother cell then lyses, releasing a dormant spore capable of germinating under favorable conditions [265].

1.7.3.2 *B. subtilis* safety for humans

B. subtilis has a long background of safe use in food production (especially in East Asia, e.g., natto), enzyme manufacture, and as a probiotic component. Importantly, it can be described as a 'transient visitor' that completes its life cycle within the gut environment but does not permanently establish itself as a stable, lifelong resident of the human microbiome. Accordingly, certain strains have been granted favorable regulatory assessments (e.g., Qualified Presumption of Safety (QPS) by the EFSA (European Food Safety Authority) or Generally Recognized as Safe (GRAS) by the FDA for specific preparations) and have been administered to thousands of people in clinical and commercial settings, with a generally good overall safety record. However, not all *B. subtilis* strains meet the safety criteria, as some carry genes encoding toxins such as Hbl (Hemolysin BL) or Nhe (Non-Hemolytic Enterotoxin), making them unsuitable for use in foods or pharmaceutical products. Consequently, human-safe strains are of pronounced relevance for pharmaceutical applications [264, 270, 271].

1.7.3.3 *B. subtilis* spores, immunostimulation, and delivery system

The *B. subtilis* spore is increasingly recognized as a powerful tool for immunostimulation and antigen delivery due to its exceptional stability, safety profile, and intrinsic adjuvant properties. Its multilayered structure enables it to survive harsh conditions, including gastric acidity, desiccation, heat, and enzymatic degradation. This resilience makes it highly suitable for mucosal vaccine delivery, where most other approaches are rapidly degraded. Its use as a probiotic in humans and animals underscores its safety profile [272-274].

Importantly, these spores can serve both as a carrier (via the adsorption of antigen on the spore surface or genetic engineering to display heterologous antigens) and as an intrinsic immunomodulator stimulating the innate immunity (via the recognition of peptidoglycan, lipoteichoic acid, etc., by TLR2/NOD2) with the corresponding activation of antigen presenting cells that further trigger the adaptative response, thereby mimicking a natural viral infection. This dual functionality enhances antigen uptake and presentation while stimulating local immune activation [275-277].

Several studies have shown the potential effectiveness of these spores as an adjuvant in various vaccine formulations (**Table 1.5**) [265]. However, all are preclinical studies involving lab strains and recombinant modifications, which find limitations in clinical applications.

Table 1.5. *B. subtilis* spores as an adjuvant and antigen carrier in different vaccine formulations

Pathogen targeted	Antigen	Mechanism of delivery	Strain	Route
Acinetobacter baumannii	TonB-dependent receptors	Recombinant display using a modified cry1Aa promoter [278]	WB800N	Oral
Bacillus anthracis	Protective antigen (PA)	Recombinant display using a modified cry3Aa promoter [279]	DB104 and WB800N	Oral, intranasal, sublingual, or intraperitoneal
Clostridioides difficile	C-terminal domain of the spore surface protein BclA3	Recombinant expression using CotB as an anchor motif [280]	PY79	Intranasal
	FliD protein fused with the human IL-1β domain VQGEESNDK peptide	Recombinant expression using CotG or CotB as anchor proteins [281]	168	Oral
	FliD protein	Non-recombinant adsorption onto *B. subtilis* spores [282]	168 and BHK121	Oral or intranasal
	Carboxy-terminal repeat domains of toxins A and B	Recombinant expression using CotC and CotB as anchor proteins [283]	PY79	Oral
Clostridium tetani	Tetanus toxin fragment C (TTFC)	Recombinant expression using CotC anchor motif [284]	Derivatives of strain 168 *trpC2*	Intranasal
		Non-recombinant adsorption onto *B. subtilis* spores [285]	PY79	Oral, intranasal
		Recombinant expression using CotB as an anchor motif [286-288]	PY79	Oral and intranasal
			RH103	Oral, intranasal, intraperitoneal
Entero-haemorrhagic *Escherichia coli* (EHEC)	Shiga-like toxin (Stx)	Recombinant expression induced by the stress-inducible sigma B-dependent promoter derived from the *B. subtilis gsiB* gene [289]	WW02	Oral, intranasal, subcutaneous
Enterotoxigenic *Escherichia coli* (ETEC)	B subunit of the heat-labile toxin (LTB)	Recombinant expression under the control of a stress-inducible promoter derived from the *B. subtilis* glucose starvation-inducible (*gsiB*) gene [290]	WW02	Oral, intraperitoneal

Escherichia coli	LBT	Non-recombinant adsorption onto *B. subtilis* spores [291]	PY79	Intranasal
Helicobacter acinonychis	Urease subunit B (UreB)	Recombinant expression using CotC as anchor motif mixed with IL-2-presenting spores (BKH121) [292]	BKH108	Oral
Helicobacter pylori	UreA and UreB	Recombinant display of chimeric gene by in-frame fusion to CotB using THY-X CISE® cloning technique [293]	PY79	Oral
	CTB-UreB	Recombinant expression using CotC as an anchor motif [294]	WB600	Oral
	UreB	Recombinant expression using CotC as an anchor motif with recombinant spores expressing IL-2 [295]	BKH48 and BKH108	Oral
Mycobacterium tuberculosis	Fusion protein 1 (FP1)	Non-recombinant adsorption onto heat-inactivated *B. subtilis* [296]	HU58	Intranasal
		Non-recombinant adsorption onto *B. subtilis* spores [297, 298]	HU58	Intranasal
	A truncated fusion of Ag85B191-325 and CFP101-70 antigens (T85BCFP)	Recombinant expression using CotC as an anchor motif on the spore coat of MTAG1 and in the cytosol of vegetatively grown cells of MTAG2 and MTAG3 [299]	PY79	Intranasal
Staphylococcus aureus	Mutant staphylococcal enterotoxin B (SEB)	Recombinant expression using CotC as an anchor motif [300]	WB600	Oral
Coxsackie virus	VP1	Recombinant expression using CotB as an anchor motif [301]	1A771	Intranasal
Enterovirus 71 (EV71)	VP1	Recombinant expression CotB as an anchor motif [302]	1A771	Oral, intranasal
Foot-and-mouth disease virus (FMDV)	CTB and an epitope box constituted with antigen sites from FMDV type Asia 1	Recombinant expression without using anchor proteins [303]	1A751	Oral
Group A rotaviruses	VP6	Recombinant expression through a double-crossover event at the *sacA* locus [304]	168	Intranasal
Influenza A virus (IAV)	M2e-FP protein (RSM2eFP)	Recombinant display using CotB as an anchor motif [305, 306]	PY79	Aerosolized intratracheal and intragastric
	3 molecules of the M2e consensus			Oral

	sequence of influenza A viruses (RSM2e3)			
	A tandem repeat of 4 consensus sequences coding for human—avian—swine—human M2e (M2eH-A-S-H) peptide	Recombinant expression using either CotB, CotC, CgeA, or CotZ as anchor motifs [307]	BTL 20–BTL 26	Oral
SARS-CoV-2	RBD	Recombinant display using CotC as an anchor motif [308]	WB800N	Oral
	RBD and HR1-HR2	Recombinant expression of a chimeric gene by in-frame fusion to CotB or CotC using the THY-X-CISE® cloning technique [309]	PY79	Intranasal
	RBD	Absorption onto a human probiotic strain (**Chapter 2**)	DG101	Intranasal
Clonorchis sinensis (Cs)	CsPmy	Recombinant expression using CotC as an anchor motif [310-314]	WB600	Oral and intraperitoneal
	Enolase of Cs (*Cs*ENO)			Oral
	Eucine aminopeptidase 2 of Cs (*Cs*LAP2)			
	Cs tegumental protein 22.3 kDa (*Cs*TP22.3)			
	*Cs*TP20.8			
Opisthorchis viverrini	Large extracellular loop (LEL) of *O. viverrini* tetraspanin-2 (*Ov*-TSP-2)	Recombinant expression using CotC as an anchor motif [315]	WB800N	Oral
Plasmodium falciparum	C-terminal region of the circumsporozoite surface protein	Non-recombinant coupling onto *B. subtilis* spores [316]	KO7	Intranasal
Schistosoma japonicum	Glutathione *S*-transferase (GST)	Recombinant expression using CotC as an anchor motif [317]	WB600	Oral

All in all, these spores represent a promising next-generation mucosal adjuvant with broad applicability, a safe profile, and excellent translational potential.

1.8 Therapeutic highlights in COVID-19

Therapeutic approaches for COVID-19 have evolved substantially as understanding of SARS-CoV-2 pathogenesis improved, leading to a layered strategy targeting different stages of infection [318].

1.8.1 Antiviral therapies

Antiviral drugs target SARS-CoV-2 replication. Remdesivir, an RNA polymerase inhibitor, was the first antiviral to demonstrate clinical benefit, reducing time to recovery in hospitalized patients requiring oxygen. Nirmatrelvir/ritonavir (Paxlovid) became a cornerstone outpatient therapy, significantly reducing hospitalization and death when given to high-risk individuals soon after diagnosis. Molnupiravir, another oral antiviral, offers an alternative for patients who are unable to take Paxlovid, albeit with comparatively weaker efficacy. These antivirals prevent disease progression by reducing viral load before the hyperinflammatory phase emerges [318-321].

1.8.2 Immunomodulatory treatments

Because severe COVID-19 is driven largely by dysregulated inflammation rather than direct viral pathology, immunomodulators form a key component of treatment for hospitalized patients. Corticosteroids, particularly dexamethasone, remain the foundation of therapy for individuals requiring supplemental oxygen or mechanical ventilation, reducing mortality by dampening excessive cytokine responses. More targeted agents, such as the monoclonals tocilizumab and sarilumab (IL-6 receptor blockers), mitigate the cytokine storm in patients with elevated inflammatory markers. Baricitinib, a JAK inhibitor, further modulates immune signaling pathways and has shown benefits both when used solely and in combination with other therapies. These therapies aim to curb the damaging host immune responses responsible for acute respiratory distress syndrome and multiorgan failure [322-324].

1.8.3 Passive immunotherapies

Passive immunotherapies provide antibodies from external sources to neutralize the virus, offering immediate but temporary protection. Early in the pandemic, most therapeutic anti-SARS-CoV-2 monoclonal antibodies targeted the Spike RBD. Representative examples include Casirivimab/Imdevimab, Bamlanivimab/ Etesevimab, Sotrovimab, Tixagevimab/Cilgavimab, and Bebtelovimab, which were effective in preventing disease progression in high-risk outpatients but lost activity as immune-evasive variants emerged [325-329]. Although the RBD was initially the most potent and clinically actionable target, its high mutation rate revealed a

key limitation: RBD antibodies are highly effective yet epitope-fragile. In contrast, the more conserved S2, which contains the fusion peptide, HR1/HR2, and stem-helix regions, provides a structurally constrained target. S2-directed antibodies are typically broader and more escape-resistant, albeit less potently neutralizing, and are now viewed as promising for durable, variant-resistant immunity against evolving coronaviruses. An example is, as previously mentioned in section 1.2.3.4, the recent discovery of a panel of VHHs targeting S2 that broadly neutralize SARS-CoV-1 and SARS-CoV-2 with unusually high potency [53, 330]. On the other hand, convalescent plasma therapy showed mixed results. Although it exhibited broad neutralization potential, outcomes varied by donor antibody levels, timing, and disease severity. In general, passive immunotherapies remain most relevant for immunocompromised patients, who often fail to mount a robust endogenous response to infection or vaccination [331-333].

1.8.4 Anticoagulation and thrombosis management

COVID-19 is associated with a high incidence of thromboembolic events due to vascular inflammation, endothelial dysfunction, and hypercoagulability. Prophylactic anticoagulation, primarily with low-molecular-weight heparin, has become standard for hospitalized patients to reduce the risk of deep vein thrombosis and pulmonary embolism. In selected high-risk or critically ill patients, intermediate or therapeutic-dose anticoagulation may be indicated. These strategies significantly reduced complications associated with COVID-related coagulopathy [334-335].

1.8.5 Respiratory and supportive care

Supportive care remains crucial for patients with severe and critical COVID-19. Oxygen therapy, including high-flow nasal cannula, prevents hypoxemia, whereas non-invasive ventilation and mechanical ventilation are used in cases of advanced respiratory failure. Prone positioning improves oxygenation and outcomes in both intubated and awake patients. Management of fluid balance, treatment of secondary infections, and careful hemodynamic support further improve survival. Innovations in ICU (Intensive Care Unit) protocols and the early identification of decompensation have markedly improved patient outcomes [336, 337].

1.8.6 Emerging and adjunctive therapies

New therapeutic avenues continue to be explored as the virus evolves. Host-directed antivirals, broad-spectrum antiviral molecules, and immunomodulatory peptides are under investigation to overcome variant resistance. Approaches targeting viral entry mechanisms, TLR modulation, interferon supplementation, and the pathophysiology of long COVID-19 are also being evaluated. The therapeutic landscape increasingly emphasizes personalized treatment tailored to variant characteristics, patient immune status, and disease stage [338, 339].

1.8.6.1 Lithium salts as potential candidates in COVID-19 therapeutics

Lithium salts are ionic compounds containing lithium (Li^+) as the cation paired with various anions. Their chemistry is defined by lithium's small ionic radius, high charge density, and strong hydration energy, giving these salts unique solubility and reactivity patterns across multiple biological and industrial contexts. The most pharmaceutically important lithium salt is lithium carbonate (Li_2CO_3), widely used as a mood stabilizer in bipolar disorder. Other common lithium salts include lithium citrate, lithium chloride, lithium sulfate, and lithium bromide, each with distinct chemical properties and applications [340, 341].

Importantly, the biological applications of lithium salts are determined by their capacity to stabilize neuronal signaling and modulate intracellular pathways, including activating neuroprotective signaling cascades, depleting inositol monophosphate, and inhibiting glycogen synthase kinase-3 (GSK-3). It is precisely this last aspect that makes lithium salts potential candidates in anti-COVID-19 therapy, specifically lithium carbonate and lithium citrate, which have been approved prescription drugs for humans since 1970 [342, 343].

GSK-3 is a highly conserved serine/threonine kinase that exists in two isoforms, GSK3α and GSK3β, each with differential regulation and tissue expression. These isoforms play a central regulatory role by intersecting with PI3K (phosphatidylinositol 3-kinase), mTOR (mammalian target of rapamycin), PKB (protein kinase B), WNT (Wingless and Int-1), and MAPK (mitogen-activated protein kinase) pathways in numerous cellular processes, including metabolism, cell proliferation, differentiation, apoptosis, inflammation, and immune responses.

Importantly, viruses can interact with it in human cells and manipulate its pathway in convenience [344, 345].

SARS-CoV-2 utilizes GSK-3 to phosphorylate its N glycoprotein at conserved serine/arginine–rich sites, which is crucial for the proper function of N in viral RNA binding, replication, and assembly. Accordingly, GSK-3 inhibition demonstrated antiviral effects *in vitro* by blocking SARS-CoV-2 infection in human lung epithelial cells [345-347].

GSK-3 inhibition also modulates host immunity, offering a host-directed booster against viruses. In immature DCs, the GSK-3β isoform, which predominates in immune cells, is continuously active, and its inhibition has been shown to enhance DC maturation and function, including DC-mediated cross-priming of $CD8^+$ T cells and cytokine production. Additionally, GSK-3β inhibition promotes NK cell maturation, thereby enhancing the antiviral cellular immune response [348, 349].

The analysis of clinical data from over 300 thousand patients in three major health systems in the United States demonstrated a 50% reduced risk of COVID-19 in patients following lithium medication, and using electronic health records of 26554 patients with documented serum lithium levels during the pandemic, it was shown that the 6-month COVID-19 infection incidence was lower among matched patients with 'therapeutic' (0.5 - 1 mmol/L) versus 'subtherapeutic' (0.05 - 0.50 mmol/L) lithium levels [347, 350].

All in all, lithium salts represent a biologically plausible antiviral strategy against SARS-CoV-2, with supportive but preliminary evidence. However, safe therapeutic plasma levels in humans are narrow, with risks of renal toxicity, thyroid dysfunction, and adverse neurologic effects that require systematic monitoring [351]. Consequently, further research is necessary to determine safe and effective doses for COVID-19 therapy.

1.9 Aim of the thesis

The COVID-19 pandemic, caused by the SARS-CoV-2, has highlighted critical limitations in current strategies for preventing and treating respiratory viral infections. Despite the rapid development and global deployment of effective systemic vaccines, the continued emergence of viral variants and the persistence

of transmission underscore the need for improved approaches that can induce robust protection at the primary site of infection, the respiratory mucosa. Mucosal vaccines offer the potential to elicit local immune responses, including secretory IgA and tissue-resident immune cells, which may provide superior protection against infection and viral spread. In parallel, the pandemic highlighted the urgent need for novel therapeutic strategies that complement vaccination, particularly for vulnerable populations and during breakthrough infections. Therefore, this thesis aims to evaluate an innovative anti-COVID-19 mucosal vaccine formulation and a novel therapeutic approach targeting SARS-CoV-2, with the broader goal of advancing to effective interventions against current and future variants of concern (VOCs) (**Figure 1.4**).

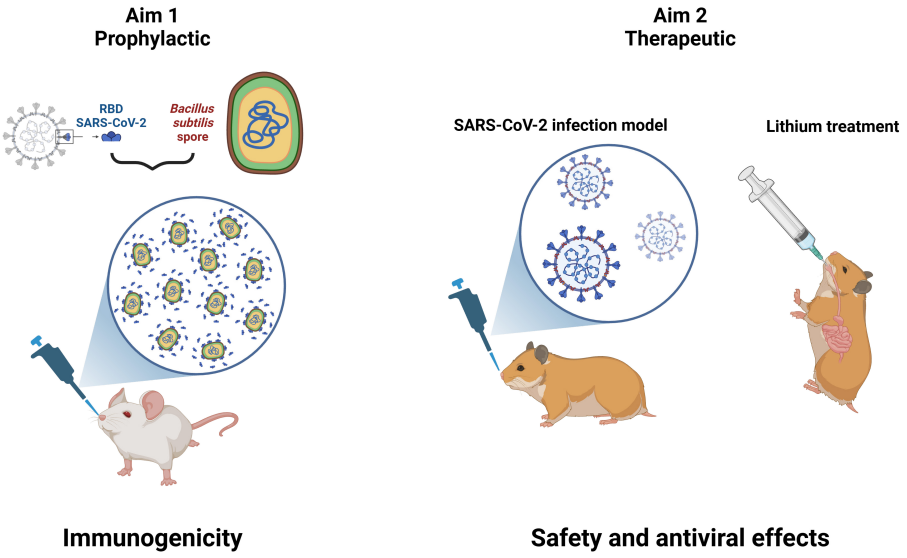

Figure 1.4. **Overview of the aims of the thesis.** Diagram of them. This thesis aims to evaluate an innovative anti-COVID-19 mucosal vaccine formulation and a novel therapeutic strategy targeting SARS-CoV-2, with the broader objective of advancing effective interventions against current and future variants of concern. Specifically, the prophylactic aim assesses the immunogenicity of an intranasal anti-SARS-CoV-2 vaccine adjuvanted with human probiotic *Bacillus subtilis* spores in a murine model, focusing on the induction of mucosal and systemic immune responses. In parallel, the therapeutic aim evaluates the safety and antiviral efficacy of lithium salts against SARS-CoV-2 infection in vitro and in a Syrian hamster model of COVID-19, determining their effects on viral replication and disease progression.

Aim 1: Evaluating the immunogenicity in mice of an anti-SARS-CoV-2 intranasal vaccine adjuvanted with human probiotic *B. subtilis* spores (Figure 1.4).

Parenteral vaccines dramatically slowed the COVID-19 pandemic [352-354]. However, despite substantial reductions in disease severity, hospitalizations, and mortality, the virus's transmissibility has persisted, allowing it to continue spreading and giving rise to several VOCs capable of evading immunity [355-357]. This has led to a prolonged battle between vaccine development and viral evolution [358-360]. Mucosal vaccine delivery has garnered significant attention for its potential to induce broad protective immunity at the primary site of infection, thereby significantly reducing the risk of viral transmission [361-363].

In **Chapter 2**, an intranasal vaccine formulation consisting of recombinant receptor-binding domain (RBD) adsorbed onto human probiotic *Bacillus subtilis* DG101 spores is evaluated. We hypothesize that these *Bacillus subtilis* spores play a dual role as antigen carrier and innate immune activator, leading to enhanced antigen uptake, presentation, and local immune activation while preserving safety. BALB/c mice are immunized intramuscularly (IM) or intranasally (IN) with three doses of RBD adsorbed onto 1 x 10^9 spores. To assess immune responses, blood samples are collected on days 35 and 42, saliva on day 38, and bronchoalveolar lavage fluid (BALF) on day 42. Additional serum is collected on day 180 to evaluate long-term immunity. NALT, spleen, and lungs are harvested for cellular analysis on day 42. Anti-SARS-CoV-2 RBD-specific IgM, IgG, and IgA are evaluated by Enzyme-Linked Immunosorbent Assay (ELISA). Moreover, the serum IgG avidity index (AI) and the 50% molecular virus neutralization titer ($mVNT_{50}$) are determined. Using flow cytometry, the systemic and local B and T cells are phenotyped for activation, polarization, homing, and memory markers. Furthermore, a CFSE (Carboxyfluorescein Succinimidyl Ester)-proliferation assay is conducted to assess antigenic recall.

Findings from this chapter of the thesis will characterize the humoral and cellular responses in mice induced by IM and IN administration of our SARS-CoV-2 vaccine candidate. This knowledge will contribute to the future approval of a human anti-SARS-CoV-2 mucosal vaccine adjuvanted with human probiotic *B. subtilis*.

Aim 2: Evaluating the safety and therapeutic effects of lithium salts against SARS-CoV-2 *in vitro* and in Syrian hamsters suffering from COVID-19 (Figure 1.4).

Despite the significant advances in anti-COVID-19 therapeutics achieved over the past few years, substantial unmet medical needs persist. SARS-CoV-2 remains globally circulating and generates new variants with altered transmissibility, pathogenicity, and susceptibility to existing treatments. In this regard, some currently available antivirals have limitations related to viral resistance, drug–drug interactions, narrow treatment windows, or reduced efficacy against emerging variants (321, 322). Consequently, novel approaches must be continually explored to ensure effective control of the virus and improve current therapeutics.

We hypothesize that lithium salts have therapeutic effects against SARS-CoV-2 while preserving safety, both *in vitro* using Vero E6 cells and *in vivo* in Syrian hamsters infected with COVID-19. In **Chapter 3**, Vero E6 monolayers are inoculated or not with 10^2 $TCID_{50}$ (50% tissue culture infectious dose) of the SARS-CoV-2 strain CUT-2010-2025, and six different concentrations of lithium (Li^+), ranging from 2 to 12 mmol/L, are added. Cytopathic effects are then assessed by microscopy 96 h after inoculation, and the antiviral efficacy of lithium is evaluated using the NR (neutral red) uptake assay [364, 365]. Next, the supernatants are collected to detect and compare the amount of viral proteins using ELISA, which is coated with an anti-SARS-CoV-2 N protein monoclonal antibody (CBSS NCoV). Additionally, an *in vivo* model of COVID-19 is evaluated using Syrian hamsters into five groups: negative and positive controls (n = 4 each); lithium control (n = 4); and two groups of infected animals treated with lithium, one on the same time point of the infection (T-0) and the other on the day before (T-1) (n = 6 each). Lithium carbonate is administered daily, intragastrically, at a dose of 15 mg/kg body weight in NaCl 0.9% to all animals, except those in the negative and positive control groups, which received only the equivalent saline solution. Lithium in the serum is measured, and the lithium-control animals are checked daily for any signs suggestive of toxicity (lethargy/inactivity, seizures, and diarrhea). To induce the animal model, anesthetized hamsters are inoculated intranasally with 10^2 $TCID_{50}$ of SARS-CoV-2 in 50 µL (25 µL in each nostril). Next, signs of the disease (lethargy, stooping,

and polypnea/abdominal breathing) are checked daily, and nasal swabs are performed on days 2, 4, 5, and 7, followed by viral load assessment by RT-qPCR and culture on Vero E6 cells. Additionally, two animals from each group are euthanized on the fifth day of infection for viral load assessment and histopathological study by scoring lung damage (0 to 4).

Findings from this chapter of the thesis will provide preclinical evidence of the safety, antiviral, and immunotherapeutic effects of lithium against SARS-CoV-2, supporting further advancement to clinical trials for COVID-19.

Chapter 2

Mucosal vaccination against SARS-CoV-2 using human probiotic *Bacillus subtilis* spores as an adjuvant induces potent systemic and mucosal immunity

Based on:

Mucosal vaccination against SARS-CoV-2 using human probiotic *Bacillus subtilis* spores as an adjuvant induces potent systemic and mucosal immunity

Ramos Pupo R, Reyes Díaz LM, Suárez Formigo GM, Borrego González Y, Lastre González M, Saavedra Hernández D, Crombet Ramos D, Sánchez Ramírez B, Grau R, Hellings N, Stinissen P, Pérez O and Bogie JFJ

Vaccines. 2025 Jul; 13(7):772

Statement of contribution

This chapter is based on collaborative research. The experimental work was conducted in Belgium and Cuban research institutions. The study was conceptualized and designed by the candidate (RRP), LMRD, OP, BSR, NH, PS, and JFJB. The candidate (RRP) contributed to the development of the methodology, performed experimental investigations together with LMRD, GMSF, and JFJB, and participated in the formal analysis of the data. The candidate also contributed to securing resources and funding acquisition for the study. The original draft of the manuscript was prepared by the candidate (RRP), NH, PS, and JFJB. The candidate further participated in manuscript review and editing together with the co-authors. Supervision of the work was provided by OP, NH, PS, and JFJB. All authors read, revised, and approved the final published version of the manuscript.

2. Mucosal vaccination against SARS-CoV-2 using human probiotic *Bacillus subtilis* spores as an adjuvant induces potent systemic and mucosal immunity

2.1 Abstract

Background: The ongoing evolution of SARS-CoV-2 has highlighted the limitations of parenteral vaccines in preventing viral transmission, largely because they fail to elicit robust mucosal immunity. **Objective/Methods**: Here, we evaluated an intranasal (IN) vaccine formulation in BALB/c mice consisting of recombinant receptor-binding domain (RBD) adsorbed onto human probiotic *Bacillus subtilis* DG101 spores. **Results**: IN spore-RBD immunization induced strong systemic and mucosal humoral responses, including elevated specific IgG, IgM, and IgA levels in serum, bronchoalveolar lavage fluid (BALF), nasal-associated lymphoid tissue (NALT), and saliva. It further promoted mucosal B cell and T cell memory, along with a Th1/Tc1-skewed T cell response, characterized by increased IFN-γ-expressing $CD4^+$ and $CD8^+$ T cells in the lungs. **Conclusions**: All in all, these findings highlight the potential of intranasal vaccines adjuvanted with probiotic *B. subtilis* spores to induce sterilizing immunity and limit SARS-CoV-2 transmission.

2.2 Introduction

The Acute Respiratory Syndrome Coronavirus 2 (SARS-CoV-2), the virus responsible for COVID-19, has presented significant challenges to global public health [17, 28, 366-369]. To date, over 180 vaccine candidates have entered clinical trials [361, 370, 371], with 14 vaccines having received validation from the World Health Organization (WHO) by December 2024 [372]. These licensed vaccines have dramatically slowed the pandemic's pace [352-354]. However, despite the substantial reduction in disease severity, hospitalizations, and mortality, the virus's transmissibility has persisted, allowing it to spread and give rise to several variants of concern (VOCs) capable of evading the immunity generated [355-357]. This has led to a prolonged battle between vaccine development and viral evolution [358-360].

While licensed parenteral SARS-CoV-2 vaccines, including mRNA vaccines, have shown high efficacy in preventing severe COVID-19, a major drawback is their limited ability to prevent virus transmission. In this context, they mainly elicit strong systemic IgG responses; however, respiratory viruses like coronaviruses spread through droplets and initially infect the upper respiratory tract, a site that systemic IgG does not sufficiently protect. As a result, these vaccines often fail to provide sterilizing immunity, allowing local viral replication in the respiratory mucosa, which can promote further transmission and potentially drive the emergence of resistant VOCs. In contrast, mucosal vaccines induce the production of specific secretory IgA (sIgA), which is expected to be more effective than IgG in neutralizing SARS-CoV-2. By blocking the virus at the portal of entry, mucosal vaccines are more likely to prevent initial viral replication and offer sterilizing immunity. Finally, mucosal immunization elicits protective tissue-resident $CD4^+$ and $CD8^+$ T cell responses within local lymphoid tissue. Despite the respiratory nature of SARS-CoV-2 infection and the potential benefits of mucosal immunization, only 10% of vaccine candidates are designed for mucosal delivery, with none yet approved [362, 363, 370, 372-375].

In this study, we evaluated a novel nasal-delivered vaccine formulation and investigated its capacity to induce both systemic and mucosal adaptive immunity. To enhance its immunogenic potential, we utilized human probiotic *Bacillus subtilis* DG101 spores [376-378] as a novel adjuvant. *B. subtilis* is an aerobic, non-pathogenic Gram-positive soil bacterium, which is widely used as a GRAS (Generally Recognized as Safe by the FDA) food ingredient for humans (e.g., natto, a traditional Japanese food) and animals, and represents an important host for the production of medicinal proteins and industrial enzymes. Its spores have proven safe and effective as vaccine carriers and adjuvants for mucosal vaccines against pathogens [275, 379-382]. Moreover, they have been reported to have intrinsic immunomodulation properties by stimulating both innate and adaptive immune responses [308, 383, 384]. The *B. subtilis* spores further exhibit heat-resistant properties that enhance vaccine stability and facilitate distribution [376, 385]. These unique characteristics make *B. subtilis* DG101 spores a promising candidate for ensuring high safety, efficacy, and room-temperature stability in mucosal vaccines. The receptor-binding domain (RBD) was chosen as a target as it engages with the angiotensin-converting enzyme 2 (ACE2) on host cells,

allowing SARS-CoV-2 to enter the cells. RBD is small (~200 aa and ~25 kDa) and folds autonomously, making it suitable for this platform [386-388]. In preclinical and clinical trials, recombinant RBD in multiple vaccine formulations has induced robust neutralizing immunity [163, 389-393]. Our findings indicate that intranasal co-administration of RBD and human probiotic *B. subtilis* DG101 spores elicits potent, specific humoral and cellular mucosal responses in the respiratory tract. We anticipate that the hydrophobic and electrostatic properties of these spores [394, 395] readily enable non-covalent binding of RBD to their surfaces, thus mimicking the natural viral infection. Overall, this mucosal vaccination strategy induces systemic responses comparable to parenteral vaccines while providing the crucial advantage of mucosal-specific immunity, making it a more effective approach to limiting virus transmission.

2.3 Materials and methods

2.3.1 Animals

Female BALB/c mice, aged 8 to 12 weeks, were obtained from Envigo or CENPALAB (National Center for the Production of Laboratory Animals, Havana). Animals were maintained under specific pathogen-free conditions and managed in accordance with the principles and procedures established in Council Directive 86/609/EEC. Mice were housed on a 12 h light/dark cycle with unrestricted access to water and a standardized, grain-based maintenance diet formulated for laboratory rodents. The investigation was approved by the Hasselt University Ethical Committee for Animal Experimentation and the Institutional Animal Care and Use Committee of the Center of Molecular Immunology. To assess immune responses, blood samples were collected at days 35 (only for IgM represented in **Figure 2.1C**) and 42 (all the other assays), saliva at day 38, and bronchoalveolar lavage fluid (BALF) at day 42. A cohort of animals was not terminated at day 42 and was intended for additional serum collection on day 180 to evaluate long-term immunity (only shown in **Figure 2.1E**). Nasal-associated lymphoid tissue (NALT), spleen, and lungs were harvested for cellular analysis at day 42 (**Figure 2.1A**).

2.3.2 Vaccine formulation and inoculation

Recombinant SARS-CoV-2 Wuhan-Hu-1 (aa 328-533) RBD-His protein was produced in a HEK293 cell expression system [396]. A total concentration of 20

µg was used for intramuscular doses. For the intranasal inoculations, 80 µg was selected based on our preliminary dose-escalation experiments, where this amount induced the highest mucosal immune activation with our formulation. This can be explained by the capacity of *B. subtilis* spores to adsorb large amounts of antigen [387], particularly relevant for the small RBD protein (~25 kDa) [388], and the lower bioavailability typically associated with the intranasal route, where higher antigen quantities are often required to overcome mucociliary clearance and enhance delivery to immune-inductive sites [397, 398]. Spores were obtained after culturing the human probiotic *B. subtilis* DG101 strain (*Instituto de Ciencias Básicas y Preclínicas*, Havana), derived from the natto strain [376, 399]. A total concentration of 1 x 10^9 *B. subtilis* DG101 spores was used for all the inoculations. The vaccine was formulated in PBS (Gibco™, Thermo Fisher Scientific, Waltham, MA, USA) by mixing the RBD and the spores, accordingly, and following an incubation step of 1 h at room temperature (RT) and 100 rpm shaking to allow the antigen adsorption [285, 400-403]. For intramuscular delivery, the left quadriceps was injected with 50 µL using a 31G syringe (Micro-Fine™, BD, Franklin Lakes, NJ, USA). For intranasal vaccination, each nostril was inoculated by pipetting 10 µL of the formulation using 10 µL tips (Sarstedt, Numbrecht, Germany).

2.3.3 Blood sampling

Mice were manually restrained, and the submandibular vein was accessed laterally to the mandible. A 25G needle (Henke Sass Wolf, Tuttlingen, Germany) was used to puncture the vein. Approximately 100 µL of blood was collected into a microcentrifuge tube (Greiner Bio-One, Kremsmünster, Austria) for further serum separation and downstream applications. Hemostasis was achieved by applying gentle pressure with sterile gauze for 30–60 s post-collection [404].

2.3.4 Saliva collection

To stimulate salivation, mice were injected intraperitoneally (IP) with pilocarpine hydrochloride (Sigma-Aldrich, St. Louis, MO, USA) at 10 mg/kg body weight in 100 µL PBS (Gibco™). Immediately after injection, mice were held slightly reclined to allow easy access to the oral cavity. Saliva was collected for 5 min following pilocarpine administration. Saliva droplets were gently aspirated from the oral

cavity using a transfer pipette (Sarstedt) and stored in a microcentrifuge tube (Greiner Bio-One). Approximately 200 µL was recovered per mouse. Collected samples were placed on ice and diluted *v*/*v* in a 2x protease inhibitor cocktail solution (cOmplete ULTRA Tablet, Mini, Roche, Basel, Switzerland) to minimize IgA degradation. Animals were monitored throughout the procedure for signs of distress or adverse reactions to pilocarpine. After collection, mice were injected IP with 200 µL PBS (Gibco™) to prevent dehydration, returned to their cages, and observed until complete recovery [405].

2.3.5 Transcardial perfusion

Mice were IP injected with pentobarbital (Dolethal®, Vetoquinol, Lure, France; 200 mg/kg) before transcardial perfusion with a heparin sodium salt (Sigma-Aldrich) in PBS (Gibco™) solution (20 U/mL). Once fully anesthetized, the thoracic cavity was opened to expose the heart. A 23G needle (Henke Sass Wolf) attached to the perfusion system was inserted into the heart's left ventricle. The right atrium was immediately incised to allow exsanguination at a steady rate of 5 mL/min until the effluent ran clear. To further remove the blood from the lungs, the needle was pushed deeper into the right ventricle, and the left atrium was immediately incised, leading to complete blood removal [406].

2.3.6 Spleen single-cell suspension

After perfusion, spleens were isolated and placed into 12-well plates (Greiner Bio-One) holding 1 mL of ice-cold RPMI 1640 medium (Gibco™) per well. Tissues were mechanically dissociated using the plungers of 5 mL syringes (Henke Sass Wolf) by pressing them through 70 µm cell strainers (Greiner Bio-One) placed over 50 mL conical tubes (Greiner Bio-One). The resulting single-cell suspensions were centrifuged at 300x g for 10 min at 4 °C. Cell pellets were resuspended in 1 mL of ACK lysis buffer (Gibco™) and incubated for 3 min at RT with gentle mixing to lyse red blood cells. This process was stopped with 10 mL of culture medium compounded by RPMI 1640 supplemented with 10% fetal bovine serum, 1% non-essential amino acids, 1% sodium pyruvate, and 1% penicillin/streptomycin (all from Gibco™), followed by centrifugation at 300x g for 10 min. After discarding the supernatant, the resuspended cells in 2 mL of culture medium were filtered through a new 70 µm filter (Greiner Bio-One). The centrifugation step was repeated, and the cells were finally resuspended in 4 mL of culture medium. To

assess viability, cells were counted using a Neubauer hemocytometer (Hausser Scientific, Horsham, PA, USA) after trypan-blue (Biochrom AG, Berlin, Germany) exclusion. Single-cell suspensions were used immediately for downstream applications [407].

2.3.7 Lung single-cell suspension

The isolated lungs from the perfused mice were placed into 12-well plates (Greiner Bio-One) holding 1 mL of ice-cold RPMI 1640 medium (Gibco™) per well. Next, the lungs were transferred into new plates and minced into small fragments using sterile scissors in 1 mL of digestion buffer per well. This buffer was compounded by culture medium, 1 mg/mL collagenase D, and 0.1 mg/mL DNase I (both from Roche). The tissue suspensions were incubated for 45 min at 37 °C, shaking at 15 min intervals to facilitate enzymatic digestion. Next, the resulting lung fragments were mechanically disrupted by pressing them using the plungers of 5 mL syringes (Henke SassWolf) through 70 µm cell strainers (Greiner Bio-One) placed over 50 mL conical tubes (Greiner Bio-One). Cells were washed through the strainer with an additional culture medium to maximize recovery, followed by centrifugation at 300x g for 10 min. After discarding the supernatant, 1 mL of 10 mM EDTA (Sigma-Aldrich) in PBS (Gibco™) was added to resuspend the cells and stop the digestion, followed by 2 mL of culture medium. Red blood cell lysis and cell counting were performed as described previously for splenic cells [408].

2.3.8 BALF collection

A small incision was made in the trachea, and a 20G catheter (Insyte™, BD) was carefully inserted and secured with surgical thread (SMI). The lungs were lavaged by slowly instilling 500 µL of PBS (Gibco™) into the lungs with a 1 mL syringe (Henke Sass Wolf), followed by gentle aspiration. The retrieved volume was transferred to a microcentrifuge tube (Greiner Bio-One), placed on ice, and diluted as described above for saliva to minimize immunoglobulin degradation [409].

2.3.9 NALT isolation and culture

Following perfusion, the upper palates were dissected by tracing along the inner edges of the incisors and molars. The palates were then carefully lifted using forceps to avoid tearing and transferred individually into 48-well plates (Greiner Bio-One) containing 250 µL of culture medium per well. After successive washing

steps, NALTs were incubated at 37 °C in 5% CO_2. After 24 h, 200 µL of supernatant medium from culture wells was collected in microcentrifuge tubes (Greiner Bio-One) for further analysis [410].

2.3.10 Specific antibody determinations

Anti-SARS-CoV-2 RBD-specific antibodies were evaluated by Enzyme-Linked Immunosorbent Assay (ELISA). The working solutions were the following: coating buffer at 0.1 M (pH 9.6) consisting of 3.18 g sodium carbonate (Na_2CO_3, Sigma-Aldrich) and 5.86 g of sodium bicarbonate ($NaHCO_3$, Sigma-Aldrich) per liter of distilled water; blocking buffer consisting of Tween 20 (Sigma-Aldrich) 0.05% *v*/*v* and fat-free milk (Marvel, Premier Foods, St Albans, UK) 4% *m*/*v* in PBS (Gibco™); assay buffer consisting of Tween 20 (Sigma-Aldrich) 0.05% *v*/*v* and fat-free milk (Marvel) 2% *m*/*v* in PBS (Gibco™); and PBS-T prepared with Tween 20 0.05% *v*/*v* in PBS (Gibco™). RBD was bound to the surface of flat-bottom 96-well microtiter plates (MaxiSorp, NUNC, Thermo Fisher Scientific) by adding 50 µL per well of coating buffer containing the antigen at a concentration of 5 µg/mL. The plates were incubated overnight at 4 °C with 50 µL per well. Next, 150 µL of blocking solution was applied per well, and the plates were incubated for 30 min at 37 °C. Serum, BALF, saliva, or NALT culture supernatant was diluted (1:1000 for serum and 1:2 for the others) in assay buffer, and 50 µL was placed per well for 2 h at 37 °C. The washings were conducted 3 times using 250 µL of PBS-T per well. Subsequently, the corresponding conjugate was added for 1 h at 37 °C in a volume of 50 µL per well: goat anti-mouse IgM-HRP (Sigma-Aldrich), goat anti-mouse IgG-HRP (Sigma-Aldrich), goat anti-mouse IgG1-HRP (Sigma-Aldrich), or goat anti-mouse IgG2a-HRP (Sigma-Aldrich), all diluted 1:10,000 in assay buffer, or biotin rat anti-mouse IgA (BioLegend, San Diego, CA, USA) diluted 1:2000 in assay buffer. Afterward, the plates were washed again in a similar manner. For IgA, an additional incubation step was required to add 50 µL of streptavidin-HRP (BioLegend) diluted 1:2000 in assay solution, followed by another washing. For developing the colorimetric reaction, 100 µL of TMB substrate (Thermo Fisher Scientific) was added per well and incubated in the dark for 20 min at RT. Reactions were stopped with 50 µL of 1 M sulfuric acid (H_2SO_4, Sigma-Aldrich), and the absorbance was measured at 450 nm in a microplate reader (CLARIOStar Plus, BMG Labtech, Ortenberg, Germany). Titers were evaluated following 2-fold

serial dilutions. The endpoint titer was demarcated as the highest serum dilution, yielding an absorbance at least four times greater than that of preimmune serum diluted 1:50. Antigen-specific serum antibody responses were interpreted according to commonly reported immunogenicity benchmarks in murine ELISA studies. Endpoint titers below $1:10^2$ were considered negative or baseline responses, titers between $1:10^2$ and $1:10^3$ were classified as weak positive responses, and titers $\geq 1:10^4$ were considered indicative of moderate to strong humoral immune responses. Titers exceeding $1:10^5$ were interpreted as highly robust antigen-specific antibody responses. [411, 412].

2.3.11 Avidity index

Antibody–antigen binding strength was evaluated by measuring the resistance to disruption with the chaotropic agent urea. Identical ELISA plates to those above were coated and blocked, as formerly described, for specific IgG antibody determinations. The sera were added at the minimal dilution so that the absorbance value exceeded 1 in the titration ELISA, and incubated for 1 h at 37 °C. Afterward, a three-time washing with PBS-T was conducted. One set of wells was then washed an additional three times with PBS-T (without urea), while the other set was washed three times with 6 M urea (CH_4N_2O, Sigma-Aldrich) in PBS-T (urea-treated) to disrupt low-affinity antibody–antigen interactions. The following steps for the ELISA were as previously presented. The avidity index (AI) was calculated as (OD with urea/OD without urea) × 100, representing the proportion of high-affinity IgG that remained bound. Antibodies were classified as high-avidity if the AI exceeded 50% [412, 413].

2.3.12 Surrogate virus neutralization assay

A surrogate virus neutralization assay was conducted to evaluate the capacity of antibodies to inhibit RBD binding to its corresponding cellular receptor, ACE2. RBD fused to human IgG1 Fc region (RBD-hFc) and ACE2 fused to murine IgG2a Fc region (ACE2-mFc) proteins were produced in a HEK293 cell expression system. Briefly, identical ELISA plates to those above were coated with ACE2-mFc at a concentration of 5 µg/mL in coating buffer. Then, 2-fold serial dilutions of sera in assay buffer were mixed 1:1 (*v*/*v*) with 40 ng/mL RBD-hFc and incubated for 1 h at 37 °C. Next, 50 µL of the mixtures were added to the wells and incubated for 2 h at 37 °C. The following steps for the ELISA were as described previously, but

using the goat anti-human IgG-HRP (Sigma-Aldrich) diluted 1:10,000 in assay buffer. Maximal recognition corresponds to RBD-hFc (40 ng/mL) mixed 1:1 (*v*/*v*) with assay buffer. The 50% molecular viral neutralization titer ($mVNT_{50}$) was defined as the highest serum dilution that resulted in half inhibition of maximal recognition [414].

2.3.13 CFSE-proliferation assay

Lung single-cell suspensions were cultured at 1 x 10^6/well in 96-well plates (Greiner Bio-One) and antigen recall was induced by adding RBD at 5 µg/mL. CFSE Cell Division Tracker Kit (BioLegend) was used according to the manufacturer's protocol. Surface staining (B and T cells) was performed, followed by fixation and permeabilization, and subsequent intracellular staining (T cells) as described below for flow cytometry [415].

2.3.14 Flow cytometry

The following reagents and fluorophores were used: Alexa Fluor® 700 anti-mouse/human CD45R/B220 (1:200, clone RA3-6B2, BioLegend), Alexa Fluor® 700 anti-mouse CD45 (1:200, clone 30-F11, BioLegend), Biotin anti-mouse IgA (1:200, clone RMA-1, BioLegend), APC Streptavidin (1:200, BioLegend), APC anti-mouse CD103 (1:200, clone 2E7, BioLegend), Brilliant Violet 421™ anti-mouse CD138 (1:100, clone 281-2, BioLegend), Brilliant Violet 510™ anti-mouse CD8a (1:200, clone 53-6.7, BioLegend), Brilliant Violet 605™ anti-mouse IgD (1:200, clone 11-26c.2a, BioLegend), Brilliant Violet 650™ anti-mouse CD19 (1:200, clone 6D5, BioLegend), Brilliant Violet 650™ anti-mouse/human CD44 (1:200, clone IM7, BioLegend), Brilliant Violet 785™ anti-mouse CD69 (1:200, clone H1.2F3, BioLegend), FITC anti-mouse CD3 (1:500, clone 17A2, BioLegend), Pacific Blue™ anti-mouse CD4 (1:200, clone RM4-5, BioLegend), PE anti-mouse CD38 (1:200, clone 90, BioLegend), PE anti-mouse IL-4 (1:200, clone 11B11, BioLegend), PE/Cyanine7 anti-mouse IFN-γ (1:200, clone XMG1.2, BioLegend), PE/Cyanine7 Goat anti-mouse IgG (1:200, clone Poly4053, BioLegend), PE/Dazzle™ 594 anti-mouse IL-17A (1:50, clone TC11-18H10.1, BioLegend), PerCP/Cyanine5.5 anti-mouse CD3 (1:200, clone 17A2, BioLegend). CFSE Cell Division Tracker Kit (BioLegend) and Zombie NIR™ Fixable Viability Kit (BioLegend). RBD was conjugated to FITC (**Table S2.1**). For stimulation and accumulation of intracellular cytokines, cells were incubated with phorbol 12-myristate 13-acetate (20 ng/mL;

Sigma-Aldrich), calcium ionomycin (1 µg/mL; Sigma-Aldrich), and GolgiPlug™ (2 µg/mL; BD Biosciences, San Jose, CA, USA) for 4 h before staining. Briefly, live/dead staining was conducted according to the manufacturer's instructions for the Zombie NIR™ Fixable Viability Kit (BioLegend). Next, extracellular staining was performed in 100 µL FACS buffer containing the appropriate stains with incubation for 15 min in the dark at RT, followed by a washing step. Cells were then fixed and permeabilized by means of the eBioscience™ Foxp3/Transcription Factor Staining Buffer Set (Thermo Fisher Scientific), following the manufacturer's instructions, and intracellularly stained for assessing IFN-γ, IL-4, and IL-17A. Samples were acquired using a BD LSRFortessa (BD Biosciences) flow cytometer. Compensation was performed using single-stained controls, and the analysis was conducted with FlowJo software v10 [416].

2.3.15 Experimental design and statistical analyses

All statistical analyses were performed with the software GraphPad Prism™ v10 and conveyed as mean ± SD. Data normality was confirmed, and, according to the number of groups in the datasets, a two-tailed unpaired Student t-test or a one-way ANOVA (post hoc: Tukey) was used. Significance levels legend: * $p < 0.05$, ** $p < 0.01$; *** $p < 0.001$ or **** $p < 0.0001$.

2.4 Results

2.4.1 SARS-CoV-2 RBD intranasal immunization adjuvanted with human probiotic *Bacillus subtilis* spores induces specific systemic and mucosal responses

To evaluate the potential efficacy of mucosal delivery of the *B. subtilis* spore-RBD vaccine formula in eliciting an Ig response, BALB/c mice were immunized intranasally (IN) with three doses of RBD (80 µg) adsorbed onto 1×10^9 *B. subtilis* DG101 spores (spore-RBD) (experimental design depicted in **Figure 2.1A**). Our findings indicate that this approach induced a robust RBD-specific serum IgG response, significantly higher than that achieved with the gold-standard intramuscular (IM) regimen of three doses of RBD (20 µg) adsorbed onto aluminum hydroxide gel (alum-RBD) (**Figure 2.1B**). Three IM doses of the spore-RBD vaccine also elicited an elevated specific IgG response, albeit lower than that observed with both the IM alum-RBD and IN spore-RBD formulations (**Figure**

2.1B). A similar trend was observed for specific IgM levels in serum (**Figure 2.1C**). Consistent with the established ability of mucosal vaccines to enhance specific IgA serum levels, only IN immunization with the spore-RBD formulation generated a significant anti-RBD response of this class in serum (**Figure 2.1D**). To further quantify the immune response, systemic anti-RBD IgG titers were assessed across the adjuvanted groups, revealing high titers in all three groups, with the highest observed in mice receiving the IN spore-RBD formulation. Moreover, we found that specific IgG titers remained above 10^4 at 180 days in most mice in the IN spore-RBD group, indicative of moderate to strong persistent humoral immune responses (**Figure 2.1E**). Finally, affinity assays demonstrated enhanced IgG affinity maturation following IN spore-RBD immunization compared with IM alum-RBD (**Figure 2.1F**). Supporting this, the anti-RBD antibodies induced by the IN spore-RBD vaccine exhibited superior neutralization capacity, most effectively inhibiting the RBD−ACE2 interaction (**Figure 2.1G**). Collectively, these findings demonstrate that IN delivery of the spore-RBD vaccine induces a potent and broad humoral immune response, characterized by elevated serum levels of specific IgG, IgM, and IgA.

Having established a potent systemic Ig response, we next evaluated respiratory mucosal immunity following IN or IM inoculation with the spore-RBD formulation. Only mice immunized with three doses of IN spore-RBD developed high levels of anti-RBD IgA and IgG in the supernatant of NALT cultures and in the BALF (**Figure 2.1H–K**). Similarly, only IN spore-RBD immunization increased anti-RBD IgA levels in saliva (**Figure 2.1L**). Neither the IN RBD (without adjuvant) nor IM spore-RBD induced a notable IgG and IgA response in BALF, NALT cultures, and saliva (**Figure 2.1 H–L**). Finally, by using FITC-conjugated RBD, we found that IN spore-RBD immunization results in an increased presence of antigen-specific B cells ($B220^+CD19^+RBD^+$) within lung tissue (**Figure 2.1M,N**), as compared to IM spore-RBD inoculation. These findings demonstrate that IN spore-RBD inoculation induces a robust, mucosal, and specific humoral immune response.

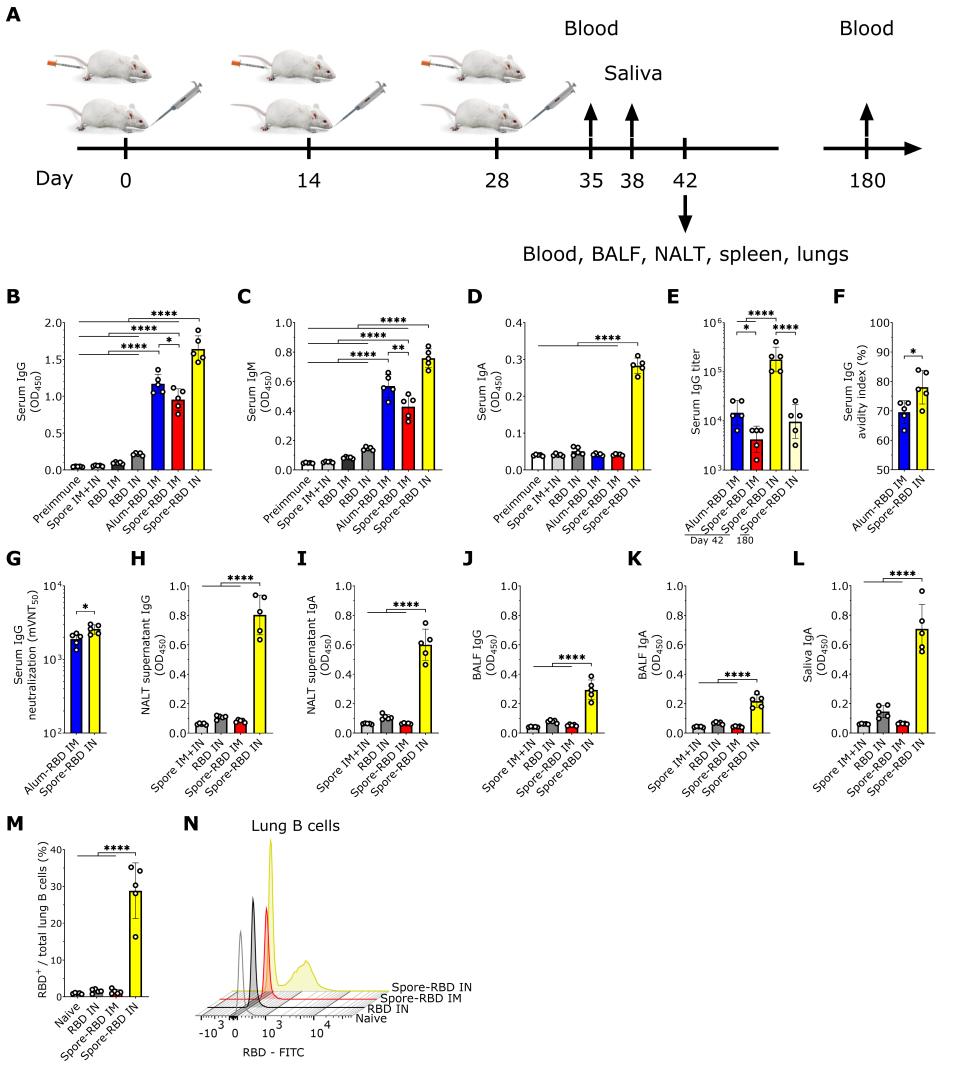

Figure 2.1. SARS-CoV-2 RBD intranasal immunization adjuvanted with *Bacillus subtilis* DG101 spores induces systemic and mucosal humoral responses. (**A**) BALB/c mice were immunized intranasally (IN) or intramuscularly (IM) with three doses of 80 µg or 20 µg, respectively, of recombinant SARS-CoV-2 Wuhan-Hu-1 receptor-binding domain (RBD) adsorbed onto 1 × 10^9 *B. subtilis* DG101 spores at 14-day intervals. To assess immune responses, blood samples were collected on days 35, 42, and 180; saliva on day 38; and bronchoalveolar lavage fluid (BALF) on day 42. Nasal-associated lymphoid tissue (NALT), spleen, and lungs were harvested for cellular analysis on day 42. (**B–D**) Anti-RBD-specific antibodies in serum (dilution 1:1000): IgG on day 42 (**B**), IgM on day 35 (**C**), and IgA on day 42 (**D**). Groups include preimmune mice; mice immunized with spores alone IM and IN (spore IM + IN); RBD alone IM (RBD IM) or IN (RBD IN); RBD adsorbed onto aluminum hydroxide IM (alum-RBD IM); and RBD adsorbed onto spores IM (spore-RBD IM) or IN (spore-RBD IN). (**E**) Anti-RBD specific IgG titers after serial dilutions of the 42-day

serum from alum-RBD IM, spore-RBD IM, and spore-RBD IN, and the 180-day serum from spore-RBD IN. (**F**) Serum IgG avidity index on day 42 after antigen–antibody dissociation using a chaotropic agent. (**G**) Half-maximal molecular virus neutralization titer ($mVNT_{50}$), indicating the 42-day serum IgG dilution required to inhibit 50% of RBD–ACE2 binding. (**H–L**) Anti-RBD-specific mucosal antibodies (dilution 1:2): IgG and IgA on day 42 in NALT culture supernatants (**H,I**); IgG and IgA in BALF on day 42 (**J,K**); and IgA in saliva collected on day 38 (**L**). Groups include spore IM + IN, RBD IN, spore-RBD IM, and spore-RBD IN. (**M,N**) Percentage of anti-RBD-specific subset from the total lung B cells of naïve, RBD IN, spore-RBD IM, and spore-RBD IN (**M**). Representative fluorescence intensity histogram from one individual mouse per group, in panel M (**N**). All data are depicted as mean ± SD. Each experimental group consists of five animals, and each dot represents an individual animal. Statistical significance was calculated by one-way analysis of variance (ANOVA) for (**B–E**) and (**H–M**) or by Student's t test for (**F,G**); * $p < 0.05$, ** $p < 0.01$; or **** $p < 0.0001$.

2.4.2 SARS-CoV-2 RBD intranasal immunization adjuvanted with human probiotic *Bacillus subtilis* spores induces mucosal B cell memory in the lungs

Essential immune effectors in long-term protection against SARS-CoV-2 in the lungs are resident memory B cells (B_{RM}), which can rapidly differentiate *in situ* into antibody-secreting cells (ASCs) upon secondary challenge with cognate antigens [417, 418]. Hence, we next assessed both subpopulations in the lungs of perfused mice, thereby circumventing carryover from blood lymphocytes. Our findings indicate that class-switched $CD19^{+/-}CD138^{+}$ASCs in lung tissue expressing IgA or IgG were significantly increased exclusively after IN spore-RBD inoculation (**Figure 2.2A–D**). A similar increase was observed for IgA^{+} or IgG^{+} class-switched B_{RM} ($CD19^{+}B220^{+}IgD^{-}CD38^{+}$) upon inoculation with spore-RBD (**Figure 2.2E–H**). To provide further evidence of efficient mucosal humoral memory, CFSE-labeled lung cells from immunized mice were analyzed for proliferative responses following antigen recall. $CD3^{-}B220^{+}CD19^{+}$ B cells proliferated efficiently (**Figure 2.2I,J**), and the IgA^{+} subset expanded significantly upon RBD challenge only for IN spore-RBD (**Figure 2.2K,L**). These findings show that IN spore-RBD inoculation induces mucosal B cell memory in the lungs, resulting from both the overall expansion and an actual increase in the percentage of class-switched antigen-specific IgA^{+} and IgG^{+} subpopulations.

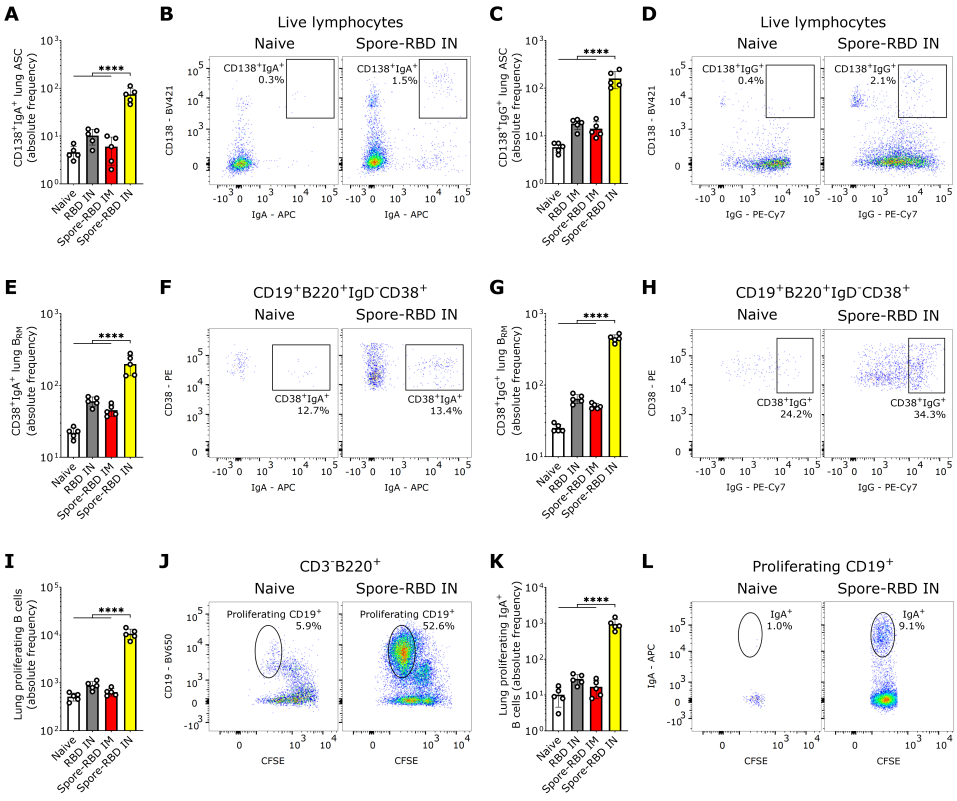

Figure 2.2. SARS-CoV-2 RBD intranasal immunization adjuvanted with *Bacillus subtilis* DG101 spores induces mucosal B cell memory in the lungs. Spleen and lungs were harvested on day 42. The data are shown in absolute frequencies and representative bivariate fluorescence histograms. (**A–D**) $CD138^+IgA^+$ASCs (**A,B**) and $CD138^+IgG^+$ASCs (**C,D**) in the lungs of naive mice, or mice immunized with RBD alone intranasally (RBD IN), or with RBD adsorbed onto *B. subtilis* DG101 spores either intramuscularly (spore-RBD IM) or intranasally (spore-RBD IN). (**E–H**) $CD38^+IgA^+B_{RM}$ (**E,F**) and $CD38^+IgG^+B_{RM}$ (**G,H**) in the lungs of naive, RBD IN, spore-RBD IM, and spore-RBD IN. (**I–L**) Lung proliferating $CD19^+B220^+$ B cells (**I,J**) and subset $CD19^+B220^+IgA^+$ B cells (**K,L**), isolated from the lungs of naive, RBD IN, spore-RBD IM, and spore-RBD IN, following *in vitro* antigen recall in a CFSE proliferation assay. All data are depicted as mean ± SD. Each experimental group consists of five animals, and each dot represents an individual animal. Statistical significance was calculated by one-way analysis of variance (ANOVA); **** $p < 0.0001$.

2.4.3 SARS-CoV-2 RBD intranasal immunization adjuvanted with human probiotic *Bacillus subtilis* spores induces systemic and mucosal T cell immunity with a Th1 bias

Given that IN vaccinations can elicit tissue-resident T cell responses within local lymphoid tissue [373], we next sought to characterize the $CD4^+$ and $CD8^+$ T cell response to spore-RBD inoculation. To this end, we immunophenotyped splenic and alveolar $CD44^{hi}CD4^+$ and $CD44^{hi}CD8^+$ T cells by flow cytometry to assess their production of IFN-γ, IL-4, and IL-17A, which are secreted from Th1/Tc1, Th2/Tc2, and Th17/Tc17 subsets, respectively. In the spleen, we found that mice immunized with spore-RBD either via IM or IN routes showed increased percentages of IFN-γ-secreting $CD4^+$ and $CD8^+$ T cells, with IN immunization eliciting the most robust response (**Figure 2.3A,B**). $CD4^+$ and $CD8^+$ T cells expressing IL-17A and IL-4 were also increased in the IN and IM spore-RBD groups, though to a lesser extent, with no significant differences between the administration routes (**Figure 2.3C–F**). In the lungs, only IN immunization with spore-RBD increased IFN-γ and IL-17A-expressing $CD44^{hi}CD4^+$ and $CD44^{hi}CD8^+$ T cells (**Figure 2.3G–J**), with a more pronounced response observed in IFN-γ-expressing cells. No changes in IL-4 expression in $CD4^+$ and $CD8^+$ T cells were observed in the lungs following administration of spore-RBD, neither via IN nor IM routes (**Figure 2.3K,L**). These patterns are consistent with Th1 and Tc1 systemic and mucosal polarization predominance after IN spore-RBD. Supporting this premise, the distribution of IgG isotypes in the sera showed that IN immunization with spore-RBD induced higher levels of IgG2a relative to IgG1, compared to IM immunization (with spore- or alum-RBD), indicating a more Th1-skewed response upon IN inoculation. It is important to notice that the IgG2a/IgG1 ratio remained below 1, still signifying a slight Th2 bias (**Figure 2.3M**).

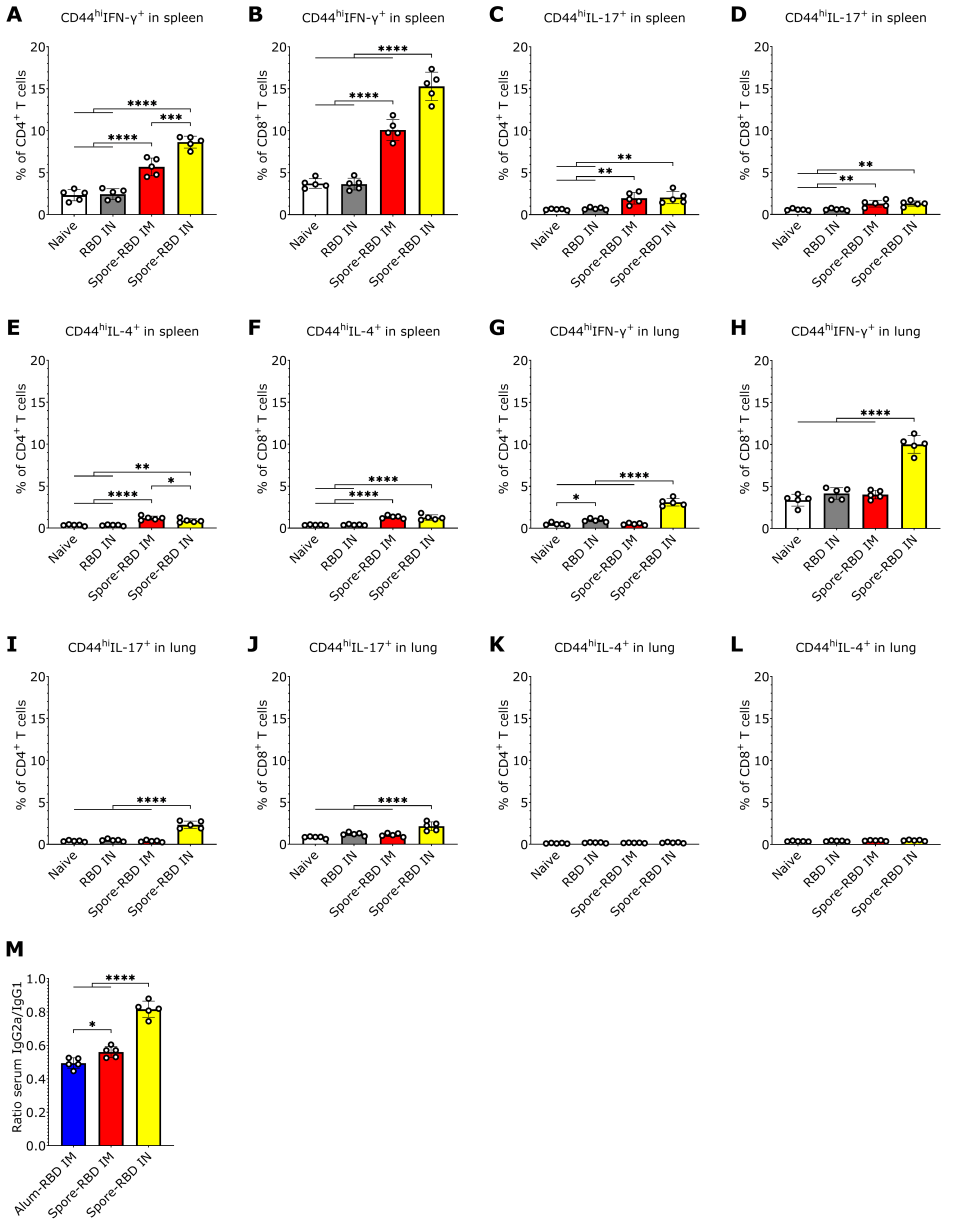
A
CD44hiIFN-γ+ in spleen
% of CD4+ T cells
B
CD44hiIFN-γ+ in spleen
% of CD8+ T cells
C
CD44hiIL-17+ in spleen
% of CD4+ T cells
D
CD44hiIL-17+ in spleen
% of CD8+ T cells
E
CD44hiIL-4+ in spleen
% of CD4+ T cells
F
CD44hiIL-4+ in spleen
% of CD8+ T cells
G
CD44hiIFN-γ+ in lung
% of CD4+ T cells
H
CD44hiIFN-γ+ in lung
% of CD8+ T cells
I
CD44hiIL-17+ in lung
% of CD4+ T cells
J
CD44hiIL-17+ in lung
% of CD8+ T cells
K
CD44hiIL-4+ in lung
% of CD4+ T cells
L
CD44hiIL-4+ in lung
% of CD8+ T cells
Naive
RBD IN
Spore-RBD IM
Spore-RBD IN
M
Ratio serum IgG2a/IgG1
Alum-RBD IM
Spore-RBD IM
Spore-RBD IN

Figure 2.3. SARS-CoV-2 RBD intranasal immunization adjuvanted with *Bacillus subtilis* DG101 spores induces systemic and mucosal T cell immunity with a Th1 bias. Spleen and lungs were harvested on day 42. (**A–L**): Percentage of Th1 ($CD44^{hi}IFN\text{-}\gamma^{+}CD4^{+}$) from total $CD4^{+}$ T cells (**A,G**), Tc1 ($CD44^{hi}IFN\text{-}\gamma^{+}CD8^{+}$) from total $CD8^{+}$ T cells (**B,H**), Th17 ($CD44^{hi}IL\text{-}17^{+}CD4^{+}$) from total $CD4^{+}$ T cells (**C,I**), Tc17 ($CD44^{hi}IL\text{-}17^{+}CD8^{+}$) from total $CD8^{+}$ T cells (**D,J**), Th2 ($CD44^{hi}IL\text{-}4^{+}CD4^{+}$) from total $CD4^{+}$ T cells (**E,K**), and Tc2 ($CD44^{hi}IL\text{-}4^{+}CD8^{+}$) from total $CD8^{+}$ T cells (**F,L**) in spleens and lungs from naive mice, or mice immunized with RBD alone intranasally (RBD IN), or with RBD adsorbed onto *B. subtilis* DG101 spores either intramuscularly (spore-RBD IM) or intranasally (spore-RBD IN). (**M**) Specific IgG2a/IgG1 ratio in 42-day serum of BALB/c mice immunized with recombinant SARS-CoV-2 RBD adsorbed onto aluminum hydroxide intramuscularly (alum-RBD IM), or onto *B. subtilis* DG101 spores intramuscularly (spore-RBD IM) or intranasally (spore-RBD IN). All data are depicted as mean ± SD. Each experimental group consists of five animals, and each dot represents an individual animal. Statistical significance was calculated by one-way analysis of variance (ANOVA); * $p < 0.05$, ** $p < 0.01$; *** $p < 0.001$ or **** $p < 0.0001$.

2.4.4 SARS-CoV-2 RBD Intranasal Immunization Adjuvanted with Human Probiotic *Bacillus subtilis* Spores Induces Mucosal T Cell Memory in the Lungs

In light of the mucosal humoral memory responses generated in the respiratory tract, we also considered assessing lung tissue-resident memory T cell (T_{RM}) induction. Flow cytometry analysis revealed an enhanced proliferative response of CFSE-labeled $CD4^{+}$ and $CD8^{+}$ T cells from spore-RBD-immunized mice upon RBD recall (**Figure 2.4A–D**). Mirroring these findings, lung tissue from mice immunized with IN spore-RBD showed an increased presence of $CD4^{+}CD44^{hi}CD69^{+}CD103^{+/-}$ and $CD8^{+}CD44^{hi}CD69^{+}CD103^{+/-}$ T cells, indicative of enhanced T_{RM} formation (**Figure 2.4E–J**). Interestingly, we found no differences among the ratios $CD103^{+}/CD103^{-}$ for $CD4^{+}$ T_{RM}, which aligns with a proportional expansion of both subsets (**Figure S2.1A**). However, for $CD8^{+}$ T_{RM}, the highest ratio was observed for the spore-RBD intranasally immunized mice, indicating a positive bias of the $CD103^{+}$ subpopulation (**Figure S2.1B**). Our results show that, in addition to the humoral mucosal responses, the IN spore-RBD vaccination strongly induces both $CD103^{+}$ and $CD103^{-}$ subpopulations of $CD4^{+}$ T_{RM} and $CD8^{+}$ T_{RM} in the lung parenchyma, in contrast to the IM formulation.

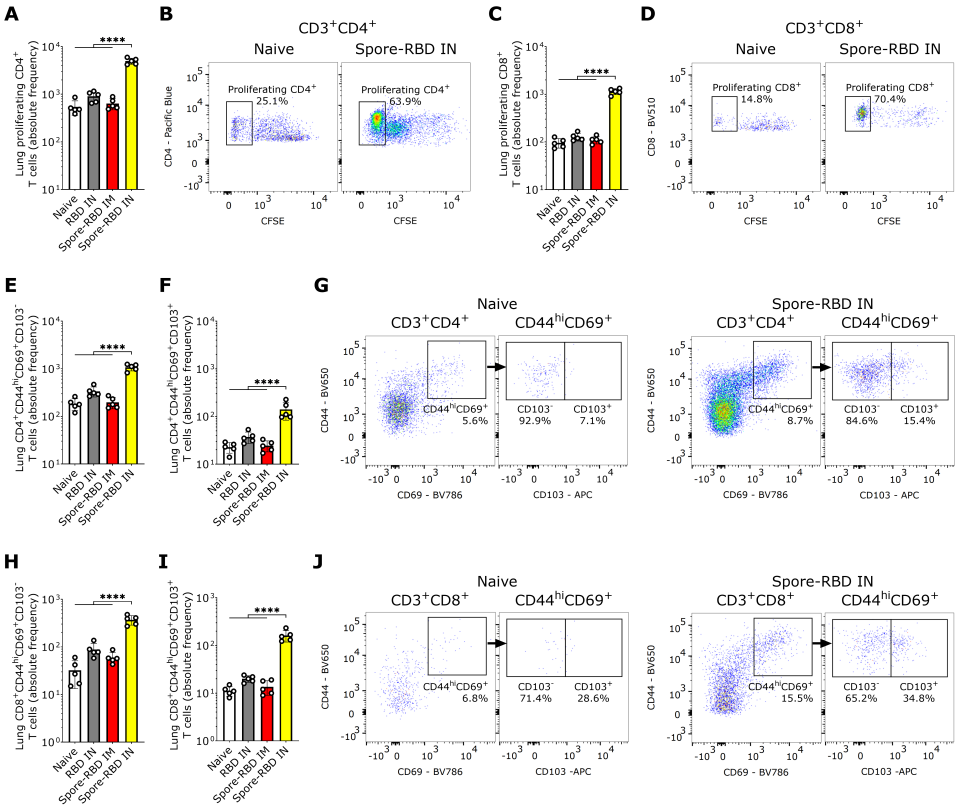

Figure 2.4. SARS-CoV-2 RBD intranasal immunization adjuvanted with *Bacillus subtilis* DG101 spores induces mucosal T cell memory in the lungs. SARS-CoV-2 RBD intranasal immunization adjuvanted with *Bacillus subtilis* DG101 spores induces mucosal T cell memory in the lungs. Spleen and lungs were harvested on day 42. The data are shown in absolute frequencies and representative bivariate fluorescence histograms. (**A–D**): Proliferating $CD4^+$ (**A,B**) and $CD8^+$ T cells (**C,D**) after *in vitro* antigen recall in a CFSE proliferation assay of lung cells from naive mice, or mice immunized with RBD alone intranasally (RBD IN), or with RBD adsorbed onto *B. subtilis* DG101 spores either intramuscularly (spore-RBD IM) or intranasally (spore-RBD IN). (**E–G**): $CD4^+CD44^{hi}CD69^+CD103^-$ (**E,G**) and $CD4^+CD44^{hi}CD69^+CD103^+$ T cells (**F,G**) in the lungs of naive, RBD IN, spore-RBD IM, and spore-RBD IN. (**H–J**): $CD8^+CD44^{hi}CD69^+CD103^-$ (**H,J**) and $CD8^+CD44^{hi}CD69^+CD103^+$ T cells (**I,J**) in the lungs of naive, RBD IN, spore-RBD IM, and spore-RBD IN. All data are depicted as mean ± SD. Each experimental group consists of five animals, and each dot represents an individual animal. Statistical significance was calculated by one-way analysis of variance (ANOVA); **** $p < 0.0001$.

2.5 Discussion

As SARS-CoV-2 transmissibility and capability for immune evasion rebound with each VOC, developing novel vaccines that allow extensive protection against current and prospective VOCs becomes increasingly necessary. In this regard, mucosal vaccine delivery has garnered significant attention for its potential to induce broad protective immunity at the primary site of infection, thereby significantly reducing viral transmission [361-363]. Here, we present a preclinical evaluation of a novel IN mucosal vaccine formulation for COVID-19, composed of the RBD and human probiotic *B. subtilis* spores as an adjuvant. Spore-RBD inoculation elicited robust mucosal and parenteral immunity in a three-dose IN schedule, characterized by the expansion of antigen-specific $CD8^+$ T_{RM}, $CD4^+$ T_{RM}, B_{RM}, and secretion of antigen-specific IgG and IgA. It also resulted in long-lasting immunity, with elevated specific IgG titers persisting after 180 days, indicating the presence of sustained, though waning, antibody responses. In contrast, IM immunization with this formulation and the gold-standard alum-RBD generated a modest systemic response without the desired mucosal immunity. These results indicate that human probiotic *B. subtilis* spores serve as a potent mucosal vaccine adjuvant and that their co-administration with the SARS-CoV-2 RBD may provide effective protection against COVID-19.

Both systemic and mucosal humoral immune responses are crucial against SARS-CoV-2. Concerning the former, serum-neutralizing antibodies targeting the RBD or the entire spike protein are key correlates of protection against symptomatic and severe COVID-19 [419-422], and are often used to assess vaccine efficacy [423-425]. However, systemic immunity alone cannot control infection at mucosal entry points, where SARS-CoV-2 invades through the nasal and oral passages, leading to respiratory tract infection and transmission. Current parenteral COVID-19 vaccines generate strong systemic but weak or no mucosal immunity, limiting their effectiveness in preventing breakthrough infections and spread [362, 363, 426].

Interestingly, we found elevated levels of specific IgM in serum at day 35 of the immunization timeline, corresponding to 7 days after the final dose. This timing supports a detectable response, particularly when induced through a mucosal tissue where immune dynamics differ from systemic responses. Specifically,

intranasal delivery using *B. subtilis* spores may contribute to extended antigen retention, potentially maintaining an ongoing immune activation [285, 397, 398]. Consequently, the continued stimulation of naive B cells or the recall to expansion of IgM^+ memory B cells could lead to our findings.

We show that IN spore-RBD induces a stronger systemic antibody response than IM. While some studies have reported higher systemic antibody responses with IM immunization, such differences likely depend on factors like adjuvant type, antigen delivery efficiency, and threshold concentration requirements for each route. For example, Yahyaei et al. (2025) found that twice the antigen dose was needed for IN delivery to match the systemic IgG levels achieved by IM administration of an mRNA-based influenza A vaccine [427], whereas Anthi et al. (2025) showed that IN vaccination with an RBD-based subunit vaccine produced higher systemic IgG than IM [428]. Hassan et al. (2021) similarly reported that an IN-administered spike protein chimpanzee adenovirus-vectored vaccine induced a superior systemic response than the IM route [429]. Our results align with these observations and can be explained by the potent adjuvant effect of *B. subtilis* spores and their capacity to deliver the antigen efficiently to mucosal sites, mimicking natural infection. We further show that IN spore-RBD inoculation results in a higher IgG2a/IgG1 ratio, suggesting a Th1-skewed response. Several factors could explain this outcome. The IN route engages the NALT, which provides a unique dendritic cell-rich microenvironment that promotes Th1 polarization [430]. *B. subtilis* spores could further enhance this effect by acting as a potent adjuvant and carrier, mimicking natural infection and delivering pathogen-associated molecular patterns (PAMPs) that activate pattern recognition receptors (PRRs) on dendritic cells, triggering Th1-skewing pathways [431]. All in all, the particulate nature of the spore-antigen complex may enhance antigen uptake and prolong presentation at mucosal surfaces, which would allow more efficient activation of antigen-presenting cells (APCs) and differentiation of $CD4^+$ T cells toward Th1 effectors [397, 398].

IgA has been reported to govern the early SARS-CoV-2–specific antibody response in COVID-19 patients, both in serum and respiratory mucosa [432-434]. In 2024, Wagstaffe et al. highlighted that an early mucosal IgA response is critical for viral control [374]. Our findings show that IN spore-RBD inoculation induces robust systemic and mucosal immunity, with high neutralizing titers and increased avidity

of serum IgG, as well as serum and respiratory mucosal IgA. These findings position the spore-RBD vaccine formulation as a highly effective and promising method to attenuate both respiratory tract infection and transmission of SARS-CoV-2. We propose that after the IN immunization, locally activated and expanded B cell clones migrate to distant mucosal lymphoid tissues and the spleen, hence allowing humoral response in the upper and lower respiratory tract, and systemic immunity.

IgA in mucosal tissues is mostly dimeric and locally produced, attached to a secretory fragment (sIgA). Multivalency increases sIgA neutralization capacity. Accordingly, it is strongly associated with early mucosal control of SARS-CoV-2 [374]. Whereas impaired mucosal IgA response in patients with severe COVID-19 has been reported, it is expected to result from plasmatic monomeric IgA (mIgA) reaching the airways through transudation, as found in BALF from severely ill patients [435]. mIgA can trigger NETosis dysregulation, ultimately leading to severe autoinflammatory lung disease [435, 436]. In contrast, sIgA is not involved in such a deleterious process, as steric hindrance prevents its interaction with Fcα receptors on neutrophils [435, 437]. Importantly, we observed no major lung pathology based on macroscopic examination for IN spore-RBD, suggesting that the detected total IgA in respiratory secretions primarily represents sIgA in our experiments. Further research should provide more insight into the IgA response induced by our vaccine formulation and assess its safety and protective capacity upon viral challenge, in an appropriate animal model.

Analogous to circulating anti-SARS-CoV-2 antibodies, specific IgG and IgA in the respiratory mucosa are reported to diminish a few months after infection [432, 434, 438, 439]. Therefore, induction of mucosal memory B cells ensures a swift rise in local antibody levels upon re-exposure to the antigen, promoting sustained viral clearance and preventing further transmission in the long term [440-442]. Following a natural infection, RBD-specific B_{RM} were found in human lungs, emphasizing the importance of mucosal priming in the induction of these cells [443]. Our results indicate that lung tissue from mice challenged with IN spore-RBD was significantly enriched in both IgG^+ and IgA^+ memory B cells, which effectively proliferated *in vitro* upon antigen recall. We therefore consider that the IN codelivery of the immunogen with this mucosal adjuvant might confer a

protective mucosal and systemic immunity that efficiently reduces infection and transmissibility.

Antiviral immunity relies on the involvement and cooperation of T cells. In this regard, an efficient Th1 response is essential for orchestrating an effective immune defense against SARS-CoV-2, while cytotoxic T cells play a critical role in eliminating infected cells [440, 444-446]. In contrast, Th2 bias after immunization has been linked to vaccine-associated enhanced respiratory disease [446-448]. Our results demonstrate a robust T cell response following IN spore-RBD inoculation, marked by a Th1/Tc1-biased immune profile without relevant Th2/Tc2 expansion, as evidenced by elevated IFN-γ without IL-4 responses in $CD4^+$ and $CD8^+$ T cells and a relatively higher IgG2a/IgG1 ratio. We also found induction of antigen-specific $CD4^+$ and $CD8^+$ T_{RM} in the lungs after IN spore-RBD inoculation. T_{RM} are the most abundant memory T cell subset in barrier tissues, which can proliferate locally upon antigen re-encounter and be primed to provide rapid, frontline immunity, playing a crucial role in long-lasting protection [449-451]. These findings underscore the importance of mucosal vaccines that directly target the airways, such as the spore-RBD formulation used in this study, positioning them as superior to peripheral vaccination strategies, which have failed to generate lasting lung T cell mucosal immunity against SARS-CoV-2 [440, 452].

In this study, we not only developed a specific vaccine formulation for SARS-CoV-2 but also proposed an optimized platform for mucosal immunization based on human probiotic *B. subtilis* spores co-administered with any immunogen. This platform is expected to have broad applications, including booster immunization against novel SARS-CoV-2 variants in previously vaccinated or infected individuals, as well as primary immunization for unexposed individuals or against other emerging respiratory pathogens. Additionally, incorporating the RBDs of newly circulating SARS-CoV-2 variants into the formulation would allow the vaccine to evolve in parallel with the virus, and potentially curb its spread. At the same time, including distinct epitopes could enable a multivalent design capable of simultaneously targeting multiple strains or variants. Notably, *B. subtilis* spores are particularly attractive as a vaccine delivery system due to their stability, resistance to harsh environments, ease of handling, and ability to interact with immune cells [272, 304, 453-455]. Moreover, they are a valuable alternative to conventional mucosal adjuvants such as cholera toxin B subunit (CTB), heat-labile

toxin (HLT) derivatives, and synthetic adjuvants (e.g., CpG-ODNs), which often raise toxicity and safety concerns [456]. Importantly, DG101 is a food-grade *B. subtilis* derived from the natto strain and widely characterized for its human probiotic properties, further supporting its excellent safety profile [376]. In particular, they are heat-stable, eliminating cold-chain requirements and enabling easy formulation, self-application, and thus broad global distribution. Additionally, their particulate nature facilitates efficient uptake by NALT, while their natural PAMPs, including peptidoglycan and lipoteichoic acid, provide strong intrinsic adjuvant effects through TLR2 and NOD2 activation [457]. This dual role as antigen carrier and innate immune activator enhances antigen uptake, presentation, and local immune activation. Although various *B. subtilis* strains are extensively documented as safe probiotics, they have not been employed as vaccine adjuvants in humans, with most prior studies relying on ones lacking human relevance, thereby limiting translational potential [453, 458-460]. All in all, by using spores from a human probiotic strain, our findings point to a safe, economical, and effective new vaccination strategy capable of inducing both systemic and mucosal immunity.

While our findings are promising, this study has some limitations that should be acknowledged. Protective efficacy was not evaluated through viral challenge, and safety assessments were limited to macroscopic observations. As this study was designed as a proof-of-concept investigation, we focused primarily on evaluating the immunogenicity and mucosal responses elicited by the intranasal formulation. Nevertheless, we observed no overt clinical signs of illness, significant weight loss, or changes in behavior, appetite, or general appearance in immunized mice compared to controls, and no major lung pathology was noted upon macroscopic examination during organ collection. We also acknowledge that the current manuscript does not provide direct experimental evidence demonstrating the efficiency and stability of RBD adsorption onto *B. subtilis* DG101 spores. Although this statement is grounded on previously established adsorption methods found in the literature [285, 400-403] and supported by theoretical fundamentals and the strong immunogenicity observed, we recognize that a detailed characterization of the adsorption process would strengthen the mechanistic understanding of our platform. To further support translational potential, future studies should validate *in vivo* protection using appropriate challenge models and

perform comprehensive safety profiling, including detailed histopathological analyses, stringent monitoring of clinical parameters, and assessment of potential spore germination or replication in the respiratory tract. In addition, further research should explore clinical development of this mucosal vaccine strategy, including its adaptation to multivalent designs or its use in next-generation formulations targeting emerging respiratory pathogens. Nevertheless, it is important to note that both *B. subtilis* spores (particularly the human probiotic DG101 strain) and recombinant RBD protein have well-established safety profiles [461, 462], as highlighted in the Introduction and Discussion sections, supporting the theoretical safety of our formulation.

2.6 Supplementary material

Table S2.1. Reagents, fluorophores, clone numbers, product codes, and dilutions used for flow cytometry.

Reagent	Fluorophore	Clone	Product code	Dilution
Anti-mouse/human CD45R/B220	Alexa Fluor® 700	RA3-6B2	103231	1:200
Anti-mouse CD45	Alexa Fluor® 700	30-F11	103127	1:200
Biotin anti-mouse IgA	N/A	RMA-1	407003	1:200
Streptavidin	APC	N/A	405207	1:200
Anti-mouse CD103	APC	2E7	121413	1:200
Anti-mouse CD138	Brilliant Violet 421™	281-2	142507	1:100
Anti-mouse CD8a	Brilliant Violet 510™	53-6.7	100751	1:200
Anti-mouse IgD	Brilliant Violet 605™	11-26c.2a	405727	1:200
Anti-mouse CD19	Brilliant Violet 650™	6D5	115541	1:200
Anti-mouse/human CD44	Brilliant Violet 650™	IM7	103049	1:200
Anti-mouse CD69	Brilliant Violet 785™	H1.2F3	104543	1:200
Anti-mouse CD3	FITC	17A2	100203	1:500
Anti-mouse CD4	Pacific Blue™	RM4-5	100534	1:200
Anti-mouse CD38	PE	90	102707	1:200
Anti-mouse IL-4	PE	11B11	504103	1:200
Anti-mouse IFN-γ	PE/Cyanine7	XMG1.2	505825	1:200
Goat anti-mouse IgG	PE/Cyanine7	Poly4053	405315	1:200
Anti-mouse IL-17A	PE/Dazzle™ 594	TC11-18H10.1	506937	1:50
Anti-mouse CD3	PerCP/Cyanine5.5	17A2	100217	1:200

All the reagents were supplied by BioLegend.

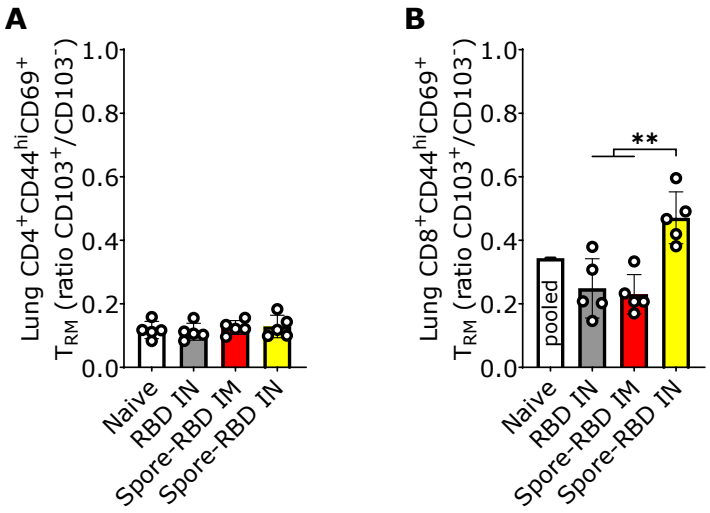

Figure S2.1. CD103$^+$/CD103$^-$ ratios of CD4$^+$ and CD8$^+$ T_{RM} after SARS-CoV-2 RBD intranasal immunization adjuvanted with *Bacillus subtilis* DG101 spores. (**A,B**) CD103$^+$/CD103$^-$ ratios of CD4$^+$ (**A**) and CD8$^+$ T_{RM} (**B**) in the lungs of naive mice, or mice immunized with RBD alone intranasally (RBD IN), or with RBD adsorbed onto *B. subtilis* DG101 spores either intramuscularly (spore-RBD IM) or intranasally (spore-RBD IN). All data are depicted as mean ± SD, except naive mice (controls) in (**B**), which are shown as the ratio of the pooled data. Each experimental group consists of 5 animals, and each dot represents an individual animal. Statistical significance was calculated by one-way analysis of variance (ANOVA); ** $p < 0.01$.

Chapter 3

Lithium salts as a treatment for COVID-19: Preclinical outcomes

Based on:

Lithium salts as a treatment for COVID-19: Preclinical outcomes

Soriano-Torres O, Noa Romero E, Gonzalez Sosa NL, Enriquez Puertas JM, Fragas Quintero A, Garcia Montero M, Martin Alfonso D, Infante Hernandez Y, Lastre M, Rodriguez-Perez L, Borrego Y, Gonzalez VE, Vega IG, Ramos Pupo R, Reyes LM, Zumeta Dube MT, Amaro Hernandez I, Garcia de la Rosa I, Minguez Suarez A, Alarcon Camejo LA, Rodriguez M, Oliva Hernandez R, Rudd CE, Perez O

Biomedicine & Pharmacotherapy. 2022 May; 149:112872.

Statement of contribution

This chapter is based on collaborative research. The experimental work was conducted in Cuban research institutions. The study was designed and led by OP, OST, and ENR. The experimental work and virological assays were performed by ENR, OST, NGS, ROH, JMEP, MGM, AFQ, YIH, DMA, MTZD, and IAH, who also contributed to data analysis and figure preparation. ML, LRP, the candidate (RRP), LMR, IGV, VEG, MRA, IGR, AMS, LAC, and YB contributed to the study design and analysis of the results. The candidate (RRP) additionally contributed to supervision, figure preparation, manuscript writing, review, and editing, and played an essential role in funding acquisition and in coordinating and ensuring the resources required for the successful execution of this study. All authors revised the manuscript and approved the final version for submission.

3. Lithium salts as a treatment for COVID-19: Preclinical outcomes

3.1 Abstract

Introduction: Identifying effective drugs for Coronavirus disease 2019 (COVID-19) is urgently needed. An efficient approach is to evaluate whether existing approved drugs have anti-SARS-CoV-2 effects. The antiviral properties of lithium salts have been studied for many years. Their anti-inflammatory and immune-potentiating effects result from the inhibition of glycogen synthase kinase-3 (GSK-3). **Aims:** To obtain preclinical evidence on the safety and therapeutic effects of lithium salts in the treatment of COVID-19. **Results:** Six different concentrations of lithium, ranging from 2 to 12 mmol/L, were evaluated. Lithium inhibited SARS-CoV-2 replication in a dose-dependent manner, with an IC_{50} of 4 mmol/L. Lithium-treated wells showed a significantly higher percentage of monolayer conservation than the viral control, particularly at concentrations above 6 mmol/L, as verified by microscopic observation, the neutral red assay, and the determination of N protein in the supernatants of treated wells. Hamsters treated with lithium showed less intense disease with fewer signs. No lithium-related mortality or overt signs of toxicity were observed during the experiment. A trend toward decreased viral load in nasopharyngeal swabs and lungs was observed in treated hamsters compared with controls. **Conclusions:** These results provide preclinical evidence of the antiviral and immunotherapeutic effects of lithium against SARS-CoV-2, supporting advancement to clinical trials in patients with COVID-19.

3.2 Introduction

SARS-CoV-2 causes a severe respiratory disease (COVID-19) characterized by significant deregulation of the immune system with over-production of pro-inflammatory cytokines (cytokine storm) [463]. It shares about 80% genetic homology with SARS-CoV, which caused the severe acute respiratory syndrome epidemic in 2003 [464] and began in the Chinese province of Guangdong [465]. Like other coronaviruses, its viral particles include genetic material of a single chain of positive-sense ribonucleic acid (RNA) and structural proteins necessary for the invasion of host cells, which include the surface or spike (S) glycoprotein,

the membrane (M) glycoprotein, the envelope (E) glycoprotein, the nucleocapsid (N) glycoprotein and the dimeric glycohemagglutinin-esterase [466]. Once inside the cells, the infective RNA encodes structural and non-structural proteins that control assembly, transcription, and viral replication [467]. The N protein supports the viral RNA and is involved in its packaging [468, 469]. The native hypophosphorylated form of this protein favors its binding to genetic material [470], forming RNA-protein condensates.

Coronaviruses require the activity of a host's kinase termed GSK-3 for their replication. This enzyme phosphorylates the N-glycoprotein [347, 471], reducing RNA-protein interactions and forming a looser conglomerate [468], which favors genome transcription, an essential step in the generation of long sub-genomic and genomic mRNAs that code for structural proteins in the cell cytosol during viral replication [471]. GSK-3 is constitutively expressed in all mammalian cells [472] and plays a crucial role in several biological processes [473]. At the immune level, inhibition of cytosolic and nuclear GSK-3 increases the transcription of TBX21 (also known as T-box expressed in T cells, Tbet), which in turn suppresses the transcription and expression of programmed cell death protein 1 (PD-1) in activated lymphocytes, particularly the T $CD8^+$ [474]. PD-1 is a cell surface receptor expressed transiently in multiple cells of the immune system, including T and B lymphocytes [475], macrophages [476], natural killer (NK) cells [477], and dendritic cells [478]. It functions as an immune checkpoint and plays an important role in the negative regulation of the immune system [479]. Blockade of PD-1 is known to increase self-renewal and proliferation of stem-like T $CD8^+$ in lymph nodes, increasing effector functions of cytolytic T lymphocytes (CTL) against infections and cancer [480, 481]. A similar inhibitory effect on the expression of another inhibitory receptor, LAG-3, has been observed [482]. GSK-3 inhibition down-regulates the inhibitory co-receptor LAG-3 on $CD4^+$ and $CD8^+$ T-cells to enhance anti-viral and anti-tumor immunity [482, 483].

Lithium was the first natural GSK-3 inhibitor described [484]. In psychiatry, lithium has been used as a specific treatment for mania since 1949 [485]. The antiviral properties of lithium have been studied since 1980 [486]. Although a detailed review of lithium's antiviral effects lies outside the scope of this work, some other potential mechanisms may be relevant besides GSK-3 inhibition, such as the regulation of autophagy, the inhibition of the phosphatidylinositol signaling

pathway [487], and the inhibition of RNA polymerases [488]. *In vitro* experiments have demonstrated that, at non-toxic concentrations in cell cultures, it is capable of inhibiting the replication of different viral types, including herpes viruses [486], coxsackievirus [489, 490], hepatitis C virus [491], and coronaviruses [488, 492, 493].

Clinical administration of lithium is typically in the form of salts (lithium carbonate) as oral tablets (in doses of 0.4–2.0 g/day), and its effective therapeutic range lies between 0.5 and 1.2 mmol/L in blood serum [494]. Besides its antiviral properties, lithium has immunomodulatory/anti-inflammatory effects [495-499]. Despite the longstanding use of lithium salts in humans, including a proof of concept in COVID-19 [500], no preclinical trials have been conducted.

The study of viral characteristics and the evaluation of drugs with antiviral properties is initially conducted in cell cultures. Vero E6 cells are African green monkey (*Cercopithecus aethiops*) kidney epithelial cells commonly used in virology studies. Research projects on SARS-CoV and SARS-CoV-2 have been carried out using these cells because of their high expression of angiotensin-converting enzyme 2 (ACE2) receptor and their ability to support a high rate of viral replication [501-503].

The availability and use of animal models for studying the pathogenesis of COVID-19 are also of great significance for preclinical evaluation of new therapeutics. Syrian hamsters (*Mesocricetus auratus*) are widely used as experimental animals and, due to the high degree of homology of their ACE2 receptor with that of humans, they have been used previously in SARS studies [504, 505], and have been defined as a biomodel for SARS-CoV-2 studies [506-509]. After intranasal inoculation of hamsters with SARS-CoV-2, moderate interstitial pneumonia occurs with a high viral load in lungs, although only a mild and rapidly resolving disease is observed [506].

Even though most studies in hamsters have been carried out using high infectious doses (10^3–10^5 $TCID_{50}$, 50% Tissue Culture Infectious Dose) [507, 509, 510], it has been reported that the mean infective dose is only 5 $TCID_{50}$ for this animal model [506]. The most common manifestations of the disease in hamsters are weight loss, ruffled fur, lethargy (reduced mobility), hunched back, and polypnea [506, 508-510].

The present work aims to obtain preclinical evidence on the safety and therapeutic effects of lithium salts in the treatment of COVID-19.

3.3 Materials and methods

3.3.1 Reagents

Minimal Essential Medium (MEM) (Gibco, Paisley, UK), gentamicin and L-glutamine (Capricorn Scientific, Ebsdorfergrund, Germany), lithium chloride monohydrate ($LiCl \cdot H_2O$), sulfuric acid (H_2SO_4), sodium carbonate (Na_2CO_3), sodium bicarbonate ($NaHCO_3$), balanced salts solution (BSS) and Tween-20 (Merck, Darmstadt, Germany), bovine serum albumin (BSA), fetal bovine serum (FBS) and horseradish peroxidase (Sigma-Aldrich, St. Louis, MO, USA), neutral red (NR) (PanReac AppliChem, Darmstadt, Germany), tetramethylbenzidine (TMB) (Sigma-Aldrich, Darmstadt, Germany), anti-SARS-CoV-2 N protein monoclonal antibody (CBSS NCoV) (Center for Genetic Engineering and Biotechnology, Sancti-Spíritus, Cuba) and lithium carbonate tablets (250 mg) (MedSol Laboratories, Havana, Cuba) were used.

3.3.2 Cell culture, virus strain, and animal model

Vero E6 cells (ATCC CRL-1586, CICDC) cryo-preserved at −80 °C were defrosted and then subcultured twice a week at 3×10^4 cells/cm^2 in MEM supplemented with 10% FBS, 2 mmol/L of 1% L-glutamine, and 7.5% sodium bicarbonate. Cells were seeded in 96-well flat-bottom plates (Nunclon Delta Surface, Roskilde, Denmark) at a density of 20×10^3 cells/well in 100 µL of supplemented MEM and grown overnight at 37 °C in a 5% CO_2 atmosphere, with 4% FBS. The SARS-CoV-2 strain (CUT-2010-2025) isolated at CICDC from a Cuban patient's nasopharyngeal swab and stored at −80 °C was used. The $TCID_{50}$ was determined by endpoint microtitration in Vero E6 cells at 10×10^3 cells/well [511, 512].

Twenty-four female Syrian hamsters from the National Center for the Production of Laboratory Animals (CENPALAB, Havana, Cuba), with an age of 4-6 weeks and a weight of 70-80 g at the beginning of the experiments, were used. The sample size calculation was based on the law of diminishing returns (resource equation method), with a degree of freedom for analysis of variance of 19 [513]. After a satisfactory clinical inspection, two hamsters were housed per polycarbonate box

(1264 C Eurostandard Type II, Tecniplast, Italy) with a surface area of 370 cm^2 at the CICDC's facility. Cages were identified by the following information: species, sex, age, project name, randomization group, number, and physical mark for identification. The hamsters enter the experiment after one week of acclimatization.

Animals received sterile pelletized feed EMO-1002 (AlyCo®, CENPALAB, Havana, Cuba) and acidified water *ad libitum*. During the experimental phase, animals were kept in a Biosafety Laboratory Level 3 (BSL-3) at CICDC under the required environmental conditions: temperature (20 ± 2 °C), relative humidity between 50% and 60%, and a 12 by 12 h light-dark cycle. All experiments with animals were carried out in conformity with Directive 2010/63/EU of the European Parliament and of the European Union Council (22 September 2010) on the protection of animals used for scientific purposes. All efforts were made to minimize animal suffering and to reduce the number of animals used. Animals were euthanized with an overdose of thiopental.

All work with viable SARS-CoV-2 was performed in BSL-3 facilities.

3.3.3 Antiviral assay on Vero E6 cells

Vero E6 monolayers were inoculated with 10^2 $TCID_{50}$ of SARS-CoV-2 strain CUT-2010-2025 in 100 µL/well of supplemented MEM and incubated for 1 h. Then, cells were washed twice with phosphate-buffered saline (PBS) solution at pH 7.3–7.5. Six different concentrations of lithium (Li^+), ranging from 2 to 12 mmol/L, were prepared from a stock solution of $LiCl{\cdot}H_2O$ dissolved in MEM with 2% FBS. A volume of 100 µL/well of each concentration was added to the Vero E6 monolayer using six replicates. Each assay plate contained cells, either inoculated or not, as viral or cellular controls, respectively.

Microplates were incubated for 96 h at 37 °C in a 5% CO_2 atmosphere. Cytopathic effects were recorded 96 h after inoculation under an inverted microscope. The antiviral efficacy of lithium was evaluated spectrophotometrically using the NR uptake assay [514] with slight modifications. Briefly, after removing the supernatant, 100 µL of 0.02% NR was added to each well. After incubating cells for 1 h at room temperature (20–25 °C) in the dark, the NR solution was removed, and cells were washed twice with 0.05% Tween-20 in PBS. A volume of 50 µL of

lysis buffer (absolute ethanol/ultrapure water/glacial acetic acid, 50:49:1, *v*/*v*/*v*) was added per well, and the plates were incubated for 15 min. Absorbance was measured using a PR621 microplate reader (Immunoassay Center, Havana, Cuba) at 520 nm [515].

Results were expressed as a percentage (%) of inhibition of lithium over SARS-CoV-2 replication. It was calculated using the following equation: *% inhibition = 100 [(As – Avc)/(Acc – Avc)]*, where *As* is the absorbance of the sample, *Avc* is the absorbance of the viral control, and *Acc* is the absorbance of the cellular control. The half-maximal inhibitory concentration (IC_{50}) is the most widely used and informative measure of a drug's efficacy, indicating the amount of drug required to inhibit a biological process by half. The lithium IC_{50} was defined as the concentration that achieved 50% inhibition of virus-induced cytopathic effects and was determined through a non-linear regression analysis of the concentration-response curve shown in **Figure 3.3**, using GraphPad Prism™ v8 [516].

After visualizing the cytopathic effect, the supernatants were collected to detect and compare the amount of viral proteins. A standardized sandwich ELISA was performed in polypropylene 96-well plates, coated with 10 µg/mL of CBSS NCoV for capture. Sensitization was performed in a humid chamber at 37 °C for 2 h, with 100 µL/well of Na_2CO_3-$NaHCO_3$ (0.05 M, pH 9.6). Plates were washed four times with BSS-Tween-20 that contains NaH_2PO_4 (0.6 g/L), NaCl (4 g/L), KCl (0.2 g/L), and $Na_2HPO_4 \cdot 12H_2O$ (1.9 g/L) at a pH of 7.2–7.4 and 0.05% of Tween-20. Plates were blocked with BSA and dried at room temperature for 24 h.

The N protein of SARS-CoV-2 was used as a positive control. The supernatant of non-infected Vero E6 was used as a negative control. BSS-Tween-20 was used as a washing solution. CBSS NCoV conjugated to horseradish peroxidase was used for detection. TMB at 1:100 was used as chromogenic substrate.

Six replicates of the samples were added to plates (100 µL/well) and incubated for 24 h at 37 °C in the dark in a humid chamber. Plates were washed three times. Peroxidase conjugate was added to the wells, followed by incubation at 37 °C for 1 h in the dark, and the plates were then washed. A revealing reaction was performed by adding 100 µL of TMB and incubating for 20 min. The reaction was stopped with 50 µL/well of 4 molar sulfuric acid. Absorbance was measured using a PR621 reader at 450 nm. The cut-off value was established as the mean of the

OD values of the negative controls plus three standard deviations (SDs). Samples with an absorbance value greater than or equal to the cut-off value were considered positive for the test.

Toxicity controls were set up in parallel on uninfected cells in every experiment.

3.3.4 Syrian hamsters and lithium carbonate administration

Animals were randomized into five groups: negative and positive controls (n = 4 each); lithium control (n = 4); and two groups of infected animals treated with lithium, one on the same day of the infection (T-0) and the other on the day before (T-1) (n = 6 each).

Lithium carbonate was administered daily, intragastrically, at a dose of 15 mg/kg body weight in NaCl 0.9% to all animals, except those in the control groups, which received only the equivalent saline solution. The determination of lithium in the serum of treated hamsters was performed using a Roche/Hitachi Cobas C system (Cobas 6000). The blood samples were allowed to clot, and the sera were separated by centrifugation at 1000 × g for 5 min and stored at −20 °C until analysis. Lithium-control animals were checked daily for any signs suggestive of toxicity. Studied signs were lethargy/inactivity, seizures, and gastrointestinal signs (diarrhea).

Hamsters were anesthetized using a ketamine/xylazine cocktail and inoculated via intranasal instillation of 10^2 $TCID_{50}$ of SARS-CoV-2 in 50 µL (25 µL in each nostril). Signs of the disease were monitored daily for all animals. The studied signs included lethargy, stooping, and polypnea/abdominal breathing. Lethargy was defined as a clear state of reduced responsiveness and spontaneous activity. Stooping was determined when the animal moved with a hunched posture or rested upright with the back hunched. To simplify the analysis of these signs, a value of 1 was assigned to each sign observed per animal per day, resulting in a maximum of 3 points per animal per day (lethargy, stooping, and polypnea/ abdominal breathing). Every animal was placed into an individual cage for 3 min. During this time, a blind observer to the study's experimental conditions scored the hamsters for the presence (=1) or absence (=0) of the evaluated sign (**Figure 3.5**). All data were collected by observers blinded to the protocol.

Two animals of each group were euthanized on the fifth day post-infection. Nasal swabs followed by Reverse Transcription quantitative Polymerase Chain Reaction (RT-qPCR) and culture on Vero E6 cells on days 2, 4, 5, and 7 were performed. The presence of the virus in the nasopharynx and lungs was determined. A histopathological study of the lung tissue was conducted. The left lung was fixed in 10% formalin, then embedded in paraffin. Tissue sections (3 µm) were analyzed after staining with hematoxylin and eosin (H:E) and scored blindly for lung damage by an expert pathologist. To facilitate analysis, a score of 0-4 was assigned for lung injury.

3.3.5 Statistical analyses

Statistical analysis was performed using GraphPad Prism™ v8.0 software. Six replicates of all cell experiments were made, and results were reported as the mean ± SEM. A Student t-test was used to analyze data sets with two groups, and a one-way ANOVA (post hoc: Tukey) for those with more than two groups. Statistical significance levels were considered as * $p < 0.05$, ** $p < 0.01$, or *** $p < 0.001$.

3.4 Results

3.4.1 Lithium treatment directly inhibits SARS-CoV-2 replication on Vero E6 cells

Initially, to examine the effect of lithium salts on SARS-CoV-2, Vero E6 cells were cultured as monolayers in the presence or absence of lithium chloride monohydrate. Cells treated with lithium showed significantly less cytopathic effect and greater cellular viability than viral controls, as determined by inverted microscopy (**Figure 3.1**) and the Neutral Red (NR) uptake assay (**Figure 3.2**), respectively. The maximal cytopathic effect was observed in the viral control wells at 96 h after inoculation. The cytopathic effect was characterized by destruction of the cell monolayer, with blank spaces, multinucleated giant cells (syncytia), and cell rounding. Lithium-treated wells showed a significantly higher percentage of monolayer conservation than the viral control, particularly at concentrations above 6 mmol/L (**Figure 3.1**).

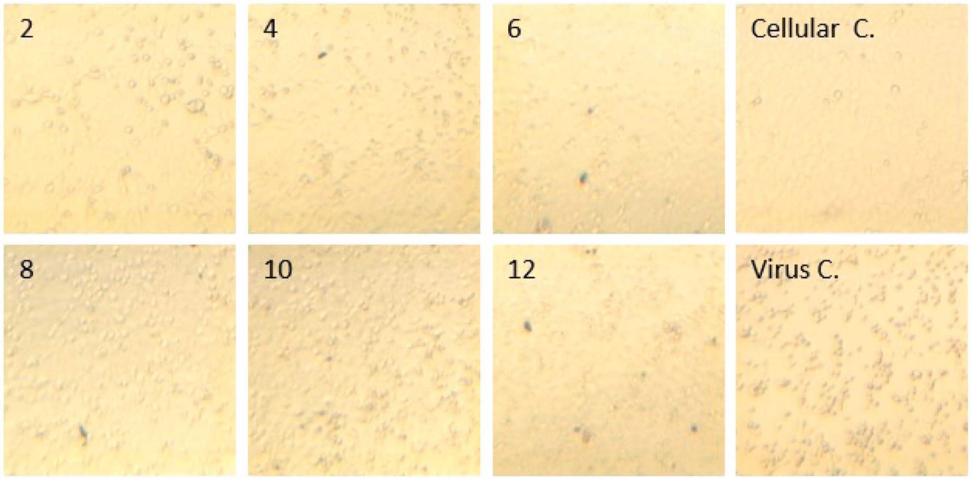

Figure 3.1. Cytopathic effect of SARS-CoV-2 on Vero E6 monolayer treated with different concentrations of lithium (mmol/L). Inverted microscope (100x). Legend: Numbers in the upper left corner of each photo indicate the lithium concentration in mmol/L; Cellular C. is the Vero E6 monolayer cultured under normal conditions; Virus C. is the Vero E6 monolayer infected with 10^2 $TCID_{50}$ of SARS-CoV-2.

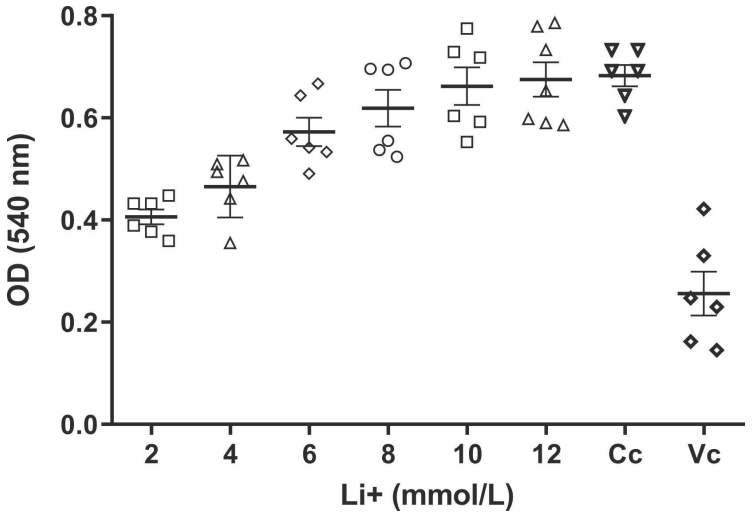

Figure 3.2. Neutral Red (NR) uptake assay in Vero E6 cells infected with SARS-CoV-2, treated with different concentrations of lithium (mmol/L). Legend: NR absorption expressed as optical density (OD) correlates with cellular viability. Infected-treated wells at increasing lithium concentrations are shown. Cc represents the cellular control; Vc represents the viral control (infected-untreated). Absorbance was measured using a PR621 reader at 540 nm. Error bars represent the standard error of the mean (SEM).

Lithium inhibited the replication of SARS-CoV-2 in a dose-dependent manner with an IC_{50} value of 4 mmol/L (**Figure 3.3**). Viability of non-infected Vero E6 cells in the presence of lithium is shown.

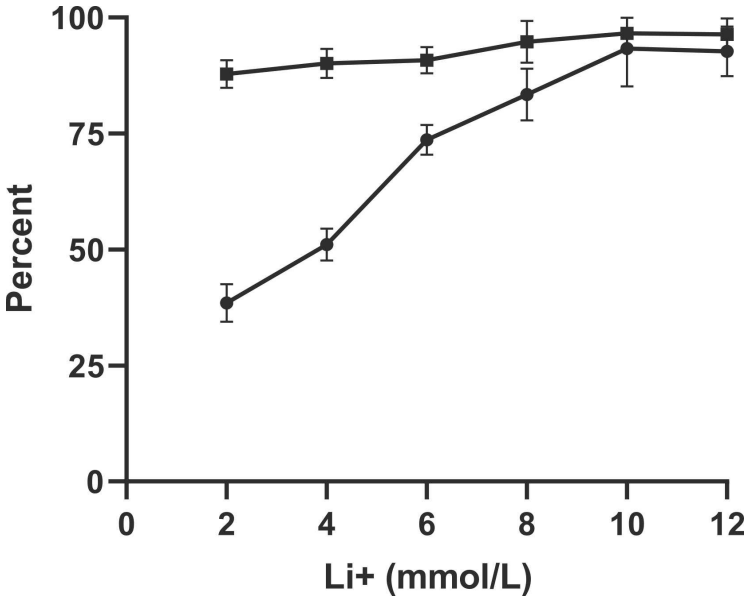

Figure 3.3. Antiviral activity of lithium against SARS-CoV-2 in Vero E6 cells and viability of lithium-treated cells. Legend: Percent of inhibition of SARS-CoV-2 replication in Vero E6 cells, under increasing concentrations of lithium, is represented with circles; black squares represent the viability of lithium-treated cells. Absorbance was measured using a PR621 reader at 540 nm. Error bars represent the SEM.

To further confirm the efficacy of lithium in inhibiting SARS-CoV-2 replication in Vero E6 cells, an ELISA was performed to detect the viral N protein in harvested supernatant from a subset of wells, and not all lithium concentrations were evaluated. The determination of N protein in treated wells matched that of the uninfected cellular control, observing a significant downgrading ($p < 0.001$). **Figure 3.4** shows the mean OD in the supernatant of treated cells for the concentrations evaluated. This semi-quantitative method enabled us to compare the concentrations of the N protein of SARS-CoV-2 in supernatants from treated and untreated infected cells. Overall, the direct anti-SARS-CoV-2 effect of lithium, as evidenced by cytopathic effects, cell viability, and the absence of viral replication, was demonstrated.

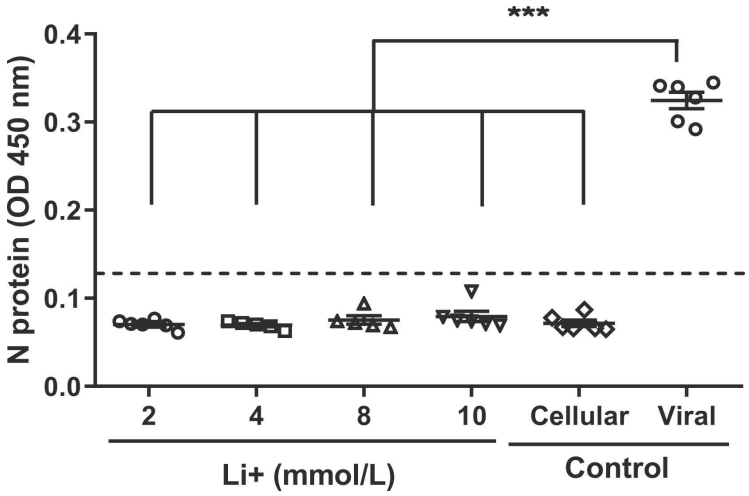

Figure 3.4. Concentration of N protein of SARS-CoV-2 in the supernatant of culture Vero E6 treated with lithium. Legend: A standardized sandwich ELISA was performed to determine the N protein of SARS-CoV-2 in the harvested supernatant of treated wells. Absorbance was measured using a PR621 reader at 450 nm. The cut-off value was set at 0.129. *** $p < 0.001$.

3.4.2 Lithium treatment affects SARS-CoV-2 infection, decreasing the appearance and intensity of signs of COVID-19 in Syrian hamsters

Clinical signs of COVID-19 were markedly reduced in both groups of Syrian hamsters treated with lithium. There were no significant differences between these groups, and the signs of both were presented together in **Figure 3.5**. The absence of signs prevailed in four animals, while another four presented signs for only one day, one animal for two days, and none had polypnea. Meanwhile, all animals in the viral control group exhibited lethargy and stooping between days 3 and 5 post-infection, and 2 developed polypnea on day 5 (**Table 3.1**). Three animals died after anesthesia on the first day (two in T-1 and one in T-0) and were excluded from statistical analysis.

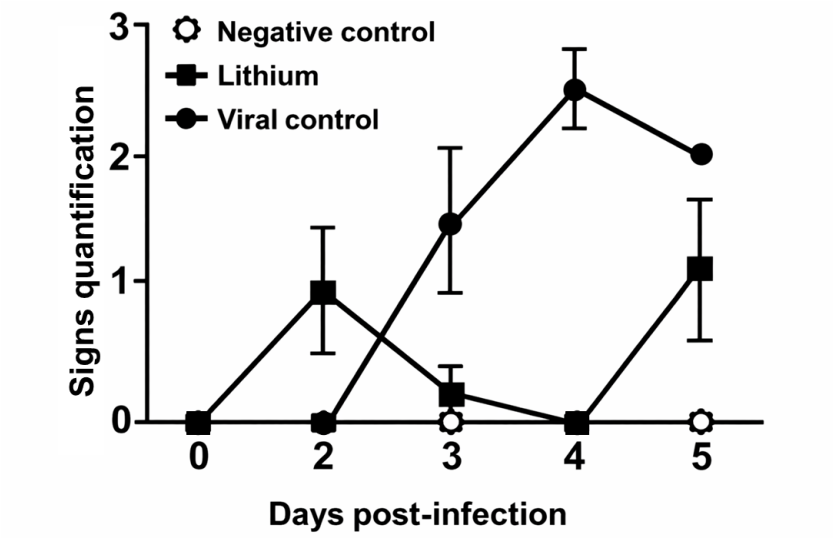

Figure 3.5. Assessment of COVID-19 signs in SARS-CoV-2-infected hamsters. Legend: Mean and error of cumulative signs for each group. Black squares represent infected hamsters treated with lithium (T-1 and T-0 groups were combined); black circles represent infected untreated hamsters. Error bars represent the SEM.

Group	No	Signs (days)												Histol. 5 PI
		2			3			4			5			
		L	S	P	L	S	P	L	S	P	L	S	P	Lungs
T-1	9	0	0	0	0	0	0	0	0	0	2	2	0	3
	11	2	2	0	0	0	0	0	0	0	2	2	0	1
	12	2	2	0	0	0	0	0	0	0	0	0	0	Nd
	13	0	0	0	0	0	0	0	0	0	0	0	0	Nd
T-0	15	0	0	0	0	0	0	0	0	0	0	0	0	1
	16	0	0	0	0	0	0	0	0	0	0	0	0	1
	18	0	0	0	0	0	0	0	0	0	0	0	0	Nd
	19	0	0	0	0	0	0	0	0	0	2	2	0	Nd
	20	0	0	0	0	0	0	0	0	0	2	2	0	Nd
C+	21	0	0	0	2	2	0	4	4	4	2	2	0	3.5
	22	0	0	0	2	2	0	2	2	0	2	2	0	2.5
	23	0	0	0	0	0	0	2	2	0	2	2	0	Nd
	24	0	0	0	2	2	0	4	4	4	2	2	0	Nd

0 1 2 3 4

Table 3.1. COVID-19 behavior in Syrian hamsters treated or not with lithium carbonate. Legend: C+ represents the positive control (infected-untreated); T-0 represents infected-treated with lithium starting on the same day of the infection; T-1 represents infected-treated with lithium starting on the day before the infection. The arrow represents the gradation of sign intensity, from absence to maximum intensity. L, lethargy; S, stooping; P, polypnea; PI, days post-infection; Nd, not done.

No signs of disease were observed in the animals of the negative control group (**Figure 3.5**). No lithium-related mortality or overt signs of toxicity were observed during the experiment. Weight loss in response to the referred infective dose was not observed (data not shown).

In the histopathological evaluation of the lungs five days after infection, large leukocyte condensates were observed, accompanied by a loss of the organ's normal histology in the infected-untreated controls, with a high percentage of lung involvement. Animals treated with lithium were characterized by small inflammatory condensates and peribronchiolar infiltrates (**Figure 3.6**), which, based on clinical manifestations, did not significantly impact the organism's dynamics. A large inflammatory condensate was observed only in one treated animal (**Table 3.1**).

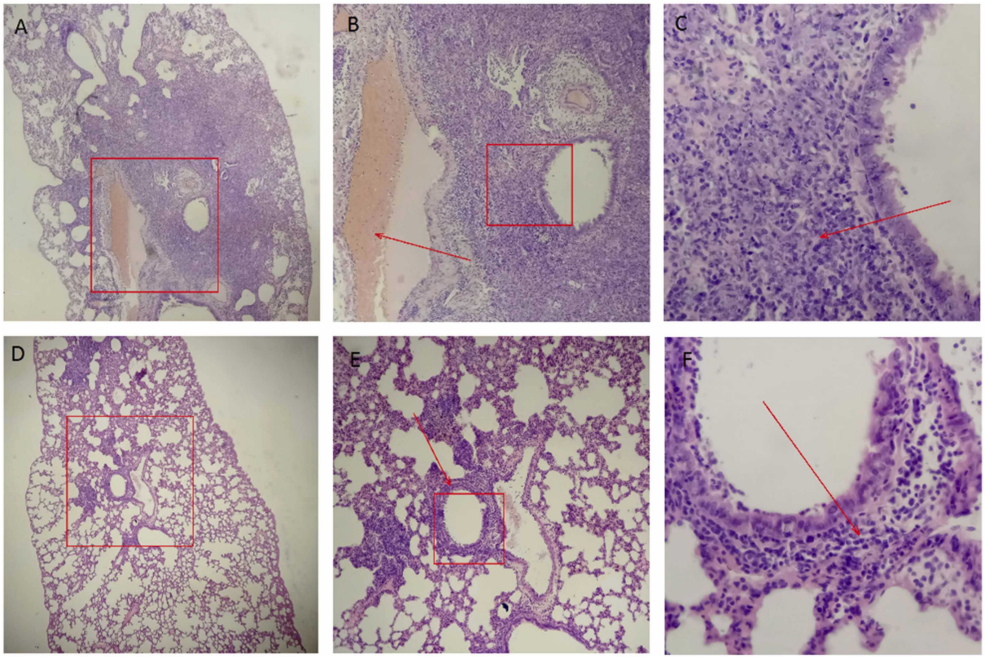

Figure 3.6. Histopathologic study of COVID-19-infected Syrian hamsters' lung tissue. Legend: Tissue section (3 µm) staining with hematoxylin and eosin A-C. Infected-untreated hamster (40x-400x): large leukocyte condensates, high percentage of lung injury; D-F: infected-treated with lithium (40x-400x), smaller inflammatory condensates and peribronchiolar infiltrates.

Samples obtained by nasopharyngeal swab, nasopharyngeal lavage, or lung maceration after euthanasia were seeded into Vero E6 cell cultures to confirm the presence of the infection. RT-qPCR was also performed to compare viral loads across animals. Between days 2 and 4 post-infection, there was a trend towards a lower viral load (higher Ct value, including three with a value higher than 35, considering negative at day 4) in hamsters treated with lithium over viral controls. This was also observed in the analysis of the lungs of euthanized hamsters on the fifth day post-infection. However, an inconclusive dispersion was observed in terms of viral load for swabbing and nasopharyngeal lavage samples on that same day post-infection (**Figure 3.7**). In our study, the intensity of clinical signs of COVID-19 in Syrian hamsters did not directly correlate with the viral load detected in each animal. At 11 days, all animals became negative by RT-qPCR (data not shown). Overall, the effects of lithium on SARS-CoV-2 infection in hamsters, particularly at the levels of signs and lung histology (regarding signs and lung injury), were demonstrated.

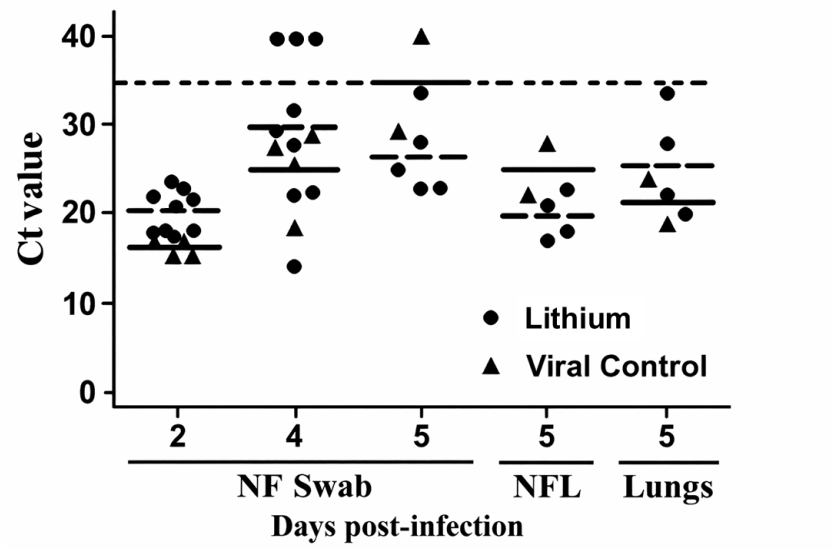

Figure 3.7. RT-qPCR for SARS-CoV-2 in infected Syrian hamsters. Legend: NF, nasopharyngeal; NFL, NF lavage. Horizontal lines represent the mean of each group (continuous for viral control; discontinuous for lithium-treated). The cut-off value of Ct was established at 35.

3.5 Discussion

SARS-CoV-2 causes a severe respiratory disease (COVID-19) that remains a global crisis [463]. Any new therapeutic approaches will be of importance and potentially could save lives. In this paper, we provide evidence that lithium salts have ablative effects on cell infection *in vitro* and in a Syrian hamster model of infection. We found that lithium inhibited SARS-CoV-2 replication in Vero E6 cells in a concentration-dependent manner. The Vero E6 monolayer was conserved as verified by microscopic observation and an NR uptake assay. Cell viability is directly proportional to the NR absorption. **Figure 3.2** clearly shows a higher NR uptake (expressed as OD) in lithium-treated wells compared to the viral control (infected-untreated). This is consistent with an important antiviral effect of lithium, as shown in **Figure 3.3**. Further, using an ELISA, we showed that lithium effectively reduced viral titers by comparing the OD of supernatants from treated wells with those from viral control cells ($p < 0.001$).

Previous studies have shown that lithium salts can reduce coronavirus infection when used at concentrations ranging from 5 to 25 mmol/L [488, 492, 517, 518]. The tested concentrations in our study correlate with the antiviral evaluation led by Harrison et al. on the avian coronavirus infectious bronchitis virus, a study that demonstrated that 5 mmol/L of LiCl causes a 50% reduction in virus titers [488]. Liu et al. [347] showed that GSK-3 inhibitors, including lithium, inhibit SARS-CoV-2 N protein phosphorylation, an essential step in viral replication. LiCl inhibited N phosphorylation with an IC_{50} of ~10 mM in 293 T cells, above the concentration needed to inhibit viral replication in Vero E6 cells in our study. Liu et al. also demonstrated that low doses of the highly selective GSK-3 inhibitor CHIR99021 reduced viral titers over 15-fold in the supernatant from SARS-CoV-2–infected human lung epithelium-derived cell line Calu-3.

Our findings are consistent with and supported by the recent *in vitro* studies of Shapira et al. [345], who tested three active compounds with GSK-3β inhibitory effects and demonstrated their ability to reduce SARS-CoV-2 infection in various cell lines, with a significant 2-log reduction 48 h after infection and treatment.

In vitro, non-toxic concentrations of lithium chloride have been reported to range from 15 to 50 mmol/L [492, 517, 518]. Our study evaluated Li^+ concentrations up

to 12 mmol/L. Although we did not perform a full toxicity assay, we assessed the non-toxicity of the used concentrations in parallel.

As coronaviruses require host GSK-3 activity for their replication [347, 480], their inhibition represents a direct antiviral mechanism of lithium. Additionally, lithium can potentiate CTL activity by inhibiting PD-1 and LAG3, thereby favoring indirect antiviral activity. Although it is difficult to translate preclinical results into actual clinical treatment in patients, lithium has advantages over other antiviral drugs. In addition to its antiviral activity, lithium has anti-inflammatory effects by decreasing the production/expression of inflammatory-associated mediators [497] such as prostaglandin E2, cyclooxygenase-2 [519], and various pro-inflammatory cytokines, including interleukin (IL) -1, IL-6 [499, 520], and tumor necrosis factor-alpha (TNF-α) [497].

Based on these results from cellular cultures, we decided to assess the therapeutic effect and safety of lithium in Syrian hamsters infected with SARS-CoV-2. A 10^2 $TCID_{50}$ infective dose was used, which was at least 10 times lower than reported in similar studies, but still higher than the mean necessary for the induction of this animal model [506, 507, 509, 510]. This allowed us to observe the development of moderate-to-severe disease in these animals. As the most frequent signs of COVID-19 described in Syrian hamsters are loss of weight, stooping, lethargy, and polypnea [506, 508-510], it was decided to evaluate them on a daily basis. Surprisingly, no significant weight loss was observed in infected animals. This may be due to the lower infective dose used compared to other studies [506, 508-510]. We hypothesized that the higher the infective dose, the greater the weight loss. We found that hamsters treated with lithium showed a less intense disease with fewer signs. Some animals treated with lithium did not show any signs of the disease. The presence of signs in the viral control group (infected, untreated) was significantly higher than in those treated with lithium. This is more evident in **Figure 3.5**, since although the n in the groups treated with lithium was significantly higher ($n = 9$) than in the untreated group ($n = 4$), the average number of signs of hamsters per day was higher in the group of the infected-untreated animals. Even two animals in the viral control group showed polypnea, a sign of the disease's greater severity.

As a worsening peak has been described on the fifth day post-infection in this animal model, followed by rapid improvement [509], it was therefore decided to euthanize two animals in each group to compare the viral load and histological lesions in the lungs.

We evaluated *in vivo* the antiviral and immunotherapeutic potential of lithium. Despite the fact that between days 2 and 4 post-infection, a trend towards a decrease in viral load was observed in treated hamsters compared to controls, on the fifth day post-infection, an inconclusive dispersion was noted in the Ct values of the swab and nasopharyngeal lavage samples. However, viral load in lungs on the fifth day post-infection was also discreetly inferior in treated animals. Early antiviral effects of lithium, suppressing initial viral replication, may limit the antigen exposure required for robust adaptive immune priming, thereby delaying immune control and leading to late viral load resurgence.

Finally, the histopathologic study of the lungs showed less tissue damage in those treated animals compared to the untreated ones, which is consistent with the decreased amount of signs of the disease found in the study group. Given that the freedom of analysis in this case [513] was below 10, these findings should be interpreted carefully, and further investigations with a larger sample size are required.

The assessment of the immunotherapeutic effect of lithium salts in animal models enables us not only to evaluate their antiviral capacity but also to assess other properties, such as their immune-potentiating and anti-inflammatory effects.

Due to the rapid evolution of the disease in Syrian hamsters and the high replication rate of SARS-CoV-2 in this animal model [508, 509], we decided to explore whether there were differences between hamsters treated 24 h before infection in comparison to those that started treatment the same day of infection. There were no significant differences between the groups treated with lithium. This may be due to the rapid intestinal absorption of lithium [494] that does not require starting treatment from the day before in this animal model.

Unlike other drugs that could not replicate *in vivo* with Syrian hamsters, the *in vitro* antiviral results obtained in cell cultures [521, 522], lithium showed, although slightly, a tendency to decrease the viral load in nasopharyngeal swabs and lungs. Although it must be noted that the infective dose used in those studies

was higher than ours, it has been demonstrated that a low-dose challenge inoculum induces a comparable viral load and disease pathology compared with higher viral dose challenges [523].

A dose of 15 mg/kg of body weight of lithium carbonate per day was chosen for treatment. This dosing regimen is equivalent to the usual daily dose in humans, approximately 1000 mg/day [494], and it yielded a serum lithium level of 0.91 ± 0.27 mmol/L, within the therapeutic range for humans. Hence, the data obtained from the current study could be extrapolated to clinical scenarios. For estimating the toxicity of a drug, the median lethal dose (LD_{50}) is a commonly used pharmacological parameter, determined in laboratory animals, preferably in mice and rats. For lithium carbonate, the LD_{50} in rats is ~700 mg/kg after oral administration [524]. In our search, we did not find the LD_{50} for Syrian hamsters, and its determination is beyond the scope of this work. The lithium regimen used is markedly below the LD_{50} for lithium application in rats, and also below the usual doses in pre-clinical toxicology studies [525, 526].

Considering the preclinical results presented here, it appears that the immunomodulatory/anti-inflammatory properties of lithium play a significant role in improving outcomes for subjects affected by COVID-19. This gains relevance as the inflammatory host response drives much of the pathology of SARS-CoV-2 infection. A reduced incidence of COVID-19 in patients taking lithium compared to the general population was demonstrated after the analysis of clinical data from four major health systems [347, 500]. Unfortunately, severity and mortality data were not obtained and compared between the two groups of infected patients, since modulation of the inflammatory response by lithium may also contribute to reducing the risk of COVID-19 severity and mortality [527].

Spuch et al. [500] treated six patients with severe COVID-19 with lithium carbonate. They found that lithium carbonate decreased plasma C-reactive protein levels and increased lymphocyte counts, thereby reducing the neutrophil-lymphocyte ratio. All patients treated with lithium carbonate showed improvement in their clinical status, and no side effects related to lithium carbonate treatment were reported. These preliminary data suggest that lithium treatment reduces the inflammatory state in patients with COVID-19, improving both inflammatory activity and the immune response. Because of the limitations of this study, such

as the small number of cases and the lack of randomization, these findings should be interpreted with caution and warrant further investigation in a larger cohort.

Four cases of lithium toxicity in COVID-19 patients under long-term lithium treatment have been reported [528, 529]. A recent study established a 1% incidence of lithium intoxication in chronically treated patients [530]. They assessed the incidence, clinical course, and renal function based on a retrospective cohort study, and concluded that lithium intoxication seems rare and can be safely managed in most cases. Also, lithium intoxication is associated with prolonged use, and short-term treatment could minimize the events associated with toxicity [531].

Given the current global status resulting from the SARS-CoV-2 pandemic, we consider the findings from this study support conducting clinical trials of lithium treatment for patients with COVID-19.

Our study has the limitation of not having determined pro-inflammatory markers (i.e., C-reactive protein and IL-6) in Syrian hamsters treated or not with lithium.

All in all, lithium directly inhibits the replication of SARS-CoV-2 in Vero E6 cells in a concentration-dependent manner. It was effective in treating Syrian hamsters with COVID-19, as evidenced by decreased viral load and reduced signs of the disease and/or its severity. These results reaffirm the possible therapeutic effect of lithium salts and support further clinical trials in patients with COVID-19.

Chapter 4

General discussion, conclusion, and future perspective

4. General discussion, conclusion, and future perspective

The unprecedented scale and speed of SARS-CoV-2 transmission, combined with its ability to cause both asymptomatic and severe disease, have posed immense challenges for disease control and prevention. COVID-19 has not only tested global healthcare capacity but also accelerated scientific innovation, leading to rapid advances in diagnostics, therapeutics, and vaccine development [5-8].

As of August 2025, over 780 million confirmed cases of COVID-19 have been reported worldwide, and more than seven million confirmed deaths have been attributed directly to the virus. In many countries, there have also been indirect deaths or excess mortality beyond those officially counted. COVID-19 is now being managed much more like a long-term endemic respiratory disease with ongoing surveillance, vaccination, treatment, and public health measures adapted to local risk [27-29].

Respiratory pathogens, such as SARS-CoV-2, enter the body through the upper airway, where systemic vaccines provide limited protection. Unlike live attenuated intranasal vaccines, which are effective but unsuitable for immunocompromised individuals and difficult to adapt rapidly to virus evolution, non-replicating vaccines require an adjuvant to overcome the airway's tolerogenic environment, rapid mucociliary clearance, and weak innate immune activation. Thereby, effective mucosal adjuvants would promote local, specific response with IgA secretion and tissue-resident memory T cells (T_{RM}), providing sterilizing immunity that would reduce both infection and transmission. Because no intranasal adjuvant is yet licensed for human use (and in total, only one mucosal adjuvant has been, rCTB in the oral Dukoral vaccine), discovering safe activators of mucosal immune pathways remains a key priority for enabling next-generation, needle-free mucosal vaccines. Consequently, developing safe and potent mucosal adjuvants for intranasal vaccines is crucial in immunoepidemiology. In this context, *B. subtilis* spores stand out as a promising candidate [219, 231, 232, 247, 263-266].

On the other hand, despite significant advances in anti-COVID-19 therapeutics, substantial unmet medical needs persist, as some currently available antivirals have limitations related to viral resistance, drug–drug interactions, narrow treatment windows, or reduced efficacy against emerging variants [321, 322].

Consequently, in parallel to vaccine development, novel approaches must be continually explored to ensure effective morbidity control and improve current therapeutics.

SARS-CoV-2 utilizes glycogen synthase kinase-3 (GSK-3) to phosphorylate its nucleocapsid (N) glycoprotein at conserved serine/arginine–rich sites, which is crucial for the proper function of N in viral RNA binding, replication, and assembly. Accordingly, GSK-3 inhibition demonstrated antiviral effects *in vitro* by blocking SARS-CoV-2 infection in human lung epithelial cells [345-347]. GSK-3 inhibition also modulates host immunity, offering a host-directed booster against viruses. In immature DCs, the GSK-3β isoform, which predominates in immune cells, is continuously active, and its inhibition has been shown to enhance DC maturation and function, including DC-mediated cross-priming of $CD8^+$ T cells and cytokine production. Additionally, GSK-3β inhibition promotes the maturation of NK cells, thereby enhancing the antiviral cellular immune response [348, 349]. Consequently, the capacity of lithium salts to inhibit GSK-3 makes them potential candidates in anti-COVID-19 therapeutics, specifically lithium carbonate and lithium citrate, which have been approved prescription drugs for humans since 1970 [342, 343].

This thesis aimed to evaluate the immunogenicity of an anti-SARS-CoV-2 intranasal vaccine adjuvanted with human probiotic *Bacillus subtilis* spores in mice. Additionally, preclinical evidence on the safety and therapeutic effects of lithium salts against SARS-CoV-2 was obtained both *in vitro* and *in vivo* in Syrian hamsters infected with COVID-19. In this chapter, the main findings of the thesis are summarized and discussed.

4.1 Human probiotic *Bacillus subtilis* spores serve as an effective mucosal adjuvant and delivery system in an anti-SARS-CoV-2 vaccine, inducing potent systemic and mucosal immunity.

In **Chapter 2**, we presented a preclinical evaluation of a novel IN mucosal vaccine formulation for COVID-19, composed of the RBD and human probiotic *B. subtilis* spores as an adjuvant and intranasal delivery system. Spore-RBD inoculation

elicited robust mucosal and parenteral immunity in a three-dose IN schedule, characterized by the expansion of antigen-specific $CD8^+$ T_{RM}, $CD4^+$ T_{RM}, and B_{RM}, and by the secretion of antigen-specific IgG and IgA. It also resulted in long-lasting immunity, with elevated specific IgG titers persisting after 180 days, indicating the presence of sustained, though waning, antibody responses. In contrast, IM immunization with this formulation and the gold-standard alum-RBD elicited a modest systemic response but failed to confer the desired mucosal immunity. These results indicate that human probiotic *B. subtilis* spores function as a potent mucosal vaccine adjuvant and delivery system, and their co-administration with the SARS-CoV-2 RBD may provide effective protection against COVID-19.

Both systemic and mucosal humoral immune responses are crucial against SARS-CoV-2. Concerning the former, serum-neutralizing antibodies targeting the RBD or the entire spike protein are key correlates of protection against symptomatic and severe COVID-19 [419-422], and are often used to assess vaccine efficacy [423-425]. However, systemic immunity alone cannot control infection at mucosal entry points, where SARS-CoV-2 invades through the nasal and oral passages, leading to respiratory tract infection and transmission. Current parenteral COVID-19 vaccines generate strong systemic but weak or no mucosal immunity, limiting their effectiveness in preventing breakthrough infections and spread [362, 363, 426]. Therefore, in **Chapter 2,** BALB/c mice were immunized intranasally (IN) or intramuscularly (IM) with three doses of RBD (80 or 20 µg, respectively) adsorbed onto 1 x 10^9 *B. subtilis* DG101 spores (spore-RBD)

We demonstrated that IN spore-RBD elicits a stronger systemic antibody response compared to IM. While some studies have reported higher systemic antibody responses with IM immunization, these differences likely depend on factors such as adjuvant type, antigen delivery efficiency, and threshold concentration requirements for each route. For example, Yahyaei et al. (2025) found that twice the antigen dose was needed for IN delivery to match the systemic IgG levels achieved by IM administration of an mRNA-based influenza A vaccine [427], whereas Anthi et al. (2025) showed that IN vaccination with an RBD-based subunit vaccine produced higher systemic IgG than IM [428]. Hassan et al. (2021) similarly reported that an IN-administered spike protein chimpanzee adenovirus-vectored vaccine induced a superior systemic response than the IM route [429].

Our results align with these observations and can be explained by the potent adjuvant effect of *B. subtilis* spores and their capacity to deliver the antigen efficiently to mucosal sites, mimicking natural infection.

We further showed in **Chapter 2** that IN spore-RBD inoculation results in a higher IgG2a/IgG1 ratio, suggesting a Th1-skewed response. Several factors could explain this outcome. The IN route engages the NALT, which provides a unique dendritic cell-rich microenvironment that promotes Th1 polarization [430]. *B. subtilis* spores could further enhance this effect by acting as a potent adjuvant and carrier, mimicking natural infection and delivering pathogen-associated molecular patterns (PAMPs) that activate pattern recognition receptors (PRRs) on dendritic cells, triggering Th1-skewing pathways [431]. All in all, the particulate nature of the spore-antigen complex may enhance antigen uptake and prolong presentation at mucosal surfaces, thereby allowing more efficient activation of antigen-presenting cells (APCs) and differentiation of $CD4^+$ T cells toward Th1 effectors [397, 398].

IgA has been reported to govern the early SARS-CoV-2–specific antibody response in COVID-19 patients, both in serum and respiratory mucosa [432-434]. In 2024, Wagstaffe et al. highlighted that an early mucosal IgA response is critical for viral control [374]. Our findings showed in **Chapter 2** that IN spore-RBD inoculation induces robust systemic and mucosal immunity, with high neutralizing titers and increased avidity of serum IgG, as well as serum and respiratory mucosal IgA. These findings position the spore-RBD vaccine formulation as a highly effective and promising approach to attenuate both respiratory tract infection and SARS-CoV-2 transmission. We propose that after IN immunization, locally activated and expanded B cell clones migrate to distant mucosal lymphoid tissues and the spleen, thereby enabling humoral response in the upper and lower respiratory tracts and systemic immunity.

IgA in mucosal tissues is mostly dimeric and locally produced, attached to a secretory fragment (sIgA). Multivalency increases sIgA neutralization capacity. Accordingly, it is strongly associated with early mucosal control of SARS-CoV-2 [374]. Whereas impaired mucosal IgA response in patients with severe COVID-19 has been reported, it is expected to result from plasmatic monomeric IgA (mIgA) reaching the airways through transudation, as found in BALF from severely ill

patients. mIgA can trigger NETosis dysregulation, ultimately leading to severe autoinflammatory lung disease [435, 436]. In contrast, sIgA is not involved in such a deleterious process, as steric hindrance prevents its interaction with Fcα receptors on neutrophils [435, 437]. Importantly, we observed no major lung pathology based on macroscopic examination for IN spore-RBD, suggesting that the detected total IgA in respiratory secretions primarily represents sIgA in our experiments. Further research should provide more insight into the IgA response induced by our vaccine formulation and assess its safety and protective capacity upon viral challenge, in an appropriate animal model.

Analogous to circulating anti-SARS-CoV-2 antibodies, specific IgG and IgA in the respiratory mucosa are reported to decline a few months after infection [432, 434, 438, 439]. Therefore, an induction of mucosal memory B cells ensures a swift rise in local antibody levels upon re-exposure to the antigen, promoting sustained viral clearance and preventing further transmission in the long term [440-442]. Following a natural infection, RBD-specific B_{RM} were found in human lungs, emphasizing the importance of mucosal priming in the induction of these cells [443]. Our results indicate that lung tissue from mice challenged with IN spore-RBD was significantly enriched in both IgG^+ and IgA^+ memory B cells, which effectively proliferated *in vitro* upon antigen recall. We therefore consider that the IN codelivery of the immunogen with this mucosal adjuvant might confer protective mucosal and systemic immunity, efficiently reducing infection and transmissibility.

Antiviral immunity relies on the involvement and cooperation of T cells. In this regard, an efficient Th1 response is essential for orchestrating an effective immune defense against SARS-CoV-2, while cytotoxic T cells play a critical role in eliminating infected cells [440, 444-446]. In contrast, Th2 bias after immunization has been linked to vaccine-associated enhanced respiratory disease [446-448]. In **Chapter 2**, our results demonstrated a robust T cell response following IN spore-RBD inoculation, characterized by a Th1/Tc1-biased immune profile without relevant Th2/Tc2 expansion, as evidenced by elevated IFN-γ and no IL-4 responses in $CD4^+$ and $CD8^+$ T cells, and a relatively higher IgG2a/IgG1 ratio. We also found induction of antigen-specific $CD4^+$ and $CD8^+$ T_{RM} in the lungs after IN spore-RBD inoculation. T_{RM} are the most abundant memory T cell subset in barrier tissues, which can proliferate locally upon antigen re-encounter and be primed to

provide rapid, frontline immunity, playing a crucial role in long-lasting protection [449-451]. These findings underscore the importance of mucosal vaccines that directly target the airways, such as the spore-RBD formulation used in this study, positioning them as superior to peripheral vaccination strategies, which have failed to generate lasting lung T cell mucosal immunity against SARS-CoV-2 [440, 452].

As a result of this thesis, we not only developed a specific anti-SARS-CoV-2 vaccine formulation but also proposed an optimized platform for mucosal immunization based on human probiotic *B. subtilis* spores co-administered with any immunogen. This platform is expected to have broad applications, including booster immunization against novel SARS-CoV-2 variants in previously vaccinated or infected individuals, as well as primary immunization for unexposed individuals or against other emerging respiratory pathogens. Additionally, incorporating the RBDs of newly circulating SARS-CoV-2 variants into the formulation would allow the vaccine to evolve in parallel with the virus, and potentially curb its spread. At the same time, including distinct epitopes could enable a multivalent design that simultaneously targets multiple strains or variants. Notably, *B. subtilis* spores are particularly relevant as a vaccine delivery system due to their stability, resistance to harsh environments, ease of handling, and ability to interact with immune cells [272, 304, 453-455].

While our findings are promising, this investigation has some limitations that should be acknowledged. Protective efficacy was not evaluated through viral challenge, and safety assessments were limited to macroscopic observations. **Chapter 2** was a proof-of-concept investigation that primarily evaluated the immunogenicity and mucosal responses elicited by the intranasal formulation. Nevertheless, we observed no overt clinical signs of illness, significant weight loss, or changes in behavior, appetite, or general appearance in immunized mice compared to controls, and no major lung pathology was noted upon macroscopic examination during organ collection. We also acknowledge that the current manuscript does not provide direct experimental evidence demonstrating the efficiency and stability of RBD adsorption onto *B. subtilis* DG101 spores. Although this statement is grounded on previously established adsorption methods found in the literature [285, 400-403] and supported by theoretical fundamentals and the strong immunogenicity observed, we recognize that a detailed

characterization of the adsorption process would strengthen the mechanistic understanding of our platform. To further support translational potential, future studies should validate *in vivo* protection using appropriate challenge models that faithfully recapitulate key aspects of human infection, transmission, and immunopathology, such as the K18-hACE2 mouse, Syrian hamster, ferret, and non-human primates [532-534], and perform comprehensive safety profiling, including detailed histopathological analyses, stringent monitoring of clinical parameters, and assessment of potential spore germination or replication in the respiratory tract. In addition, further research should explore clinical development of this mucosal vaccine strategy, including its adaptation to multivalent designs or its use in next-generation formulations targeting emerging respiratory pathogens. Nevertheless, it is important to note that both *B. subtilis* spores (particularly the human probiotic DG101 strain) and recombinant RBD protein have well-established safety profiles [461, 462], as highlighted in **Chapters 1 and 2**, supporting the theoretical safety of our formulation.

4.2 Lithium salts serve as a safe and effective treatment for COVID-19 in Syrian hamsters

In **Chapter 3**, we provide evidence that lithium salts have ablative effects on cell infection *in vitro* and in a Syrian hamster model of COVID-19. We found that lithium inhibited SARS-CoV-2 replication in Vero E6 cells in a concentration-dependent manner. The Vero E6 monolayer was maintained, as verified by microscopy and an NR uptake assay. In this regard, a higher uptake of NR was observed in lithium-treated wells compared with the viral control (infected-untreated), consistent with a relevant antiviral effect. Furthermore, we showed that lithium effectively reduced viral titers, as indicated by an N-SARS-CoV-2 ELISA of supernatants from treated and viral control wells ($p < 0.001$).

Previous *in vitro* studies have shown that lithium salts can reduce coronavirus infection at concentrations ranging from 5 to 25 mmol/L, and non-toxic concentrations have been reported up to 50 mmol/L [488, 492, 517, 518]. In **Chapter 3,** we evaluated Li^+ concentrations up to 12 mmol/L. Although we did not perform a full toxicity assay, we demonstrated that the used concentrations were non-toxic. Our investigation correlated with an antiviral evaluation by

Harrison et al. of the avian coronavirus infectious bronchitis virus, which found that 5 mmol/L of LiCl reduced virus titers by 50% (IC_{50}) [488]. Additionally, Liu et al. [347] showed that GSK-3 inhibitors impaired SARS-CoV-2 N protein phosphorylation, an essential step in viral replication, with an IC_{50} achieved for 10 mM lithium in HEK 293 T cells, which resulted above our required concentration of 4 mmol/L in Vero E6 cells. Moreover, our findings were consistent with the *in vitro* study by Shapira et al. [345], who tested three active compounds with GSK-3β inhibitory effects and demonstrated their ability to reduce SARS-CoV-2 infection in various cell lines, achieving a significant 2-log reduction 48 h after infection and treatment.

As coronaviruses require host GSK-3 activity for their replication [347, 480], its inhibition represents a direct antiviral mechanism of lithium. Additionally, lithium can potentiate CTL activity by inhibiting PD-1 and LAG3, thereby favoring indirect antiviral activity. Moreover, it has anti-inflammatory effects by decreasing the production/expression of inflammatory-associated mediators [497] such as prostaglandin E2, cyclooxygenase-2 [519], and various pro-inflammatory cytokines, including interleukin (IL) -1, IL-6 [499, 520], and tumor necrosis factor-alpha (TNF-α) [497].

Based on the above *in vitro* results, we next assessed the therapeutic effect and safety of lithium in Syrian hamsters infected with SARS-CoV-2. A 10^2 $TCID_{50}$ infective dose was used per animal, which was at least 10 times lower than reported in similar studies but still higher than the mean required to induce this model, allowing us to develop moderate-to-severe disease. As the most frequent signs of COVID-19 in Syrian hamsters are weight loss, stooping, lethargy, and polypnea, they were evaluated daily. Surprisingly, despite the other signs behaving as expected, no significant weight loss was observed in infected animals. This might be due to the lower infective dose we used compared to other studies [506-510]. No signs of lithium toxicity were shown in treated control animals (non-infected).

We showed in **Chapter 3** that infected hamsters treated with lithium showed less severe disease, with fewer signs of it. Even some of them did not show any. In contrast, the disease severity and, accordingly, the average daily score were

significantly higher in the viral control group (infected, untreated), with two animals showing polypnea, a sign of greater disease severity.

On days 2, 4, 5, and 7, we collected nasal swabs from all animals to quantify viral load by RT-qPCR and cultured them on Vero E6 cells. As a peak in disease severity has been described on the fifth day of infection in this animal model, followed by rapid improvement [509], two animals from each group were euthanized at this time point to compare lung viral load and histological lesions.

Despite a trend towards lower swab viral load on the second and fourth days of infection in treated hamsters compared to controls, on the fifth day of infection, swab and nasopharyngeal lavage results showed inconclusive dispersion. However, viral load in the lungs at this time point was also discretely lower in treated animals.

Additionally, the histopathologic study of the lungs showed less tissue damage in the infected-treated animals than in the infected-untreated controls, consistent with the lower disease signs observed as well in this study group. These results support the immunotherapeutic effect of lithium salts *in vivo* and allow not only the evaluation of their antiviral capacity but also the assessment of potential immune-boosting and antinflammatory effects. However, given the small sample size [513], these findings should be interpreted with caution, and further investigations with a larger sample are required.

Due to the rapid evolution of the disease and the high SARS-CoV-2 replication rate in this animal model [508, 509], we further explored whether there were differences between hamsters that started lithium treatment 24 h before the infection time point and those that started treatment and were infected simultaneously, showing no significant differences among these groups. This result may be supported by the rapid intestinal absorption of lithium [494], which would not require earlier initiation of treatment to achieve systemic therapeutic levels in this animal model.

Unlike other drugs that could not replicate *in vivo* the *in vitro* antiviral results obtained in cell cultures [521, 522], lithium showed, although slightly, to decrease the viral load in nasopharyngeal swabs and lungs. Although it must be noted that the infective dose in those studies was higher than ours, it has been demonstrated

that a low-dose challenge inoculum induces a viral load and disease pathology comparable to those observed with higher viral-dose challenges [523].

A dose of 15 mg/kg/day of lithium carbonate was chosen for the hamsters' treatment, as it is equivalent to the standard daily human dose and yielded a serum lithium level of 0.91 ± 0.27 mmol/L, within the therapeutic range in humans [494]. Hence, the data obtained from the current study can be safely extrapolated to clinical scenarios.

According to the results presented here, lithium's immunomodulatory properties appear to play a significant role in improving outcomes in subjects with COVID-19, which is relevant given that the inflammatory host response drives much of the pathology of SARS-CoV-2 infection. Importantly, a reduced incidence of COVID-19 among patients taking lithium compared to the general population was demonstrated in an analysis of clinical data from four major health databases [347, 500]. Additionally, Spuch et al. [500] reported that in six patients with severe COVID-19, treatment with lithium carbonate reduced plasma C-reactive protein levels and increased lymphocyte counts, reducing the neutrophil-lymphocyte ratio and improving clinical status without side effects. Moreover, a recently published retrospective cohort study has found that lithium use was associated with significantly lower odds of severe COVID-19, even though users were older and had more medical comorbidities [535]. However, another recent study has challenged those previous findings, even though the researchers reported, in an ad hoc analysis, that lithium monotherapy was associated with reduced hospitalizations and ICU admissions [536]. Overall, lithium treatment shows direct antiviral effects and may both enhance antiviral immunity and reduce the inflammatory state in COVID-19 patients, but further, broader clinical investigations are required.

Regarding the safety of lithium treatment, a recent study established a 1% incidence of lithium intoxication in chronically treated patients [530]. They assessed the incidence, clinical course, and renal function based on a retrospective cohort study, and concluded that lithium intoxication seems rare and can be safely managed in most cases. Consequently, lithium intoxication is associated with prolonged use, and short-term treatment would further minimize any toxicity occurrence [531].

All in all, lithium directly inhibits the *in vitro* replication of SARS-CoV-2 in Vero E6 cells in a concentration-dependent manner, and it was effective in treating Syrian hamsters with COVID-19, as evidenced by decreased viral load and reduced signs of the disease. Given the study's limitations, including the small sample size and absence of randomization, these findings should be interpreted with caution and warrant confirmation in larger cohorts. In addition, the lack of assessment of pro-inflammatory biomarkers (e.g., C-reactive protein and IL-6) restricts mechanistic interpretation. Accordingly, the results should be viewed as preliminary and hypothesis-generating, providing a rationale for conducting clinical trials.

4.3 General conclusion and future perspectives

4.3.1 Human probiotic *Bacillus subtilis* spores as a promising mucosal adjuvant and antigen delivery platform

While the present thesis establishes human probiotic *Bacillus subtilis* spores as a promising mucosal adjuvant and antigen delivery platform, allowing long-lasting immunity with antigen-specific IgG and IgA secretion, and B_{RM}, and both $CD4^+$ and $CD8^+$ T_{RM} expansion, further investigations are warranted to strengthen mechanistic understanding and translational relevance.

A more detailed characterization of the antigen–spore adsorption process will be critical to elucidate the physicochemical and molecular determinants governing antigen binding, stability, and release. Such analyses may include surface charge interactions, binding kinetics, structural visualization, and the impact of environmental conditions on antigen retention. A deeper mechanistic understanding of this process will inform rational optimization of antigen loading and improve the consistency and reproducibility of the vaccine formulation.

To further support translational potential, future studies should validate *in vivo* protective efficacy using appropriate SARS-CoV-2 challenge models. These studies should assess not only reductions in viral load and disease severity, but also the vaccine's ability to limit viral replication in the upper respiratory tract and reduce transmission potential, key advantages of mucosal immunization strategies. Longitudinal studies evaluating the durability of protection and immune memory will be particularly important in defining the clinical relevance of spore-based vaccination.

Selecting the Syrian hamster (*Mesocricetus auratus*) as an *in vivo* model for COVID-19 is critical for evaluating vaccine efficacy and immunopathogenesis, as hamsters are naturally susceptible to SARS-CoV-2 infection without genetic modification and closely recapitulate key features of human disease, including viral replication in the upper and lower respiratory tract, lung pathology, weight loss, and inflammatory responses. This makes the model particularly well-suited for assessing mucosal vaccines designed to prevent viral entry and transmission. Moreover, *in vivo* studies in hamsters enable an integrated evaluation of both protective efficacy and safety by simultaneously assessing vaccine-induced mucosal IgA responses, systemic neutralizing antibodies, T-cell immunity, and lung histopathology following viral challenge, while also allowing longitudinal monitoring of disease progression and immune memory to gain insights into the durability and quality of protection.

Comprehensive safety profiling and regulatory considerations are essential for clinical advancement. Although *B. subtilis* is widely recognized as safe and has a long history of use as a probiotic, extensive clinical evaluation will be necessary to confirm safety across diverse populations, including immunocompromised individuals, the elderly, and pediatric cohorts. Future investigations should include detailed histopathological analyses of respiratory and distal organs, stringent monitoring of clinical and behavioral parameters, and thorough evaluation of local and systemic inflammatory responses. In addition, assessment of potential spore germination, replication, and persistence within the respiratory tract will be critical to confirm biosafety. Moreover, the fact that oral administration of a probiotic *B. subtilis* strain for 8 weeks increased microbial community diversity without significantly shifting the overall gastrointestinal microbiome equilibrium [264] suggests that long-term studies examining local microbiome interactions and potential immunological tolerance will be relevant to support regulatory approval and public acceptance.

Beyond SARS-CoV-2, this platform offers considerable flexibility for broader vaccine development. Future research should explore clinical translation of this mucosal vaccine strategy, including its adaptation to multivalent formulations capable of targeting multiple viral antigens or co-circulating respiratory pathogens. The modular nature of spore-based antigen delivery also positions this approach as a promising candidate for next-generation vaccines against emerging

and re-emerging respiratory viruses, including pandemic-prone coronaviruses and influenza strains. Moreover, mucosal vaccination strategies may be extended to gastrointestinal, urogenital, or even oncological applications, where local immune activation is desirable. The ability to deliver antigens orally or intranasally without needles could significantly improve vaccine compliance and coverage.

Another important avenue involves evaluating the scalability and manufacturability of *B. subtilis* spore–based vaccines. Spores are inherently stable, heat-, desiccation-, and harsh-environment-resistant, offering a substantial advantage over conventional vaccine formulations that require cold-chain storage. Future research should focus on industrial-scale production, formulation stability, and standardized quality control measures. If successfully translated, this platform could dramatically reduce logistical barriers to vaccine distribution, particularly in low- and middle-income countries where cold-chain infrastructure remains limited.

Integration with heterologous prime–boost strategies represents another promising future direction. Spore-based mucosal vaccines could serve as priming or boosting components in combination with mRNA, viral vector, or protein subunit vaccines. Such approaches may synergistically enhance immune breadth and durability by engaging both systemic and mucosal immune compartments. Comparative studies evaluating homologous versus heterologous vaccination regimens will be critical to identify optimal strategies.

From a mechanistic standpoint, further elucidation of the innate immune pathways activated by *B. subtilis* spores will deepen our understanding of mucosal adjuvanticity. Investigating interactions with PRRs, APCs, and the gut–lung immune axis together with systems immunology approaches such as transcriptomics, single-cell analyses, and multiparameter immune profiling, could provide valuable insights into host–spore interactions at the molecular level and uncover novel immunological principles.

Finally, the success of spore-based mucosal vaccination underscores the importance of rethinking conventional vaccine paradigms. As the global community prepares for future pandemics, platforms that are safe, stable, easily deployable, and capable of inducing sterilizing mucosal immunity will be

indispensable. Human probiotic *B. subtilis* spores embody many of these desirable features and may represent a transformative tool in the global vaccine arsenal.

4.3.2 Lithium salts as a therapeutic approach

On the other hand, demonstration that lithium salts confer therapeutic benefit against SARS-CoV-2 infection in Syrian hamsters highlights the potential of drug repurposing strategies for the management of COVID-19 and other emerging viral diseases. Lithium has a long history of clinical use in psychiatry, with well-characterized pharmacokinetics and safety monitoring frameworks, making it an attractive candidate for rapid translational development. The present findings provide a strong preclinical foundation, yet several important avenues of future research are necessary to fully define the therapeutic scope, mechanism of action, and clinical applicability of lithium-based interventions in viral infections.

A key future priority is the detailed elucidation of the antiviral and immunomodulatory mechanisms underlying lithium's protective effects. Lithium is known to inhibit GSK-3β, modulate autophagy, and influence innate immune signaling pathways, all of which may contribute to its antiviral activity. Future studies should dissect how these pathways intersect during SARS-CoV-2 infection, particularly in the respiratory tract. Investigations employing transcriptomic, proteomic, and metabolomic approaches could provide insights into host pathways modulated by lithium and identify biomarkers predictive of therapeutic response.

Comprehensive safety evaluation remains a central consideration for lithium-based therapies. Despite its widespread clinical use, lithium's narrow therapeutic index necessitates careful monitoring, and future preclinical studies should include detailed histopathological analyses of respiratory, renal, hepatic, and neurological tissues, alongside monitoring of serum lithium levels and electrolyte balance. Importantly, assessing short-term lithium administration in the context of acute viral infection may reveal a favorable risk–benefit profile distinct from chronic psychiatric use. In addition, optimization of dosing regimens will be essential for clinical translation. Although lithium demonstrated efficacy and safety in the hamster model, careful evaluation of dose–response relationships, therapeutic windows, and timing of administration relative to infection is required to define optimal treatment strategies. Future work should compare prophylactic versus therapeutic administration and determine whether lithium is most effective during

early viral replication or later, during inflammatory phases of disease, thereby clarifying its potential clinical use in outpatient treatment, early post-exposure intervention, or as an adjunct therapy for hospitalized patients.

The established safety profile, global availability, and low cost of lithium position it as a compelling candidate for clinical evaluation in COVID-19. Moreover, preclinical evidence demonstrating therapeutic efficacy in a relevant animal model supports the rationale for advancing lithium into carefully designed clinical trials. Future efforts should prioritize translating these findings into rigorously controlled human studies to define lithium's clinical utility across different stages of SARS-CoV-2 infection.

Beyond SARS-CoV-2, the broad immunomodulatory and antiviral properties of lithium suggest potential applicability against other respiratory viruses and emerging pathogens. Future studies should assess lithium's efficacy across diverse viral models to determine whether its protective effects extend beyond COVID-19. This could establish lithium as a host-directed antiviral therapy relevant to pandemic preparedness.

4.3.3 Final conclusions

All in all, this thesis highlights the potential of innovative preventive and therapeutic strategies against SARS-CoV-2. The use of *B. subtilis* spores as a mucosal adjuvant and delivery platform demonstrated strong potential for developing next-generation intranasal vaccines that induce both mucosal and systemic immune responses. In parallel, lithium salts exhibited favorable safety and therapeutic effects in the Syrian hamster model of COVID-19, supporting their potential as an accessible antiviral treatment. Together, these findings provide valuable insights for the development of novel interventions against current and emerging respiratory viral diseases.

Chapter 5

Nederlandse samenvatting

5. Nederlandse samenvatting

5.1 Introductie

COVID-19, veroorzaakt door SARS-CoV-2 (*Coronaviridae*), groeide sinds eind 2019 uit tot een wereldwijde gezondheidscrisis met een blijvende impact op volksgezondheid, zorgsystemen en maatschappij. Aanvankelijk beschouwd als een primaire respiratoire infectie, wordt de ziekte inmiddels erkend als een multisysteemstoornis, gekenmerkt door immuundysregulatie en immuunpathologie [1-4]. Ondanks snelle vooruitgang in diagnostiek, therapeutica en vaccinontwikkeling [5-8], blijft COVID-19 endemisch met een aanzienlijke ziektelast wereldwijd en in België, waar sinds het begin van de pandemie meer dan 4,9 miljoen bevestigde gevallen en ruim 34.000 overlijdens werden geregistreerd [27-29].

Respiratoire pathogenen dringen het lichaam binnen via de bovenste luchtwegen, waar systemisch toegediende vaccins slechts beperkte bescherming bieden tegen initiële infectie en transmissie. Doeltreffende bescherming vereist mucosale immuniteit met lokale inductie van secretoir IgA en weefselresidente geheugen-T-cellen (T_{RM}), die snelle frontlinie-immuniteit kunnen verschaffen. Aangezien geen intranasaal adjuvans is goedgekeurd voor humaan gebruik, blijft de identificatie van veilige mucosale adjuvantia een belangrijke prioriteit. Humane probiotische *Bacillus subtilis*-sporen vormen in dit kader een veelbelovende kandidaatadjuvans [219, 231, 232, 247, 263-266].

Daarnaast blijven therapeutische noden bestaan. SARS-CoV-2 gebruikt gastheer-GSK-3 voor fosforylering van het nucleocapside-eiwit, dat essentieel is voor virale replicatie. *In vitro* kan GSK-3-inhibitie infectie blokkeren [345-349]. Lithiumzouten zijn gekende GSK-3-inhibitoren met een lang klinisch veiligheidsprofiel [342, 343] en bijgevolg potentiële antivirale kandidaten.

5.2 Doel van het proefschrift

Dit proefschrift had tot doel twee complementaire strategieën te evalueren: een innovatief mucosaal vaccinplatform en een antivirale therapie tegen SARS-CoV-2, met als doel de ontwikkeling van effectieve interventies tegen respiratoire virale infecties te ondersteunen. Daartoe werd de immunogeniciteit onderzocht van een

intranasaal (IN) RBD-subunitvaccin geadjuveerd met humane probiotische *Bacillus subtilis*-sporen. Daarnaast werd het antivirale en immunomodulerende potentieel van lithiumzouten getest *in vitro* en *in vivo* met behulp van een Syrisch hamstermodel.

5.3 Resultaten en discussie

5.3.1 Humane probiotische *Bacillus subtilis* sporen fungeren als een doeltreffend mucosaal adjuvans en afgiftesysteem in een anti-SARS-CoV-2-vaccin

In **Hoofdstuk 2** werd een nieuw IN mucosaal COVID-19-vaccin geëvalueerd, bestaande uit het RBD van SARS-CoV-2, geadjuveerd met humane probiotische *Bacillus subtilis*-sporen die fungeren als mucosaal adjuvans en antigeenafgiftesysteem. IN-toediening van spoor–RBD volgens een driedosisschema induceerde robuuste en langdurige mucosale en systemische immuniteit, gekenmerkt door expansie van antigeenspecifieke $CD4^+$- en $CD8^+$-T_{RM}, aanrijking van B_{RM}-cellen en sterke IgG- en IgA-responsen met persisterende serum-IgG-titers tot minstens 180 dagen. Intramusculaire immunisatie leidde daarentegen slechts tot beperkte systemische responsen en induceerde geen relevante mucosale immuniteit, wat de beperkingen van parenterale vaccinatiestrategieën voor luchtweginfecties onderstreept. Hoewel serumafgeleide neutraliserende antilichamen belangrijke correlaten van bescherming vormen, volstaat systemische immuniteit niet om infectie aan de respiratoire mucosa te controleren [362, 363, 419-426].

IN-sporen–RBD-vaccinatie induceerde sterkere systemische antilichaam-responsen dan intramusculaire toediening, in overeenstemming met het belang van antigeendosis, adjuvanspotentie en toedieningsroute [427-429]. De immuunrespons vertoonde een uitgesproken Th1-polarisatie, gekenmerkt door verhoogde IgG2a/IgG1-ratio's en IFN-γ-productie zonder IL-4, waarschijnlijk als gevolg van activatie van het NALT [430], spore-gemedieerde activatie van patroonherkenningsreceptoren [431] en verbeterde antigeenpresentatie door de partikelachtige aard van het sporen–antigeencomplex [397, 398]. Parallel hieraan induceerde IN-vaccinatie robuuste IgA-responsen in serum en respiratoire secreties, die essentieel zijn voor vroege controle van SARS-CoV-2 [374, 432-

434]. In tegenstelling tot pathogene monomere IgA geassocieerd met NETose bij ernstige COVID-19 [435, 436], interageert secretoir IgA niet met Fcα-receptoren [435, 437], wat overeenstemt met het uitblijven van macroscopische longpathologie.

Aangezien mucosale IgG- en IgA-responsen na verloop van tijd afnemen [432, 434, 438, 439], berust duurzame bescherming op de inductie van immunologisch geheugen. Overeenkomstig hiermee leidde IN-spoor–RBD-vaccinatie tot aanrijking van IgG^+- en IgA^+-B_{RM} cellen in longweefsel en inductie van antigeenspecifieke $CD4^+$- en $CD8^+$-T_{RM} cellen sleutelpopulaties voor snelle frontlinie-immuniteit [440-443, 449-451]. Gezien het cruciale belang van Th1- en cytotoxische T-celresponsen voor effectieve controle van SARS-CoV-2 [440, 444-446] en de associatie van Th2-geskewde immuniteit met vaccin-geassocieerde versterkte respiratoire ziekte [446-448], benadrukt dit Th1/Tc1-gedomineerde profiel het voordeel van mucosale boven perifere vaccinatiestrategieën [440, 452]. Naast een specifieke COVID-19-vaccinformulering introduceert dit werk een modulair mucosaal vaccinatieplatform op basis van *B. subtilis*-sporen met gunstige stabiliteits- en veiligheidskenmerken [272, 304, 453-455]. Ondanks het ontbreken van virale challenge-experimenten en directe adsorptiekarakterisering, wordt deze benadering ondersteund door gevestigde methodologieën en veiligheidsprofielen [285, 400-403, 461, 462].

5.3.2 Lithiumzouten fungeren als een veilige en doeltreffende behandeling voor COVID-19 in Syrische hamsters

In **Hoofdstuk 3** tonen wij aan dat lithiumzouten zowel antivirale als immunomodulerende effecten uitoefenen tegen SARS-CoV-2, zowel *in vitro* als *in vivo*. Lithium remde de replicatie van SARS-CoV-2 in Vero E6-cellen op concentratie-afhankelijke wijze, met behoud van de monolaagintegriteit en een significante reductie van virale titers, bevestigd via neutraalrood-opnameassays en N-SARS-CoV-2-ELISA ($p < 0{,}001$). De gebruikte concentraties (≤12 mmol/L) waren niet-toxisch en stemmen overeen met eerdere rapporten over antivirale effecten van lithium tegen coronavirussen [488, 492, 517, 518]. Onze bevindingen zijn consistent met studies die aantonen dat inhibitie van glycogeensynthasekinase-3 (GSK-3), een gastheerfactor die essentieel is voor coronavirusreplicatie, de fosforylering van het SARS-CoV-2-nucleocapside-eiwit

verstoort en zo virale replicatie belemmert [345, 347, 480]. Naast deze directe antivirale werking kan lithium ook indirect antiviraal werken door versterking van cytotoxische T-celactiviteit en door anti-inflammatoire effecten, onder meer via reductie van prostaglandine E2, cyclo-oxygenase-2 en pro-inflammatoire cytokines zoals IL-1, IL-6 en TNF-α [497, 499, 519, 520].

Op basis van deze *in vitro*-resultaten werd lithium vervolgens geëvalueerd in een Syrisch hamstermodel van COVID-19, waarbij lithiumcarbonaat werd toegediend aan een klinisch relevante dosis (15 mg/kg/dag), resulterend in serum-lithiumspiegels binnen het therapeutische bereik bij de mens [494]. Met lithium behandelde geïnfecteerde hamsters vertoonden een minder ernstig ziektebeeld en minder klinische tekenen dan onbehandelde controledieren, zonder aanwijzingen voor lithiumtoxiciteit. Hoewel reducties in nasofaryngale virale lading variabel waren, werden in de longen consistent lagere virale ladingen en minder histopathologische schade waargenomen bij behandelde dieren. Er werden geen significante verschillen vastgesteld tussen dieren die vóór infectie of gelijktijdig met infectie met lithium werden behandeld, wat waarschijnlijk samenhangt met de snelle systemische absorptie van lithium [494]. In tegenstelling tot verschillende antivirale middelen die hun *in vitro*-effectiviteit niet konden reproduceren *in vivo* [521, 522], vertoonde lithium in dit model een bescheiden maar reproduceerbaar therapeutisch effect.

De klinische relevantie van deze bevindingen wordt ondersteund door observationele studies waarin een lagere incidentie en ernst van COVID-19 werden gerapporteerd bij patiënten die lithium gebruiken [347, 500, 535], hoewel ook tegenstrijdige resultaten zijn beschreven [536]. Wat betreft veiligheid is lithiumintoxicatie zeldzaam (ongeveer 1%) en voornamelijk geassocieerd met chronisch gebruik, wat suggereert dat kortdurende behandeling in het kader van acute virale infecties een gunstig veiligheidsprofiel heeft [530, 531]. Samen genomen wijzen deze resultaten erop dat lithium de replicatie van SARS-CoV-2 rechtstreeks kan inhiberen en de ziekte-ernst *in vivo* kan verminderen, waarschijnlijk via een combinatie van antivirale en immunomodulerende mechanismen. Gezien de beperkingen van deze studie, waaronder de kleine steekproefomvang, het ontbreken van randomisatie en het niet bepalen van inflammatoire biomerkers, dienen deze bevindingen te worden beschouwd als

hypothesevormend en vereisen zij verdere bevestiging in grotere preklinische studies en gecontroleerde klinische trials.

5.4 Conclusie en toekomstperspectieven

Dit proefschrift toont aan dat humane probiotische *Bacillus subtilis*-sporen een veelbelovend mucosaal adjuvans en antigeenafgifteplatform vormen dat robuuste en langdurige systemische en mucosale immuniteit kan induceren, inclusief T_{RM}- en B_{RM}-celresponsen. Hoewel verdere validatie in virale challengemodellen, gedetailleerde karakterisering van antigeenbinding en uitgebreide veiligheidsprofilering vereist zijn voor klinische translatie, biedt dit platform een solide basis voor de ontwikkeling van multivalente, stabiele en logistiek toegankelijke mucosale vaccins tegen respiratoire pathogenen. Parallel hieraan tonen de resultaten aan dat lithiumzouten antivirale en immunomodulerende effecten vertonen in een relevant diermodel van COVID-19, wat drug-repurposing ondersteunt als aanvullende therapeutische strategie. Verdere studies gericht op mechanistische opheldering, doseringsoptimalisatie en veiligheidsprofilering zijn noodzakelijk ter voorbereiding van gecontroleerde humane studies. Samen onderstrepen deze bevindingen het potentieel van een geïntegreerde aanpak, waarbij mucosale immunisatie wordt gecombineerd met gastheer-gerichte therapie, voor de preventie en behandeling van huidige en toekomstige respiratoire virale infecties.

References

1. Park SE. Epidemiology, virology, and clinical features of severe acute respiratory syndrome-coronavirus-2 (SARS-CoV-2; Coronavirus Disease-19). Clinical and Experimental Pediatrics. 2020;63(4):119–24.
2. Wong L-YR, Perlman S. Immune dysregulation and immunopathology induced by SARS-CoV-2 and related coronaviruses—are we our own worst enemy? Nature Reviews Immunology. 2022;22(1):47–56.
3. Parotto M, Gyöngyösi M, Howe K, Myatra SN, Ranzani O, Shankar-Hari M, et al. Post-acute sequelae of COVID-19: understanding and addressing the burden of multisystem manifestations. The Lancet Respiratory Medicine. 2023;11(8):739–54.
4. Sharma C, Bayry J. High risk of autoimmune diseases after COVID-19. Nature Reviews Rheumatology. 2023;19(7):399–400.
5. Li R, Pei S, Chen B, Song Y, Zhang T, Yang W, et al. Substantial undocumented infection facilitates the rapid dissemination of novel coronavirus (SARS-CoV-2). Science. 2020;368(6490):489–93.
6. Ranney ML, Griffeth V, Jha AK. Critical supply shortages—the need for ventilators and personal protective equipment during the COVID-19 pandemic. New England journal of medicine. 2020;382(18):e41.
7. Asselah T, Durantel D, Pasmant E, Lau G, Schinazi RF. COVID-19: Discovery, diagnostics and drug development. Journal of Hepatology. 2021;74(1):168–84.
8. Krammer F. SARS-CoV-2 vaccines in development. Nature. 2020;586(7830): 516–27.
9. Zmasek CM, Lefkowitz EJ, Niewiadomska A, Scheuermann RH. Genomic evolution of the *Coronaviridae* family. Virology. 2022;570:123–33.
10. Kesheh MM, Hosseini P, Soltani S, Zandi M. An overview on the seven pathogenic human coronaviruses. Reviews in Medical Virology. 2022; 32(2):e2282.
11. Badar MS, Irfan UH, Siddique ZH, Karimi AM, Ansari MA, Ahmad F, et al. History of Coronaviruses. In: Badar MS, editor. COVID-19: Causes, Transmission, Diagnosis, and Treatment. Singapore: Bentham Science Publishers; 2024. p. 1–36.
12. Liu WJ, Liu P, Lei W, Jia Z, He X, Shi W, et al. Surveillance of SARS-CoV-2 at the Huanan seafood market. Nature. 2024;631(8020):402–8.
13. Holmes EC. The emergence and evolution of SARS-CoV-2. Annual Review of Virology. 2024;11(1):21-42.
14. Crits-Christoph A, Levy JI, Pekar JE, Goldstein SA, Singh R, Hensel Z, et al. Genetic tracing of market wildlife and viruses at the epicenter of the COVID-19 pandemic. Cell. 2024;187(19):5468–82.
15. Wang C, Nan X, Deng Y, Fan S, Lan J. Cross-species recognition of squirrel ACE2 by the receptor binding domains of SARS-CoV-2, RaTG13, PCoV-GD and PCoV-GX. Structure. 2025;33(10):1750-59.

16. Yang J, Skaro M, Chen J, Zhan D, Lyu L, Gay S, et al. The species coalescent indicates possible bat and pangolin origins of the COVID-19 pandemic. Scientific Reports. 2023;13(1):5571.
17. Hu B, Guo H, Zhou P, Shi Z-L. Characteristics of SARS-CoV-2 and COVID-19. Nature Reviews Microbiology. 2021;19(3):141–54.
18. Reis J, Le Faou A, Buguet A, Sandner G, Spencer P. Covid-19: Early cases and disease spread. Annals of Global Health. 2022;88(1):83.
19. Torner N. The end of COVID-19 public health emergency of international concern (PHEIC): And now what? Vacunas (English Edition). 2023.
20. Russell TW, Wu JT, Clifford S, Edmunds WJ, Kucharski AJ, Jit M. Effect of internationally imported cases on internal spread of COVID-19: a mathematical modelling study. The Lancet Public Health. 2021;6(1):e12–e20.
21. Clinical and virologic characteristics of the first 12 patients with coronavirus disease 2019 (COVID-19) in the United States. Nature Medicine. 2020;26(6):861–8.
22. Downing S. COVID-19: a global pandemic. SA Pharmaceutical Journal. 2020;87(2):31–4.
23. Vannabouathong C, Devji T, Ekhtiari S, Chang Y, Phillips SA, Zhu M, et al. Novel coronavirus COVID-19: current evidence and evolving strategies. The Journal of Bone and Joint Surgery (American Volume). 2020;102(9):734–44.
24. Anttiroiko A-V. Successful government responses to the pandemic: Contextualizing national and urban responses to the COVID-19 outbreak in East and West. International Journal of E-Planning Research. 2021;10(2):1–17.
25. Sarker R, Roknuzzaman A, Hossain MJ, Bhuiyan MA, Islam MR. The WHO declares COVID-19 is no longer a public health emergency of international concern: benefits, challenges, and necessary precautions to come back to normal life. International Journal of Surgery. 2023;109(9):2851–2.
26. Alsayed R, Zainualbdeen K, Ahmed D, Younus R, Mohammed AH, Ismael S, et al. The incidence of COVID-19 is once again increasing. Baghdad Journal of Biochemistry and Applied Biological Sciences. 2025;6(3):153–9.
27. Kania M, Terlecki M, Batko K, Rajzer M, Malecki MT, Krzanowski M. Impact of Prior Chronic Kidney Disease and Newly Detected eGFR Impairment at Admission on Outcomes and Prognosis of Hospitalized COVID-19 Patients–A Single-Center Cohort Study. International Journal of General Medicine. 2025;18(0):593–602.
28. Wang H, Paulson KR, Pease SA, Watson S, Comfort H, Zheng P, et al. Estimating excess mortality due to the COVID-19 pandemic: a systematic analysis of COVID-19-related mortality, 2020–21. The Lancet. 2022;399(10334):1513–36.
29. Contreras S, Iftekhar EN, Priesemann V. From emergency response to long-term management: the many faces of the endemic state of COVID-19. The Lancet Regional Health–Europe. 2023;30:100664.

30. Islam MJ, Islam NN, Alom MS, Kabir M, Halim MA. A review on structural, non-structural, and accessory proteins of SARS-CoV-2: Highlighting drug target sites. Immunobiology. 2023;228(1):152302.
31. Yang H, Rao Z. Structural biology of SARS-CoV-2 and implications for therapeutic development. Nature Reviews Microbiology. 2021;19(11):685–700.
32. Chen T, Zhu R, Du T, Yang H, Zhang X, Wang Z, et al. Stem loop binding protein promotes SARS-CoV-2 replication via-1 programmed ribosomal frameshifting. Signal Transduction and Targeted Therapy. 2025;10(1):192.
33. Rashid F, Xie Z, Suleman M, Shah A, Khan S, Luo S. Roles and functions of SARS-CoV-2 proteins in host immune evasion. Frontiers in Immunology. 2022;13:940756.
34. Coronavirus SARS. Isolate Wuhan-Hu-1, Complete Genome. NCBI Reference Sequence: NC_045512.2.
35. Steiner S, Kratzel A, Barut GT, Lang RM, Aguiar Moreira E, Thomann L, et al. SARS-CoV-2 biology and host interactions. Nature Reviews Microbiology. 2024;22(4):206–25.
36. Hoffmann M, Kleine-Weber H, Schroeder S, Krüger N, Herrler T, Erichsen S, et al. SARS-CoV-2 cell entry depends on ACE2 and TMPRSS2 and is blocked by a clinically proven protease inhibitor. Cell. 2020;181(2):271–80.
37. Tai W, He L, Zhang X, Pu J, Voronin D, Jiang S, et al. Characterization of the receptor-binding domain (RBD) of 2019 novel coronavirus: implication for development of RBD protein as a viral attachment inhibitor and vaccine. Cellular & Molecular Immunology. 2020;17(6):613–20.
38. Walls AC, Park Y-J, Tortorici MA, Wall A, McGuire AT, Veesler D. Structure, function, and antigenicity of the SARS-CoV-2 spike glycoprotein. Cell. 2020; 181(2):281–92.
39. V'kovski P, Kratzel A, Steiner S, Stalder H, Thiel V. Coronavirus biology and replication: implications for SARS-CoV-2. Nature Reviews Microbiology. 2021; 19(3):155–70.
40. Finkel Y, Mizrahi O, Nachshon A, Weingarten-Gabbay S, Morgenstern D, Yahalom-Ronen Y, et al. The coding capacity of SARS-CoV-2. Nature. 2021; 589(7840):125–30.
41. Blanco-Melo D, Nilsson-Payant BE, Liu W-C, Uhl S, Hoagland D, Møller R, et al. Imbalanced host response to SARS-CoV-2 drives development of COVID-19. Cell. 2020;181(5):1036–45.
42. Schubert K, Karousis ED, Jomaa A, Scaiola A, Echeverria B, Gurzeler L-A, et al. SARS-CoV-2 Nsp1 binds the ribosomal mRNA channel to inhibit translation. Nature Structural & Molecular Biology. 2020;27(10):959–66.
43. Snijder EJ, Limpens RW, de Wilde AH, de Jong AW, Zevenhoven-Dobbe JC, Maier HJ, et al. A unifying structural and functional model of the coronavirus replication organelle: Tracking down RNA synthesis. PLoS Biology. 2020;18(6): e3000715.

44. Jiang H-w, Zhang H-n, Meng Q-f, Xie J, Li Y, Chen H, et al. SARS-CoV-2 Orf9b suppresses type I interferon responses by targeting TOM70. Cellular & Molecular Immunology. 2020;17(9):998–1000.
45. Zhang Y, Chen Y, Li Y, Huang F, Luo B, Yuan Y, et al. The ORF8 protein of SARS-CoV-2 mediates immune evasion through down-regulating MHC-I. Proceedings of the National Academy of Sciences. 2021;118(23):e2024202118.
46. Miorin L, Kehrer T, Sanchez-Aparicio MT, Zhang K, Cohen P, Patel RS, et al. SARS-CoV-2 Orf6 hijacks Nup98 to block STAT nuclear import and antagonize interferon signaling. Proceedings of the National Academy of Sciences. 2020; 117(45):28344–54.
47. Diao B, Wang C, Tan Y, Chen X, Liu Y, Ning L, et al. Reduction and functional exhaustion of T cells in patients with coronavirus disease 2019 (COVID-19). Frontiers in Immunology. 2020;11:544639.
48. Wilk AJ, Rustagi A, Zhao NQ, Roque J, Martínez-Colón GJ, McKechnie JL, et al. A single-cell atlas of the peripheral immune response in patients with severe COVID-19. Nature medicine. 2020;26(7):1070–6.
49. Watanabe Y, Berndsen ZT, Raghwani J, Seabright GE, Allen JD, Pybus OG, et al. Vulnerabilities in coronavirus glycan shields despite extensive glycosylation. Nature Communications. 2020;11(1):2688.
50. Carabelli AM, Peacock TP, Thorne LG, Harvey WT, Hughes J, 6 C-GUCdSTI, et al. SARS-CoV-2 variant biology: immune escape, transmission and fitness. Nature Reviews Microbiology. 2023;21(3):162–77.
51. Cao Y, Wang J, Jian F, Xiao T, Song W, Yisimayi A, et al. Omicron escapes the majority of existing SARS-CoV-2 neutralizing antibodies. Nature. 2022;602 (7898):657–63.
52. Raharinirina NA, Gubela N, Börnigen D, Smith MR, Oh D-Y, Budt M, et al. SARS-CoV-2 evolution on a dynamic immune landscape. Nature. 2025;639(8053): 196–204.
53. De Cae S, Van Molle I, van Schie L, Shoemaker SR, Deckers J, Debeuf N, et al. Ultrapotent SARS coronavirus-neutralizing single-domain antibodies that clamp the spike at its base. Nature Communications. 2025;16(1):5040.
54. Clausen TM, Sandoval DR, Spliid CB, Pihl J, Perrett HR, Painter CD, et al. SARS-CoV-2 infection depends on cellular heparan sulfate and ACE2. Cell. 2020; 183(4):1043–57.
55. Choi B, Choudhary MC, Regan J, Sparks JA, Padera RF, Qiu X, et al. Persistence and evolution of SARS-CoV-2 in an immunocompromised host. New England Journal of Medicine. 2020;383(23):2291–3.
56. Payne S. Family *Coronaviridae*. Viruses. 2017:149-58.
57. Duffy S. Why are RNA virus mutation rates so damn high? PLoS Biology. 2018; 16(8):e3000003.
58. Robson F, Khan KS, Le TK, Paris C, Demirbag S, Barfuss P, et al. Coronavirus RNA proofreading: molecular basis and therapeutic targeting. Molecular Cell. 2020;79(5):710–27.
59. Focosi D, Maggi F. Recombination in Coronaviruses, with a Focus on SARS-CoV-2. Viruses. 2022;14(6):1239.

60. Di Giorgio S, Martignano F, Torcia MG, Mattiuz G, Conticello SG. Evidence for host-dependent RNA editing in the transcriptome of SARS-CoV-2. Science Advances. 2020;6(25):eabb5813.
61. Simmonds P. Rampant C→ U hypermutation in the genomes of SARS-CoV-2 and other coronaviruses: causes and consequences for their short-and long-term evolutionary trajectories. mSphere. 2020;5(3):e00408-20.
62. COVID S. Tracking changes in SARS-CoV-2 spike: evidence that D614G increases infectivity of the COVID-19 virus. Cell. 2020;182(4):812–27.
63. Harvey WT, Carabelli AM, Jackson B, Gupta RK, Thomson EC, Harrison EM, et al. SARS-CoV-2 variants, spike mutations and immune escape. Nature Reviews Microbiology. 2021;19(7):409–24.
64. Jian F, Wang J, Yisimayi A, Song W, Xu Y, Chen X, et al. Evolving antibody response to SARS-CoV-2 antigenic shift from XBB to JN. 1. Nature. 2025; 637(8047):921–9.
65. Smith EC, Blanc H, Vignuzzi M, Denison MR. Coronaviruses lacking exoribonuclease activity are susceptible to lethal mutagenesis: evidence for proofreading and potential therapeutics. PLoS Pathogens. 2013;9(8): e1003565.
66. Ogando NS, Zevenhoven-Dobbe JC, van Der Meer Y, Bredenbeek PJ, Posthuma CC, Snijder EJ. The enzymatic activity of the nsp14 exoribonuclease is critical for replication of MERS-CoV and SARS-CoV-2. Journal of Virology. 2020;94(23):e01246-20.
67. Riccio AA, Sullivan ED, Copeland WC. Activation of the SARS-CoV-2 NSP14 3'–5' exoribonuclease by NSP10 and response to antiviral inhibitors. Journal of Biological Chemistry. 2022;298(1):101518.
68. Domingo E, García-Crespo C, Lobo-Vega R, Perales C. Mutation rates, mutation frequencies, and proofreading-repair activities in RNA virus genetics. Viruses. 2021;13(9):1882.
69. Batool S, Chokkakula S, Jeong JH, Baek YH, Song M-S. SARS-CoV-2 drug resistance and therapeutic approaches. Heliyon. 2025;11(2):e41980.
70. Shannon A, Le NT-T, Selisko B, Eydoux C, Alvarez K, Guillemot J-C, et al. Remdesivir and SARS-CoV-2: Structural requirements at both nsp12 RdRp and nsp14 Exonuclease active-sites. Antiviral Research. 2020;178:104793.
71. Simon-Loriere E, Holmes EC. Why do RNA viruses recombine? Nature Reviews Microbiology. 2011;9(8):617–26.
72. Williams R, Hales J, Collier W, Gould P. Coronavirus Replication: Genomes, Subgenomic RNAs, and Defective Viral Genomes. Viruses. 2025;17(6):767.
73. Colson P, Fournier PE, Delerce J, Million M, Bedotto M, Houhamdi L, et al. Culture and identification of a "Deltamicron" SARS-CoV-2 in a three-case cluster in southern France. Journal of Medical Virology. 2022;94(8):3739–49.
74. Karim B, Barary M, Fereydouni Z, Sanjari E, Hosseinzadeh R, Salehi-Vaziri M, et al. The nuts and bolts of recombination in the generation of SARS-CoV-2 variants; from XA to XBB. Letters in Applied Microbiology. 2024;77(8): ovae074.

75. Amoutzias GD, Nikolaidis M, Tryfonopoulou E, Chlichlia K, Markoulatos P, Oliver SG. The remarkable evolutionary plasticity of coronaviruses by mutation and recombination: insights for the COVID-19 pandemic and the future evolutionary paths of SARS-CoV-2. Viruses. 2022;14(1):78.
76. Markov PV, Ghafari M, Beer M, Lythgoe K, Simmonds P, Stilianakis NI, et al. The evolution of SARS-CoV-2. Nature Reviews Microbiology. 2023;21(6):361–79.
77. Triggle CR, Bansal D, Ding H, Islam MM, Farag EABA, Hadi HA, et al. A comprehensive review of viral characteristics, transmission, pathophysiology, immune response, and management of SARS-CoV-2 and COVID-19 as a basis for controlling the pandemic. Frontiers in Immunology. 2021;12:631139.
78. Nguyen KV. Containing the spread of COVID-19 virus facing to its high mutation rate: approach to intervention using a nonspecific way of blocking its entry into the cells. Nucleosides, Nucleotides & Nucleic Acids. 2022;41(8):778–814.
79. Zhu N, Zhang D, Wang W, Li X, Yang B, Song J, et al. A novel coronavirus from patients with pneumonia in China, 2019. New England Journal of Medicine. 2020;382(8):727–33.
80. Plante JA, Liu Y, Liu J, Xia H, Johnson BA, Lokugamage KG, et al. Spike mutation D614G alters SARS-CoV-2 fitness. Nature. 2021;592(7852):116–21.
81. Daniloski Z, Jordan TX, Ilmain JK, Guo X, Bhabha G, TenOever BR, et al. The Spike D614G mutation increases SARS-CoV-2 infection of multiple human cell types. Elife. 2021;10:e65365.
82. Salehi-Vaziri M, Fazlalipour M, Seyed Khorrami SM, Azadmanesh K, Pouriayevali MH, Jalali T, et al. The ins and outs of SARS-CoV-2 variants of concern (VOCs). Archives of Virology. 2022;167(2):327–44.
83. Volz E, Mishra S, Chand M, Barrett JC, Johnson R, Geidelberg L, et al. Assessing transmissibility of SARS-CoV-2 lineage B. 1.1. 7 in England. Nature. 2021;593 (7858):266–9.
84. Dhawan M, Sharma A, Priyanka N, Thakur N, Rajkhowa TK, Choudhary OP. Delta variant (B. 1.617. 2) of SARS-CoV-2: Mutations, impact, challenges and possible solutions. Human Vaccines & Immunotherapeutics. 2022;18(5): 2068883.
85. Huai Luo C, Paul Morris C, Sachithanandham J, Amadi A, Gaston DC, Li M, et al. Infection with the severe acute respiratory syndrome coronavirus 2 (SARS-CoV-2) delta variant is associated with higher recovery of infectious virus compared to the alpha variant in both unvaccinated and vaccinated individuals. Clinical Infectious Diseases. 2022;75(1):e715–25.
86. Bhattacharya M, Chatterjee S, Sharma AR, Lee S-S, Chakraborty C. Delta variant (B. 1.617. 2) of SARS-CoV-2: current understanding of infection, transmission, immune escape, and mutational landscape. Folia Microbiologica. 2023;68(1):17–28.
87. Viana R, Moyo S, Amoako DG, Tegally H, Scheepers C, Althaus CL, et al. Rapid epidemic expansion of the SARS-CoV-2 Omicron variant in southern Africa. Nature. 2022;603(7902):679–86.

88. Tamura T, Ito J, Uriu K, Zahradnik J, Kida I, Anraku Y, et al. Virological characteristics of the SARS-CoV-2 XBB variant derived from recombination of two Omicron subvariants. Nature Communications. 2023;14(1):2800.
89. Ito J, Suzuki R, Uriu K, Itakura Y, Zahradnik J, Kimura KT, et al. Convergent evolution of SARS-CoV-2 Omicron subvariants leading to the emergence of BQ. 1.1 variant. Nature Communications. 2023;14(1):2671.
90. Bálint G, Vörös-Horváth B, Széchenyi A. Omicron: increased transmissibility and decreased pathogenicity. Signal Transduction and Targeted Therapy. 2022;7(1):151.
91. Russell TW, Townsley H, Abbott S, Hellewell J, Carr EJ, Chapman LA, et al. Combined analyses of within-host SARS-CoV-2 viral kinetics and information on past exposures to the virus in a human cohort identifies intrinsic differences of Omicron and Delta variants. Plos Biology. 2024;22(1):e3002463.
92. Tegally H, Moir M, Everatt J, Giovanetti M, Scheepers C, Wilkinson E, et al. Emergence of SARS-CoV-2 omicron lineages BA. 4 and BA. 5 in South Africa. Nature Medicine. 2022;28(9):1785–90.
93. Thakur P, Thakur V, Kumar P, Patel SKS. Emergence of novel omicron hybrid variants: BA (x), XE, XD, XF more than just alphabets. International Journal of Surgery. 2022;104:106727.
94. Mohapatra RK, Kandi V, Tuli HS, Chakraborty C, Dhama K. The recombinant variants of SARS-CoV-2: Concerns continue amid COVID-19 pandemic. Journal of Medical Virology. 2022;94(8):3506.
95. Ma K, Chen J. Omicron XE emerges as SARS-CoV-2 keeps evolving. The Innovation. 2022;3(3):100248.
96. Chen Q, Shi P-D, Qin C-F. XBB: the chosen one from SARS-CoV-2 homologous recombination. Oxford University Press UK; 2024.
97. Zhang X, Chen L-L, Ip JD, Chan W-M, Hung IF-N, Yuen K-Y, et al. Omicron sublineage recombinant XBB evades neutralising antibodies in recipients of BNT162b2 or CoronaVac vaccines. The Lancet Microbe. 2023;4(3):e131.
98. Ao D, He X, Hong W, Wei X. The rapid rise of SARS-CoV-2 Omicron subvariants with immune evasion properties: XBB. 1.5 and BQ. 1.1 subvariants. MedComm. 2023;4(2):e239.
99. Kumar S, Jain S, Wali B, Zarnitsyna VI, Joshi D, Ellis ML, et al. The XBB. 1.5 COVID-19 vaccine elicits a durable antibody response to ancestral and XBB. 1.5 SARS-CoV-2 spike proteins. Science Translational Medicine. 2025;17(814): eadu8067.
100. Tamura T, Mizuma K, Nasser H, Deguchi S, Padilla-Blanco M, Oda Y, et al. Virological characteristics of the SARS-CoV-2 BA. 2.86 variant. Cell Host & Microbe. 2024;32(2):170–80.
101. Du P, Wu C, Hu S, Fan R, Gao GF, Wang Q. The omicron BA. 2.86 subvariant as a new serotype of SARS-CoV-2. The Lancet Microbe. 2024;5(6):e516.
102. Planas D, Staropoli I, Michel V, Lemoine F, Donati F, Prot M, et al. Distinct evolution of SARS-CoV-2 Omicron XBB and BA. 2.86/JN. 1 lineages combining increased fitness and antibody evasion. Nature Communications. 2024;15(1):2254.

103. Uriu K, Ito J, Kosugi Y, Tanaka YL, Mugita Y, Guo Z, et al. Transmissibility, infectivity, and immune evasion of the SARS-CoV-2 BA. 2.86 variant. The Lancet Infectious Diseases. 2023;23(11):e460–1.
104. Li P, Faraone JN, Hsu CC, Chamblee M, Zheng Y-M, Carlin C, et al. Neutralization escape, infectivity, and membrane fusion of JN. 1-derived SARS-CoV-2 SLip, FLiRT, and KP. 2 variants. Cell reports. 2024;43(8):114520.
105. Ruan W, Gao P, Qu X, Jiang J, Zhao Z, Qiao S, et al. SARS-CoV-2 serotyping based on spike antigenicity and its implications for host immune evasion. EBioMedicine. 2025;114:105634.
106. Lu Y, Ao D, He X, Wei X. The rising SARS-CoV-2 JN. 1 variant: evolution, infectivity, immune escape, and response strategies. MedComm. 2024;5(8): e675.
107. Guo C, Yu Y, Liu J, Jian F, Yang S, Song W, et al. Antigenic and virological characteristics of SARS-CoV-2 variants BA. 3.2, XFG, and NB. 1.8.1. The Lancet Infectious Diseases. 2025;25(7):e374-77.
108. Zhang L, Kempf A, Nehlmeier I, Chen N, Stankov MV, Happle C, et al. Host cell entry and neutralisation sensitivity of SARS-CoV-2 BA. 3.2. The Lancet Microbe. 2025;6(11):101165.
109. Branda F, Ciccozzi M, Scarpa F. SARS-CoV-2 XFG: a genomic insight into the new recombinant. Infectious Diseases. 2025;57(10):1017-1020.
110. Uriu K, Okumura K, Uwamino Y, Chen L, Tolentino JE, Asakura H, et al. Virological characteristics of the SARS-CoV-2 NB. 1.8. 1 variant. The Lancet Infectious Diseases. 2025;25(8):e443.
111. Lauer SA, Grantz KH, Bi Q, Jones FK, Zheng Q, Meredith HR, et al. The incubation period of coronavirus disease 2019 (COVID-19) from publicly reported confirmed cases: estimation and application. Annals of Internal Medicine. 2020;172(9):577–82.
112. Ilyicheva T, Netesov S, Gureyev V. COVID-19, Influenza, and Other Acute Respiratory Viral Infections: Etiology, Immunopathogenesis, Diagnosis, and Treatment. Part I. COVID-19 and Influenza. Molecular Genetics, Microbiology, and Virology. 2022;37(1):1–9.
113. Oran DP, Topol EJ. The proportion of SARS-CoV-2 infections that are asymptomatic: a systematic review. Annals of Internal Medicine. 2021; 174(5):655–62.
114. Mehta OP, Bhandari P, Raut A, Kacimi SEO, Huy NT. Coronavirus disease (COVID-19): comprehensive review of clinical presentation. Frontiers in Public Health. 2021;8:582932.
115. Kim G-U, Kim M-J, Ra SH, Lee J, Bae S, Jung J, et al. Clinical characteristics of asymptomatic and symptomatic patients with mild COVID-19. Clinical microbiology and infection. 2020;26(7):948.e1–3.
116. Gandhi RT, Lynch JB, Del Rio C. Mild or moderate Covid-19. New England Journal of Medicine. 2020;383(18):1757–66.
117. Weiss P, Murdoch DR. Clinical course and mortality risk of severe COVID-19. The Lancet. 2020;395(10229):1014–5.

118. Hu J, Wang Y. The clinical characteristics and risk factors of severe COVID-19. Gerontology. 2021;67(3):255-266.
119. Celik I, Öztürk R. From asymptomatic to critical illness: decoding various clinical stages of COVID-19. Turkish Journal of Medical Sciences. 2021;51(7):3284–300.
120. Maslove DM, Tang B, Shankar-Hari M, Lawler PR, Angus DC, Baillie JK, et al. Redefining critical illness. Nature Medicine. 2022;28(6):1141–8.
121. Ginestra JC, Mitchell OJ, Anesi GL, Christie JD. COVID-19 critical illness: a data-driven review. Annual Review of Medicine. 2022;73(1):95–111.
122. Gupta A, Madhavan MV, Sehgal K, Nair N, Mahajan S, Sehrawat TS, et al. Extrapulmonary manifestations of COVID-19. Nature Medicine. 2020;26(7): 1017–32.
123. Abobaker A, Raba AA, Alzwi A. Extrapulmonary and atypical clinical presentations of COVID-19. Journal of Medical Virology. 2020;92(11):2458–64.
124. Elrobaa IH, New KJ. COVID-19: pulmonary and extra pulmonary manifestations. Frontiers in Public Health. 2021;9:711616.
125. Sanyaolu A, Marinkovic A, Prakash S, Zhao A, Balendra V, Haider N, et al. Post-acute sequelae in COVID-19 survivors: an overview. SN Comprehensive Clinical Medicine. 2022;4(1):91.
126. Peter RS, Nieters A, Kräusslich H-G, Brockmann SO, Göpel S, Kindle G, et al. Post-acute sequelae of COVID-19 six to 12 months after infection: population-based study. BMJ. 2022;379:e071050.
127. Jennifer K, Shirley SBD, Avi P, Daniella R-C, Naama SS, Anat EZ, et al. Post-acute sequelae of COVID-19 infection. Preventive Medicine Reports. 2023; 31:102097.
128. Halaji M, Heiat M, Faraji N, Ranjbar R. Epidemiology of COVID-19: An updated review. Journal of Research in Medical Sciences. 2021;26(1):82.
129. Ge H, Wang X, Yuan X, Xiao G, Wang C, Deng T, et al. The epidemiology and clinical information about COVID-19. European Journal of Clinical Microbiology & Infectious Diseases. 2020;39(6):1011–9.
130. Zaidi AK, Singh RB. Epidemiology of COVID-19. Progress in Molecular Biology and Translational Science. 2024;202:25–38.
131. Wang CC, Prather KA, Sznitman J, Jimenez JL, Lakdawala SS, Tufekci Z, et al. Airborne transmission of respiratory viruses. Science. 2021;373(6558): eabd9149.
132. Greenhalgh T, Jimenez JL, Prather KA, Tufekci Z, Fisman D, Schooley R. Ten scientific reasons in support of airborne transmission of SARS-CoV-2. Lancet. 2021;397(10285):1603-05.
133. Chaudhuri S, Kasibhatla P, Mukherjee A, Pan W, Morrison G, Mishra S, et al. Analysis of overdispersion in airborne transmission of COVID-19. Physics of Fluids. 2022;34(5):051914.
134. Marking U, Bladh O, Aguilera K, Pongracz T, Havervall S, Greilert-Norin N, et al. Impact of systemic SARS-CoV-2 vaccination on mucosal IgA responses to subsequent breakthrough infection. EBioMedicine. 2025;120:105912.

135. Al Noman Z, Tasnim S, Masud RI, Anika TT, Islam MS, Rahman AMMT, et al. A systematic review on reverse-zoonosis: global impact and changes in transmission patterns. Journal of Advanced Veterinary and Animal Research. 2024;11(3):601.
136. Heydarifard Z, Chegeni AM, Heydarifard F, Nikmanesh B, Salimi V. An overview of SARS-CoV-2 natural infections in companion animals: A systematic review of the current evidence. Reviews in Medical Virology. 2024;34(1):e2512.
137. Quaade ML, Jensen MM, Rasmussen TB, Jensen TK, Hammer AS. Subclinical and long-term effects of severe acute respiratory syndrome coronavirus 2 infection in Danish farmed mink: implications for disease surveillance. Acta Veterinaria Scandinavica. 2025;67(1):29.
138. Mawalla WF, Njiro BJ, Bwire GM, Nasser A, Sunguya B. No evidence of SARS-CoV-2 transmission through transfusion of human blood products: A systematic review. EJHaem. 2021;2(3):601–6.
139. Gaussen A, Hornby L, Rockl G, O'Brien S, Delage G, Sapir-Pichhadze R, et al. Evidence of SARS-CoV-2 infection in cells, tissues, and organs and the risk of transmission through transplantation. Transplantation. 2021;105(7):1405–22.
140. Monroe JM, Quach HQ, Punia S, Enninga EAL, Fedyshyn Y, Girsch JH, et al. Vertical Transmission of SARS-CoV-2–Specific Antibodies and Cytokine Profiles in Pregnancy. The Journal of Infectious Diseases. 2024;229(2):473–84.
141. Li A, Schwartz DA, Vo A, VanAbel R, Coler C, Li E, et al. Impact of SARS-CoV-2 infection during pregnancy on the placenta and fetus. Seminars in Perinatology. 2024;48(4):151919.
142. Pennanen-Iire C, Prereira-Lourenço M, Padoa A, Ribeirinho A, Samico A, Gressler M, et al. Sexual health implications of COVID-19 pandemic. Sexual Medicine Reviews. 2021;9(1):3–14.
143. Tur-Kaspa I, Tur-Kaspa T, Hildebrand G, Cohen D. COVID-19 may affect male fertility but is not sexually transmitted: a systematic review. F&S Reviews. 2021;2(2):140–9.
144. Ahammed T, Anjum A, Rahman MM, Haider N, Kock R, Uddin MJ. Estimation of novel coronavirus (COVID-19) reproduction number and case fatality rate: A systematic review and meta-analysis. Health Science Reports. 2021;4(2): e274.
145. Riccardo F, Ajelli M, Andrianou XD, Bella A, Del Manso M, Fabiani M, et al. Epidemiological characteristics of COVID-19 cases and estimates of the reproductive numbers 1 month into the epidemic, Italy, 28 January to 31 March 2020. Eurosurveillance. 2020;25(49):2000790.
146. Kumar R, Saxena B, Shrivastava R, Bhardwaj R, editors. Mathematical modelling for COVID-19. AIP Conference Proceedings; 2025: AIP Publishing LLC.
147. Vilella A, Trilla A. The COVID-19 pandemic—an epidemiological perspective. Current Allergy and Asthma Reports. 2021;21(4):29.
148. Leung TC. Comparing the Change in R 0 for the COVID-19 Pandemic in Eight Countries Using an SIR Model for Specific Periods. COVID. 2024;4(7):930–51.

149. Anazawa K. Evaluating a novel reproduction number estimation method: a comparative analysis. Scientific Reports. 2025;15(1):5423.
150. Buss LF, Prete Jr CA, Abrahim CM, Mendrone Jr A, Salomon T, de Almeida-Neto C, et al. Three-quarters attack rate of SARS-CoV-2 in the Brazilian Amazon during a largely unmitigated epidemic. Science. 2021;371(6526):288–92.
151. Shah K, Saxena D, Mavalankar D. Secondary attack rate of COVID-19 in household contacts: a systematic review. QJM: An International Journal of Medicine. 2020;113(12):841–50.
152. Rader B, Scarpino SV, Nande A, Hill AL, Adlam B, Reiner RC, et al. Crowding and the shape of COVID-19 epidemics. Nature Medicine. 2020;26(12):1829–34.
153. Luo G, Zhang X, Zheng H, He D. Infection fatality ratio and case fatality ratio of COVID-19. International Journal of Infectious Diseases. 2021;113:43–6.
154. Du J, Lang H-m, Ma Y, Chen A-w, Qin Y-y, Zhang X-p, et al. Global trends in COVID-19 incidence and case fatality rates (2019–2023): a retrospective analysis. Frontiers in Public Health. 2024;12:1355097.
155. Xia Q, Yang Y, Wang F, Huang Z, Qiu W, Mao A. Case fatality rates of COVID-19 during epidemic periods of variants of concern: A meta-analysis by continents. International Journal of Infectious Diseases. 2024;141:106950.
156. Wolff D, Nee S, Hickey NS, Marschollek M. Risk factors for Covid-19 severity and fatality: a structured literature review. Infection. 2021;49(1):15–28.
157. Zsichla L, Müller V. Risk factors of severe COVID-19: a review of host, viral and environmental factors. Viruses. 2023;15(1):175.
158. Russell CD, Lone NI, Baillie JK. Comorbidities, multimorbidity and COVID-19. Nature Medicine. 2023;29(2):334–43.
159. Zhang J-j, Dong X, Liu G-h, Gao Y-d. Risk and protective factors for COVID-19 morbidity, severity, and mortality. Clinical Reviews in Allergy & Immunology. 2023;64(1):90–107.
160. Ayouni I, Maatoug J, Dhouib W, Zammit N, Fredj SB, Ghammam R, et al. Effective public health measures to mitigate the spread of COVID-19: a systematic review. BMC Public Health. 2021;21(1):1015.
161. Talic S, Shah S, Wild H, Gasevic D, Maharaj A, Ademi Z, et al. Effectiveness of public health measures in reducing the incidence of COVID-19, SARS-CoV-2 transmission, and COVID-19 mortality: systematic review and meta-analysis. BMJ. 2021;375:e068302.
162. Galbán-García E, Más-Bermejo P. COVID-19 in Cuba: assessing the national response. MEDICC Review. 2021;22:29–34.
163. Hernández-Bernal F, Ricardo-Cobas MC, Martín-Bauta Y, Rodríguez-Martínez E, Urrutia-Pérez K, Urrutia-Pérez K, et al. A phase 3, randomised, double-blind, placebo-controlled clinical trial evaluation of the efficacy and safety of a SARS-CoV-2 recombinant spike RBD protein vaccine in adults (ABDALA-3 study). The Lancet Regional Health–Americas. 2023;21:100497.
164. Toledo-Romaní ME, García-Carmenate M, Valenzuela-Silva C, Baldoquín-Rodríguez W, Martínez-Pérez M, Rodríguez-González M, et al. Safety and efficacy of the two doses conjugated protein-based SOBERANA-02 COVID-19

vaccine and of a heterologous three-dose combination with SOBERANA-Plus: a double-blind, randomised, placebo-controlled phase 3 clinical trial. The Lancet Regional Health–Americas. 2023;18:100423.
165. Perez Riverol A. The Cuban strategy for combatting the COVID-19 pandemic. MEDICC Review. 2022;22:64–8.
166. Praet P. Reflections on the COVID-19 Restrictions in Belgium and the Rule of Law. Juridica Int'l. 2021;30:194–207.
167. Luyten J, Schokkaert E. Belgium's response to the COVID-19 pandemic. Health Economics, Policy and Law. 2022;17(1):37–47.
168. Popelier P, Van de Heyning C, Van Drooghenbroeck S. National Report on Belgium. In: Vedaschi A, editor. Governmental Policies to Fight Pandemic: The Boundaries of Extraordinary Powers. Leiden: Brill Nijhoff; 2024. p. 137–58.
169. Fajgenblat M, Molenberghs G, Verbeeck J, Willem L, Crèvecoeur J, Faes C, et al. Evaluating the direct effect of vaccination and non-pharmaceutical interventions during the COVID-19 pandemic in Europe. Communications Medicine. 2024;4(1):178.
170. Braeye T, van Loenhout JA, Brondeel R, Stouten V, Hubin P, Billuart M, et al. COVID-19 vaccine effectiveness against symptomatic infection and hospitalisation in Belgium, July 2021 to May 2022. Eurosurveillance. 2023; 28(26):2200768.
171. Crevecoeur J, Hens N, Neyens T, Lariviere Y, Verhasselt B, Masson H, et al. Changes in COVID-19 outbreak patterns following vaccination in long-term care facilities in Flanders, Belgium. Vaccine. 2022;40(43):6218–24.
172. Haynes WA, Kamath K, Bozekowski J, Baum-Jones E, Campbell M, Casanovas-Massana A, et al. High-resolution epitope mapping and characterization of SARS-CoV-2 antibodies in large cohorts of subjects with COVID-19. Communications Biology. 2021;4(1):1317.
173. Liu H, Wilson IA. Protective neutralizing epitopes in SARS-CoV-2. Immunological Reviews. 2022;310(1):76–92.
174. López-Aladid R, Bueno-Freire L, Farriol-Duran R, Porta-Pardo E, Aguilar R, Vidal M, et al. Epitope mapping of SARS-CoV-2 Spike protein using naturally-acquired immune responses to develop monoclonal antibodies. Scientific Reports. 2025;15(1):16269.
175. Atanasova M, Dimitrov I, Ralchev N, Markovski A, Manoylov I, Bradyanova S, et al. Design, development and immunogenicity study of a multi-epitope vaccine prototype against SARS-CoV-2. Pharmaceuticals. 2024;17(11):1498.
176. Palatnik-de-Sousa I, Wallace ZS, Cavalcante SC, Ribeiro MPF, Silva JABM, Cavalcante RC, et al. A novel vaccine based on SARS-CoV-2 $CD4^+$ and $CD8^+$ T cell conserved epitopes from variants Alpha to Omicron. Scientific Reports. 2022;12(1):16731.
177. Fan X, Song J-W, Cao W-J, Zhou M-J, Yang T, Wang J, et al. T-cell epitope mapping of SARS-CoV-2 reveals coordinated IFN-γ Production and clonal expansion of T cells facilitates recovery from COVID-19. Viruses. 2024;16(7):1006.

178. Kurup D, Myers J, Schnell MJ. Current vaccine strategies against SARS-CoV-2: promises and challenges. Journal of Allergy and Clinical Immunology. 2022;150(1):17–21.
179. Kyriakidis NC, López-Cortés A, González EV, Grimaldos AB, Prado EO. SARS-CoV-2 vaccine strategies: a comprehensive review of phase 3 candidates. NPJ Vaccines. 2021;6(1):28.
180. Bettini E, Locci M. SARS-CoV-2 mRNA vaccines: immunological mechanism and beyond. Vaccines. 2021;9(2):147.
181. Goel RR, Painter MM, Apostolidis SA, Mathew D, Meng W, Rosenfeld AM, et al. mRNA vaccines induce durable immune memory to SARS-CoV-2 and variants of concern. Science. 2021;374(6572):abm0829.
182. Fanti S, Dyer C, Ingimarsdóttir IJ, Harding D, Wang G, D'Amati A, et al. Combined adaptive immune mechanisms mediate cardiac injury after COVID-19 vaccination. Circulation. 2025 Oct 31;152(18):1485-1500.
183. Mascellino MT, Di Timoteo F, De Angelis M, Oliva A. Overview of the main anti-SARS-CoV-2 vaccines: mechanism of action, efficacy and safety. Infection and Drug Resistance. 2021:3459–76.
184. Chavda VP, Bezbaruah R, Athalye M, Parikh PK, Chhipa AS, Patel S, et al. Replicating viral vector-based vaccines for COVID-19: potential avenue in vaccination arena. Viruses. 2022;14(4):759.
185. Lenart K, Arcoverde Cerveira R, Hellgren F, Ols S, Sheward DJ, Kim C, et al. Three immunizations with Novavax's protein vaccines increase antibody breadth and provide durable protection from SARS-CoV-2. NPJ Vaccines. 2024;9(1):17.
186. Toledo-Romaní ME, Valenzuela-Silva C, Montero-Díaz M, Iñiguez-Rojas L, Rodríguez-González M, Martínez-Cabrera M, et al. Real-world effectiveness of the heterologous SOBERANA-02 and SOBERANA-Plus vaccine scheme in 2–11 years-old children during the SARS-CoV-2 Omicron wave in Cuba: a longitudinal case-population study. The Lancet Regional Health–Americas. 2024;34:100750.
187. Wang C, Chen L-Y, Lu Q-B, Cui F. Vaccination with the inactivated vaccine (Sinopharm BBIBP-CorV) ensures protection against SARS-CoV-2 related disease. Vaccines. 2022;10(6):920.
188. Jin L, Li Z, Zhang X, Li J, Zhu F. CoronaVac: A review of efficacy, safety, and immunogenicity of the inactivated vaccine against SARS-CoV-2. Human Vaccines & Immunotherapeutics. 2022;18(6):2096970.
189. Yadav PD, Kumar S, Agarwal K, Jain M, Patil DR, Maithal K, et al. Needle-free injection system delivery of ZyCoV-D DNA vaccine demonstrated improved immunogenicity and protective efficacy in rhesus macaques against SARS-CoV-2. Journal of Medical Virology. 2023;95(2):e28484.
190. Blakney AK, Bekker L-G. DNA vaccines join the fight against COVID-19. The Lancet. 2022;399(10332):1281–2.
191. Mallapaty S. India's DNA COVID vaccine is a first—more are coming. Nature. 2021;597:161–2.

192. Castrodeza-Sanz J, Sanz-Muñoz I, Eiros JM. Adjuvants for COVID-19 vaccines. Vaccines. 2023;11(5):902.
193. Zhao T, Cai Y, Jiang Y, He X, Wei Y, Yu Y, et al. Vaccine adjuvants: mechanisms and platforms. Signal Transduction and Targeted Therapy. 2023;8(1):283.
194. Facciolà A, Visalli G, Laganà A, Di Pietro A. An overview of vaccine adjuvants: current evidence and future perspectives. Vaccines. 2022;10(5):819.
195. Glenny A, Pope C, Waddington H, Wallace U. Immunological notes. XVII–XXIV. The Journal of Pathology and Bacteriology. 1926;29(1):31–40.
196. Iwasaki A, Omer SB. Why and how vaccines work. Cell. 2020;183(2):290–5.
197. Medzhitov R, Janeway CA. Innate immunity: the virtues of a nonclonal system of recognition. Cell. 1997;91(3):295–8.
198. Garçon N, Leroux-Roels G, Cheng W-F. Vaccine adjuvants. Perspectives in Vaccinology. 2011;1(1):89–113.
199. Tamargo B, Márquez Y, Ramírez W, Cedré B, Fresno M, Sierra G. New proteoliposome vaccine formulation from *N. meningitidis* serogroup B, without aluminum hydroxide, retains its antimeningococcal protectogenic potential as well as Th-1 adjuvant capacity. BMC Immunology. 2013;14(Suppl 1):S12.
200. Ambrosch F, Wiedermann G, Jonas S, Althaus B, Finkel B, Glück R, et al. Immunogenicity and protectivity of a new liposomal hepatitis A vaccine. Vaccine. 1997;15(11):1209–13.
201. Ko E-J, Kang S-M. Immunology and efficacy of MF59-adjuvanted vaccines. Human Vaccines & Immunotherapeutics. 2018;14(12):3041–5.
202. Tateno M, Stone BJ, Srodulski SJ, Reedy S, Gawriluk TR, Chambers TM, et al. Synthetic biology-derived triterpenes as efficacious immunomodulating adjuvants. Scientific Reports. 2020;10(1):17090.
203. Hernán-García C, Sánchez-Carmona DL, Mateo-Otero LC, Fernández-Espinilla V, Rodríguez-Ducuara PA, Castrodeza-Sanz JJ, et al. Immunogenicity and predictive factors of hepatitis B vaccination with Fendrix® in chronic kidney disease patients. Frontiers in Public Health. 2025;13:1523733.
204. Hayek H, Hasan L, Amarin JZ, Qwaider YZ, Hamdan O, Rezende W, et al. Vaccine Adjuvants in the Immunocompromised Host: Science, Safety, and Efficacy. Transplant Infectious Disease. 2025;27(3):e70053.
205. Evans JT, Cluff CW, Johnson DA, Lacy MJ, Persing DH, Baldridge JR. Enhancement of antigen-specific immunity via the TLR4 ligands MPL™ adjuvant and Ribi. 529. Expert Review of Vaccines. 2003;2(2):219–29.
206. Akhtar A, Styles TM, Gu C, León AN, Tharp GK, Stokdyk K, et al. Influenza vaccine based on AS03-adjuvanted chimeric HA induces long-lived stalk-specific plasma cells in bone marrow and lymph nodes of nonhuman primates. Nature Immunology. 2025;26(11):2045-2058.
207. Khurana S, Coyle EM, Manischewitz J, King LR, Gao J, Germain RN, et al. AS03-adjuvanted H5N1 vaccine promotes antibody diversity and affinity maturation, NAI titers, cross-clade H5N1 neutralization, but not H1N1 cross-subtype neutralization. NPJ Vaccines. 2018;3(1):40.

208. van Doorn E, Liu H, Huckriede A, Hak E. Safety and tolerability evaluation of the use of Montanide ISA™ 51 as vaccine adjuvant: A systematic review. Human Vaccines & Immunotherapeutics. 2016;12(1):159–69.
209. Nan L, Zhang X, Ziyi L, Li S, Xia N. Montanide ISA-51: a promising adjuvant in cancer vaccine immunotherapy. Expert Review of Vaccines. 2025;24(1):958-971.
210. Tregoning JS, Russell RF, Kinnear E. Adjuvanted influenza vaccines. Human Vaccines & Immunotherapeutics. 2018;14(3):550–64.
211. Mokalla VR, Gundarapu S, Kaushik RS, Rajput M, Tummala H. Influenza Vaccines: Current Status, Adjuvant Strategies, and Efficacy. Vaccines. 2025; 13(9):962.
212. Roman F, Burny W, Ceregido MA, Laupèze B, Temmerman ST, Warter L, et al. Adjuvant system AS01: from mode of action to effective vaccines. Expert Review of Vaccines. 2024;23(1):715–29.
213. James SF, Chahine EB, Sucher AJ, Hanna C. Shingrix: the new adjuvanted recombinant herpes zoster vaccine. Annals of Pharmacotherapy. 2018;52(7): 673–80.
214. Lee G-H, Lim S-G. CpG-adjuvanted hepatitis B vaccine (HEPLISAV-B®) update. Expert Review of Vaccines. 2021;20(5):487–95.
215. Champion CR. Heplisav-B: a hepatitis B vaccine with a novel adjuvant. Annals of Pharmacotherapy. 2021;55(6):783–91.
216. Zarnegar B, Carow B, Eriksson J, Spennare E, Öhlund P, Akpinar E, et al. Matrix-M adjuvant triggers inflammasome activation and enables antigen cross-presentation through induction of lysosomal membrane permeabilization. NPJ Vaccines. 2025;10(1):184.
217. Stertman L, Palm A-KE, Zarnegar B, Carow B, Lunderius Andersson C, Magnusson SE, et al. The Matrix-M™ adjuvant: A critical component of vaccines for the 21st century. Human Vaccines & Immunotherapeutics. 2023;19(1): 2189885.
218. Chappell KJ, Mordant FL, Li Z, Wijesundara DK, Ellenberg P, Lackenby JA, et al. Safety and immunogenicity of an MF59-adjuvanted spike glycoprotein-clamp vaccine for SARS-CoV-2: a randomised, double-blind, placebo-controlled, phase 1 trial. The Lancet Infectious Diseases. 2021;21(10):1383–94.
219. Patel K, Chawla N, Mehta Y, Patel S. Adjuvants in Licensed Vaccines. In: Chavda VP, Apostolopoulos V, editors. Emerging Pathways of Vaccine Adjuvants: A Nonspecific Stimulant of the Immune System. Hoboken: Wiley; 2025. p. 107–36.
220. Hu Z, Chen J-P, Xu J-C, Chen Z-Y, Qu R, Zhang L, et al. A two-dose optimum for recombinant S1 protein-based COVID-19 vaccination. Virology. 2022;566: 56–9.
221. Dayan GH, Rouphael N, Walsh SR, Chen A, Grunenberg N, Allen M, et al. Efficacy of a bivalent (D614+ B. 1.351) SARS-CoV-2 recombinant protein vaccine with AS03 adjuvant in adults: a phase 3, parallel, randomised, modified double-blind, placebo-controlled trial. The Lancet Respiratory Medicine. 2023; 11(11):975–90.

222. Hsieh S-M, Liu W-D, Huang Y-S, Lin Y-J, Hsieh E-F, Lian W-C, et al. Safety and immunogenicity of a recombinant stabilized prefusion SARS-CoV-2 spike protein vaccine (MVC COV1901) adjuvanted with CpG 1018 and aluminum hydroxide in healthy adults: a phase 1, dose-escalation study. eClinicalMedicine. 2021;38:100989.
223. Sheng W-H, Hsieh S-M, Chang S-C. Achievements of COVID-19 vaccination programs: Taiwanese perspective. Journal of the Formosan Medical Association. 2024;123(1):S70–6.
224. Moderbacher CR, Kim C, Mateus J, Plested J, Zhu M, Cloney-Clark S, et al. NVX-CoV2373 vaccination induces functional SARS-CoV-2–specific $CD4^+$ and $CD8^+$ T cell responses. The Journal of Clinical Investigation. 2022;132(19): e160898.
225. Datoo MS, Natama HM, Somé A, Bellamy D, Traoré O, Rouamba T, et al. Efficacy and immunogenicity of R21/Matrix-M vaccine against clinical malaria after 2 years' follow-up in children in Burkina Faso: a phase 1/2b randomised controlled trial. The Lancet Infectious Diseases. 2022;22(12):1728–36.
226. Petrovsky N, Cooper PD. Advax™, a novel microcrystalline polysaccharide particle engineered from delta inulin, provides robust adjuvant potency together with tolerability and safety. Vaccine. 2015;33(44):5920–6.
227. Li L, Honda-Okubo Y, Huang Y, Jang H, Carlock MA, Baldwin J, et al. Immunisation of ferrets and mice with recombinant SARS-CoV-2 spike protein formulated with Advax-SM adjuvant protects against COVID-19 infection. Vaccine. 2021;39(40):5940–53.
228. Petrovsky N. Clinical development of SpikoGen®, an Advax-CpG55. 2 adjuvanted recombinant spike protein vaccine. Human Vaccines & Immunotherapeutics. 2024;20(1):2363016.
229. Ndeupen S, Qin Z, Jacobsen S, Bouteau A, Estanbouli H, Igyártó BZ. The mRNA-LNP platform's lipid nanoparticle component used in preclinical vaccine studies is highly inflammatory. iScience. 2021;24(12):103479.
230. Wilson B, Geetha KM. Lipid nanoparticles in the development of mRNA vaccines for COVID-19. Journal of Drug Delivery Science and Technology. 2022;74: 103553.
231. Shi T, Ye Y, Fan Z, Yang Q, Ma Y, Zhu J. Respiratory mucosal vaccines: Applications, delivery strategies and design considerations. Biomedicine & Pharmacotherapy. 2025;189:118326.
232. Zhang Z, Hong W, Zhang Y, Li X, Que H, Wei X. Mucosal immunity and vaccination strategies: Current insights and future perspectives. Molecular Biomedicine. 2025;6(1):1–31.
233. Song Y, Mehl F, Zeichner SL. Vaccine Strategies to Elicit Mucosal Immunity. Vaccines. 2024;12(2):191.
234. Chow MY-T, Lam JKW. Intranasal and Inhaled Vaccines. In: Lam J, Kwok PCL, editors. Respiratory Delivery of Biologics, Nucleic Acids, and Vaccines. Cham: Springer; 2024. p. 123–48
235. Harris E. FDA will evaluate first self-administered FluMist vaccine. JAMA. 2023; 330(20):1945.

236. Zhang Z, Yang Y, Huang L, Yuan L, Huang S, Zeng Z, et al. Nanotechnology-driven advances in intranasal vaccine delivery systems against infectious diseases. Frontiers in Immunology. 2025;16:1573037.
237. Gao F, Wang Q, Qiu C, Luo J, Li X. Pandemic preparedness of effective vaccines for the outbreak of newly H5N1 highly pathogenic avian influenza virus. Virologica Sinica. 2024;39(6):981–5.
238. Ward RL, Bernstein DI. Rotarix: a rotavirus vaccine for the world. Clinical Infectious Diseases. 2009;48(2):222-8.
239. Plotkin SA, Offit P. Efficacy of Rotavirus Vaccines. The Pediatric Infectious Disease Journal. 2024;43(6):518–9.
240. Clark F. A brief account of experiences leading to RotaTeq vaccine. Human Vaccines. 2008;4(4):256–9.
241. Saikia K, Ahmed R, Das B, Paul S, Ray SK, Chandra Deka R, et al. Impact of Rotavac Vaccine on Hospital-Based Disease Prevalence and Strain Diversity in India: A Systematic Review and Meta-Analysis. Reviews in Medical Virology. 2025;35(5):e70066.
242. Cárcamo-Calvo R, Muñoz C, Buesa J, Rodríguez-Díaz J, Gozalbo-Rovira R. The rotavirus vaccine landscape, an update. Pathogens. 2021;10(5):520.
243. Domingos-Pereira S, Cesson V, Chevalier MF, Derré L, Jichlinski P, Nardelli-Haefliger D. Preclinical efficacy and safety of the Ty21a vaccine strain for intravesical immunotherapy of non-muscle-invasive bladder cancer. Oncoimmunology. 2017;6(1):e1265720.
244. Burns CC, Diop OM, Sutter RW, Kew OM. Vaccine-derived polioviruses. The Journal of Infectious Diseases. 2014;210(1):S283–93.
245. Mosley JF, Smith LL, Brantley P, Locke D, Como M. Vaxchora: the first FDA-approved cholera vaccination in the United States. Pharmacy and Therapeutics. 2017;42(10):638–40.
246. Saluja T, Mogasale VV, Excler J-L, Kim JH, Mogasale V. An overview of VaxchoraTM, a live attenuated oral cholera vaccine. Human Vaccines & Immunotherapeutics. 2020;16(1):42–50.
247. Jelinek T, Kollaritsch H. Vaccination with Dukoral® against travelers' diarrhea (ETEC) and cholera. Expert Review of Vaccines. 2008;7(5):561–7.
248. Holmgren J. An update on cholera immunity and current and future cholera vaccines. Tropical Medicine and Infectious Disease. 2021;6(2):64.
249. Baik YO, Choi SK, Olveda RM, Espos RA, Ligsay AD, Montellano MB, et al. A randomized, non-inferiority trial comparing two bivalent killed, whole cell, oral cholera vaccines (Euvichol vs Shanchol) in the Philippines. Vaccine. 2015; 33(46):6360–5.
250. Song KR, Lim JK, Park SE, Saluja T, Cho S-I, Wartel TA, et al. Oral cholera vaccine efficacy and effectiveness. Vaccines. 2021;9(12):1482.
251. Choudhry A, Mathena J, Albano JD, Yacovone M, Collins L. Safety evaluation of adenovirus type 4 and type 7 vaccine live, oral in military recruits. Vaccine. 2016;34(38):4558–64.

252. Hoke Jr CH, Snyder Jr CE. History of the restoration of adenovirus type 4 and type 7 vaccine, live oral (Adenovirus Vaccine) in the context of the Department of Defense acquisition system. Vaccine. 2013;31(12):1623–32.
253. Fallah Mehrabadi MH, Hajimoradi M, Es-Haghi A, Kalantari S, Noofeli M, Mokarram AR, et al. Safety and immunogenicity of intranasal Razi Cov Pars as a COVID-19 booster vaccine in adults: promising results from a groundbreaking clinical trial. Vaccines. 2024;12(11):1255.
254. Malek E, Mehrabadi MHF, Es-Haghi A, Nofeli M, Mokaram AR, Moradi MH, et al. Analysis of immunological and biochemical parameters after booster dose vaccination using protein-based and inactivated virus vaccine for safety. Heliyon. 2024;10(22):e40124.
255. Tukhvatulin AI, Gordeychuk IV, Dolzhikova IV, Dzharullaeva AS, Krasina ME, Bayurova EO, et al. Immunogenicity and protectivity of intranasally delivered vector-based heterologous prime-boost COVID-19 vaccine Sputnik V in mice and non-human primates. Emerging Microbes & Infections. 2022;11(1):2229–47.
256. Astakhova EA, Baranov KO, Shilova NV, Polyakova SM, Zuev EV, Poteryaev DA, et al. Antibody Avidity Maturation Following Booster Vaccination with an Intranasal Adenovirus Salnavac Vaccine. Vaccines. 2024;12(12):1362.
257. Challener C. Inhalation vaccine development. Pharmaceutical Technology. 2023;47(1):26–9.
258. Aerogen and CanSinoBIO agree on landmark development and commercial supply partnership for the world’s first inhaled COVID-19 vaccine delivery. Business Wire. 2021 Dec 9.
259. Akula VR, Bhate AS, Gillurkar CS, Kushwaha JS, Singh AP, Singh C, et al. Effect of heterologous intranasal iNCOVACC® vaccination as a booster to two-dose intramuscular Covid-19 vaccination series: a randomized phase 3 clinical trial. Communications Medicine. 2025;5(1):133.
260. Singh C, Verma S, Reddy P, Diamond MS, Curiel DT, Patel C, et al. Phase III Pivotal comparative clinical trial of intranasal (iNCOVACC) and intramuscular COVID-19 vaccine (Covaxin®). NPJ Vaccines. 2023;8(1):125.
261. Zhu F, Huang S, Liu X, Chen Q, Zhuang C, Zhao H, et al. Safety and efficacy of the intranasal spray SARS-CoV-2 vaccine dNS1-RBD: a multicentre, randomised, double-blind, placebo-controlled, phase 3 trial. The Lancet Respiratory Medicine. 2023;11(12):1075–88.
262. Chu K, Quan J, Liu X, Chen Q, Zang X, Jiang H, et al. A randomized phase I trial of intranasal SARS-CoV-2 vaccine dNS1-RBD in children aged 3–17 years. NPJ Vaccines. 2025;10(1):50.
263. Sinani G, Şenel S. Advances in vaccine adjuvant development and future perspectives. Drug Delivery. 2025;32(1):2517137.
264. Williams N, Weir TL. Spore-based probiotic *Bacillus subtilis*: Current applications in humans and future perspectives. Fermentation. 2024;10(2):78.
265. Hazan A, Lee HY, Tiong V, AbuBakar S. *Bacillus subtilis* Spores as a Vaccine Delivery Platform: A Tool for Resilient Health Defense in Low-and Middle-Income Countries. Vaccines. 2025;13(10):995.

266. Hazan A, Saperi AA, Zulkifli N, MatRahim NA, Tiong V, Lee HY, et al. Recombinant Bacillus subtilis spores expressing SARS-CoV-2 spike protein induced humoral, mucosal, and cellular immunity in mice. Scientific Reports. 2025;15(1):44552.
267. Hamiot A, Lemy C, Krzewinski F, Faille C, Dubois T. Sporulation conditions influence the surface and adhesion properties of *Bacillus subtilis* spores. Frontiers in Microbiology. 2023;14:1219581.
268. Park ZM, Ramamurthi KS. To Sporulate or Not to Sporulate: Developmental Checkpoints Monitoring *Bacillus subtilis* Sporulation. Annual Review of Microbiology. 2025;79(1):87-104.
269. Zhang T, Gong Z, Zhou B, Rao L, Liao X. Recent progress in proteins regulating the germination of *Bacillus subtilis* spores. Journal of Bacteriology. 2025; 207(2):e0028524.
270. Saggese A, Baccigalupi L, Ricca E. Spore formers as beneficial microbes for humans and animals. Applied Microbiology. 2021;1(3):498–509.
271. Todorov SD, Ivanova IV, Popov I, Weeks R, Chikindas ML. Bacillus spore-forming probiotics: benefits with concerns? Critical Reviews in Microbiology. 2022;48(4):513–30.
272. Huang J-M, La Ragione RM, Nunez A, Cutting SM. Immunostimulatory activity of *Bacillus* spores. FEMS Immunology & Medical Microbiology. 2008;53(2): 195–203.
273. Yuan C, Ji X, Zhang Y, Liu X, Ding L, Li J, et al. Important role of *Bacillus subtilis* as a probiotic and vaccine carrier in animal health maintenance. World Journal of Microbiology and Biotechnology. 2024;40(9):268.
274. Mohamadzadeh M, Abbaspour S. Probiotic applications of Bacillus subtilis. In: Razafindralambo H, editor. *Bacillus subtilis* - Functionalities and One Health Applications. London: IntechOpen; 2024. Ch. 3.
275. De Souza RD, Batista MT, Luiz WB, Cavalcante RCM, Amorim JH, Bizerra RSP, et al. *Bacillus subtilis* spores as vaccine adjuvants: further insights into the mechanisms of action. PLoS One. 2014;9(1):e87454.
276. Dekeukeleire M, Vandenheuvel D, Khondee T, Delanghe L, Van Rillaer T, Thys S, et al. Immunostimulatory activity of inactivated environmental *Bacillus* isolates and their endospores. Scientific Reports. 2025;15(1):30604.
277. Liao B, Han Y, Wei Z, Ding X, Lv Y, Sun X, et al. Disruption of Spore Coat Integrity in *Bacillus subtilis* Enhances Macrophage Immune Activation. Current Issues in Molecular Biology. 2025;47(5):378.
278. MatRahim N-A, Jones KM, Keegan BP, Strych U, Zhan B, Lee H-Y, et al. Tonb-dependent receptor protein displayed on spores of *Bacillus subtilis* stimulates protective immune responses against *Acinetobacter baumannii*. Vaccines. 2023;11(6):1106.
279. Oh Y, Kim JA, Kim C-H, Choi S-K, Pan J-G. *Bacillus subtilis* spore vaccines displaying protective antigen induce functional antibodies and protective potency. BMC Veterinary Research. 2020;16(1):259.
280. Maia AR, Reyes-Ramírez R, Pizarro-Guajardo M, Saggese A, Ricca E, Baccigalupi L, et al. Nasal immunization with the C-terminal domain of BclA3

induced specific IgG production and attenuated disease symptoms in mice infected with Clostridioides difficile spores. International Journal of Molecular Sciences. 2020;21(18):6696.

281. Potocki W, Negri A, Peszyńska-Sularz G, Hinc K, Obuchowski M, Iwanicki A. IL-1 fragment modulates immune response elicited by recombinant *Bacillus subtilis* spores presenting an antigen/adjuvant chimeric protein. Molecular Biotechnology. 2018;60(11):810–9.
282. Potocki W, Negri A, Peszyńska-Sularz G, Hinc K, Obuchowski M, Iwanicki A. The combination of recombinant and non-recombinant *Bacillus subtilis* spore display technology for presentation of antigen and adjuvant on single spore. Microbial Cell Factories. 2017;16(1):151.
283. Permpoonpattana P, Hong HA, Phetcharaburanin J, Huang J-M, Cook J, Fairweather NF, et al. Immunization with *Bacillus* spores expressing toxin A peptide repeats protects against infection with *Clostridium difficile* strains producing toxins A and B. Infection and Immunity. 2011;79(6):2295–302.
284. Lee S, Belitsky BR, Brown DW, Brinker JP, Kerstein KO, Herrmann JE, et al. Efficacy, heat stability and safety of intranasally administered *Bacillus subtilis* spore or vegetative cell vaccines expressing tetanus toxin fragment C. Vaccine. 2010;28(41):6658–65.
285. Huang J-M, Hong HA, Van Tong H, Hoang TH, Brisson A, Cutting SM. Mucosal delivery of antigens using adsorption to bacterial spores. Vaccine. 2010; 28(4):1021–30.
286. Mauriello EM, Cangiano G, Maurano F, Saggese V, De Felice M, Rossi M, et al. Germination-independent induction of cellular immune response by *Bacillus subtilis* spores displaying the C fragment of the tetanus toxin. Vaccine. 2007; 25(5):788–93.
287. Uyen NQ, Hong HA, Cutting SM. Enhanced immunisation and expression strategies using bacterial spores as heat-stable vaccine delivery vehicles. Vaccine. 2007;25(2):356–65.
288. Duc LH, Hong HA, Fairweather N, Ricca E, Cutting SM. Bacterial spores as vaccine vehicles. Infection and Immunity. 2003;71(5):2810–18.
289. Gomes PADP, Bentancor LV, Paccez JD, Sbrogio-Almeida M, Palermo MS, Ferreira RdCC, et al. Antibody responses elicited in mice immunized with *Bacillus subtilis* vaccine strains expressing Stx2B subunit of enterohaemorragic *Escherichia coli* O157: H7. Brazilian Journal of Microbiology. 2009;40:333–8.
290. Paccez JD, Luiz WB, Sbrogio-Almeida ME, Ferreira RC, Schumann W, Ferreira LC. Stable episomal expression system under control of a stress inducible promoter enhances the immunogenicity of *Bacillus subtilis* as a vector for antigen delivery. Vaccine. 2006;24(15):2935–43.
291. Isticato R, Sirec T, Treppiccione L, Maurano F, De Felice M, Rossi M, et al. Non-recombinant display of the B subunit of the heat labile toxin of Escherichia coli on wild type and mutant spores of *Bacillus subtilis*. Microbial Cell Factories. 2013;12(1):98.
292. Stasiłojć M, Hinc K, Peszyńska-Sularz G, Obuchowski M, Iwanicki A. Recombinant *Bacillus subtilis* spores elicit Th1/Th17-polarized immune

response in a murine model of *Helicobacter pylori* vaccination. Molecular Biotechnology. 2015;57(8):685–91.
293. Katsande PM, Nguyen VD, Nguyen TLP, Nguyen TKC, Mills G, Bailey DM, et al. Prophylactic immunization to *Helicobacter pylori* infection using spore vectored vaccines. Helicobacter. 2023;28(4):e12997.
294. Zhou Z, Dong H, Huang Y, Yao S, Liang B, Xie Y, et al. Recombinant *Bacillus subtilis* spores expressing cholera toxin B subunit and *Helicobacter pylori* urease B confer protection against *H. pylori* in mice. Journal of Medical Microbiology. 2017;66(1):83–9.
295. Hinc K, Stasiłojć M, Piątek I, Peszyńska-Sularz G, Isticato R, Ricca E, et al. Mucosal adjuvant activity of IL-2 presenting spores of *Bacillus subtilis* in a murine model of Helicobacter pylori vaccination. PLoS One. 2014;9(4):e95187.
296. Vergara EJ, Tran AC, Kim M-Y, Mussá T, Paul MJ, Harrison T, et al. Mucosal and systemic immune responses after a single intranasal dose of nanoparticle and spore-based subunit vaccines in mice with pre-existing lung mycobacterial immunity. Frontiers in Immunology. 2023;14:1306449.
297. Copland A, Diogo GR, Hart P, Harris S, Tran AC, Paul MJ, et al. Mucosal delivery of fusion proteins with *Bacillus subtilis* spores enhances protection against tuberculosis by Bacillus Calmette-Guérin. Frontiers in Immunology. 2018;9: 346.
298. Reljic R, Sibley L, Huang J-M, Pepponi I, Hoppe A, Hong HA, et al. Mucosal vaccination against tuberculosis using inert bioparticles. Infection and immunity. 2013;81(11):4071–80.
299. Das K, Thomas T, Garnica O, Dhandayuthapani S. Recombinant *Bacillus subtilis* spores for the delivery of Mycobacterium tuberculosis Ag85B-CFP10 secretory antigens. Tuberculosis. 2016;101:S18–27.
300. Xiong Z, Mai J, Li F, Liang B, Yao S, Liang Z, et al. Oral administration of recombinant *Bacillus subtilis* spores expressing mutant staphylococcal enterotoxin B provides potent protection against lethal enterotoxin challenge. AMB Express. 2020;10(1):215.
301. Cao Y-G, Hao Y, Wang L. A Bacillus-based Coxsackie virus A16 mucosal vaccine induces strong neutralizing antibody responses. Central European Journal of Immunology. 2019;44(1):1–6.
302. Cao Y-G, Li Z-H, Yue Y-Y, Song N-N, Peng L, Wang L-X, et al. Construction and evaluation of a novel *Bacillus subtilis* spores-based enterovirus 71 vaccine. Journal of Applied Biomedicine. 2013;11(2):105–13.
303. Hu B, Li C, Lu H, Zhu Z, Du S, Ye M, et al. Immune responses to the oral administration of recombinant *Bacillus subtilis* expressing multi-epitopes of foot-and-mouth disease virus and a cholera toxin B subunit. Journal of Virological Methods. 2011;171(1):272–9.
304. Lee S, Belitsky BR, Brinker JP, Kerstein KO, Brown DW, Clements JD, et al. Development of a *Bacillus subtilis*-based rotavirus vaccine. Clinical and Vaccine Immunology. 2010;17(11):1647–55.
305. Ma D, Tian S, Qin Q, Yu Y, Jiao J, Xiong X, et al. Construction of an inhalable recombinant M2e-FP-expressing *Bacillus subtilis* spores-based vaccine and

evaluation of its protection efficacy against influenza in a mouse model. Vaccine. 2023;41(30):4402–13.
306. Zhao G, Miao Y, Guo Y, Qiu H, Sun S, Kou Z, et al. Development of a heat-stable and orally delivered recombinant M2e-expressing *B. subtilis* spore-based influenza vaccine. Human Vaccines & Immunotherapeutics. 2014;10(12): 3649–58.
307. Łęga T, Weiher P, Obuchowski M, Nidzworski D. Presenting influenza A M2e antigen on recombinant spores of *Bacillus subtilis*. PLoS One. 2016;11(11): e0167225.
308. Chan BC-L, Li P, Tsang MS-M, Sung JC-C, Kwong KW-Y, Zheng T, et al. Creating a vaccine-like supplement against respiratory infection using recombinant *Bacillus subtilis* spores expressing SARS-CoV-2 spike protein with natural products. Molecules. 2023;28(13):4996.
309. Katsande PM, Fernández-Bastit L, Ferreira WT, Vergara-Alert J, Hess M, Lloyd-Jones K, et al. Heterologous systemic prime–intranasal boosting using a spore SARS-CoV-2 vaccine confers mucosal immunity and cross-reactive antibodies in mice as well as protection in hamsters. Vaccines. 2022;10(11):1900.
310. Sun H, Lin Z, Zhao L, Chen T, Shang M, Jiang H, et al. *Bacillus subtilis* spore with surface display of paramyosin from *Clonorchis sinensis* potentializes a promising oral vaccine candidate. Parasites & Vectors. 2018;11(1):156.
311. Yu J, Chen T, Xie Z, Liang P, Qu H, Shang M, et al. Oral delivery of *Bacillus subtilis* spore expressing enolase of Clonorchis sinensis in rat model: induce systemic and local mucosal immune responses and has no side effect on liver function. Parasitology Research. 2015;114(7):2499–505.
312. Qu H, Xu Y, Sun H, Lin J, Yu J, Tang Z, et al. Systemic and local mucosal immune responses induced by orally delivered *Bacillus subtilis* spore expressing leucine aminopeptidase 2 of *Clonorchis sinensis*. Parasitology research. 2014;113(8): 3095–103.
313. Zhou Z, Xia H, Hu X, Huang Y, Li Y, Li L, et al. Oral administration of a *Bacillus subtilis* spore-based vaccine expressing Clonorchis sinensis tegumental protein 22.3 kDa confers protection against *Clonorchis sinensis*. Vaccine. 2008;26(15): 1817–25.
314. Zhou Z, Xia H, Hu X, Huang Y, Ma C, Chen X, et al. Immunogenicity of recombinant *Bacillus subtilis* spores expressing *Clonorchis sinensis* tegumental protein. Parasitology Research. 2008;102(2):293–7.
315. Phumrattanaprapin W, Chaiyadet S, Brindley PJ, Pearson M, Smout MJ, Loukas A, et al. Orally administered Bacillus spores expressing an extracellular vesicle-derived tetraspanin protect hamsters against challenge infection with carcinogenic human liver fluke. The Journal of Infectious Diseases. 2021;223 (8):1445–55.
316. de Almeida MEM, Alves KCS, de Vasconcelos MGS, Pinto TS, Glória JC, Chaves YO, et al. *Bacillus subtilis* spores as delivery system for nasal *Plasmodium falciparum* circumsporozoite surface protein immunization in a murine model. Scientific Reports. 2022;12(1):1531.

317. Li L, Hu X, Wu Z, Xiong S, Zhou Z, Wang X, et al. Immunogenicity of self-adjuvanticity oral vaccine candidate based on use of *Bacillus subtilis* spore displaying Schistosoma japonicum 26 KDa GST protein. Parasitology Research. 2009;105(6):1643–51.
318. Toussi SS, Hammond JL, Gerstenberger BS, Anderson AS. Therapeutics for COVID-19. Nature Microbiology. 2023;8(5):771–86.
319. Alves MC, da Silva RC, de Leitão-Júnior SS, de Balbino VQ. Therapeutic Approaches for COVID-19: A Review of Antiviral Treatments, Immunotherapies, and Emerging Interventions. Advances in Therapy. 2025; 42(7):3045-58.
320. Vegivinti CTR, Evanson KW, Lyons H, Akosman I, Barrett A, Hardy N, et al. Efficacy of antiviral therapies for COVID-19: a systematic review of randomized controlled trials. BMC Infectious Diseases. 2022;22(1):107.
321. Gudima G, Kofiadi I, Shilovskiy I, Kudlay D, Khaitov M. Antiviral therapy of COVID-19. International Journal of Molecular Sciences. 2023;24(10):8867.
322. Rommasi F, Nasiri MJ, Mirsaeidi M. Immunomodulatory agents for COVID-19 treatment: possible mechanism of action and immunopathology features. Molecular and Cellular Biochemistry. 2022;477(3):711–26.
323. Mathur P, Kottilil S. Immunomodulatory therapies for COVID-19. Frontiers in Medicine. 2022;9:921452.
324. Velikova T, Valkov H, Aleksandrova A, Peshevska-Sekulovska M, Sekulovski M, Shumnalieva R. Harnessing immunity: Immunomodulatory therapies in COVID-19. World Journal of Virology. 2024;13(2):92521.
325. Weinreich DM, Sivapalasingam S, Norton T, Ali S, Gao H, Bhore R, et al. REGEN-COV antibody combination and outcomes in outpatients with COVID-19. New England Journal of Medicine. 2021;385(23):e81.
326. Dougan M, Nirula A, Azizad M, Mocherla B, Gottlieb RL, Chen P, et al. Bamlanivimab plus etesevimab in mild or moderate COVID-19. New England Journal of Medicine. 2021;385(15):1382–92.
327. Gupta A, Gonzalez-Rojas Y, Juarez E, Crespo Casal M, Moya J, Falci DR, et al. Early treatment for COVID-19 with SARS-CoV-2 neutralizing antibody sotrovimab. New England Journal of Medicine. 2021;385(21):1941–50.
328. Levin MJ, Ustianowski A, De Wit S, Launay O, Avila M, Templeton A, et al. Intramuscular AZD7442 (tixagevimab–cilgavimab) for prevention of COVID-19. New England Journal of Medicine. 2022;386(23):2188–200.
329. Westendorf K, Žentelis S, Wang L, Foster D, Vaillancourt P, Wiggin M, et al. LY-CoV1404 (bebtelovimab) potently neutralizes SARS-CoV-2 variants. Cell Reports. 2022;39(7):110812.
330. Yamamoto Y, Inoue T. Current status and perspectives of therapeutic antibodies targeting the spike protein S2 subunit against SARS-CoV-2. Biological and Pharmaceutical Bulletin. 2024;47(5):917–23.
331. Knowlton KU, Siegel LK, Barkauskas CE, Bhagani S, Dharan NJ, Gardner EM, et al. Passive immunotherapy for adults hospitalized with COVID-19: An individual participant data meta-analysis of six randomized controlled trials. PLoS Medicine. 2025;22(7):e1004616.

332. Farhangnia P, Dehrouyeh S, Safdarian AR, Farahani SV, Gorgani M, Rezaei N, et al. Recent advances in passive immunotherapies for COVID-19: The Evidence-Based approaches and clinical trials. International Immunopharmacology. 2022;109:108786.
333. Strohl WR, Ku Z, An Z, Carroll SF, Keyt BA, Strohl LM. Passive immunotherapy against SARS-CoV-2: from plasma-based therapy to single potent antibodies in the race to stay ahead of the variants. BioDrugs. 2022;36(3):231.
334. Obeagu EI, Tukur M, Akaba K. Impacts of COVID-19 on hemostasis: coagulation abnormalities and management perspectives. Annals of Medicine and Surgery. 2024;86(10):5844–50.
335. Reis S, Faske A, Monsef I, Langer F, Müller OJ, Kranke P, et al. Anticoagulation in COVID-19 patients–An updated systematic review and meta-analysis. Thrombosis Research. 2024;238:141–50.
336. Focosi D, Franchini M, Maggi F, Shoham S. COVID-19 therapeutics. Clinical Microbiology Reviews. 2024;37(2):e00119–23.
337. Ñamendys-Silva SA. Respiratory support for patients with COVID-19 infection. The Lancet Respiratory Medicine. 2020;8(4):e18.
338. Trieu M, Qadir N. Adjunctive Therapies in Acute Respiratory Distress Syndrome. Critical Care Clinics. 2024;40(2):329–51.
339. Arévalo-Romero JA, Chingaté-López SM, Camacho BA, Alméciga-Díaz CJ, Ramírez-Segura CA. Next-generation treatments: Immunotherapy and advanced therapies for COVID-19. Heliyon. 2024;10(5):e26423.
340. Stober HC. Lithium Carbonate. In: Florey K, editor. Analytical Profiles of Drug Substances. Vol. 15. Orlando: Academic Press; 1986. p. 367–91.
341. Wen J, Sawmiller D, Wheeldon B, Tan J. A review for lithium: pharmacokinetics, drug design, and toxicity. CNS & Neurological Disorders Drug Targets. 2019; 18(10):769–78.
342. Gogoleva I, Gromova O, Torshin IY, Grishina T, Pronin A. The Neurobiological Role of Lithium Salts. Neuroscience and Behavioral Physiology. 2023;53(6): 939–45.
343. Hart DA. Lithium Ions as Modulators of Complex Biological Processes: The Conundrum of Multiple Targets, Responsiveness and Non-Responsiveness, and the Potential to Prevent or Correct Dysregulation of Systems during Aging and in Disease. Biomolecules. 2024;14(8):905.
344. Mathuram TL. GSK-3: An "Ace" among kinases. Cancer Biotherapy & Radiopharmaceuticals. 2024;39(9):619–31.
345. Shapira T, Vimalanathan S, Rens C, Pichler V, Peña-Díaz S, Jordana G, et al. Inhibition of glycogen synthase kinase-3-beta (GSK3β) blocks nucleocapsid phosphorylation and SARS-CoV-2 replication. Molecular Biomedicine. 2022;3 (1):43.
346. Cao Y, Wang Y, Huang D, Tan Y-J. The Role of SARS-CoV-2 Nucleocapsid Protein in Host Inflammation. Viruses. 2025;17(8):1046.
347. Liu X, Verma A, Garcia Jr G, Ramage H, Lucas A, Myers RL, et al. Targeting the coronavirus nucleocapsid protein through GSK-3 inhibition. Proceedings of the National Academy of Sciences. 2021;118(42):e2113401118.

348. Fu C, Ma T, Zhou L, Mi Q-S, Jiang A. Balancing Immunity: GSK-3's Divergent Roles in Dendritic Cell-Mediated T-Cell Priming and Memory Responses. International Journal of Molecular Sciences. 2025;26(13):6078.
349. Cichocki F, Valamehr B, Bjordahl R, Zhang B, Rezner B, Rogers P, et al. GSK3 inhibition drives maturation of NK cells and enhances their antitumor activity. Cancer Research. 2017;77(20):5664–75.
350. De Picker LJ, Leboyer M, Geddes JR, Morrens M, Harrison PJ, Taquet M. Association between serum lithium level and incidence of COVID-19 infection. The British Journal of Psychiatry. 2022;221(1):425–7.
351. Shine B, McKnight RF, Leaver L, Geddes JR. Long-term effects of lithium on renal, thyroid, and parathyroid function: a retrospective analysis of laboratory data. The Lancet. 2015;386(9992):461–8.
352. Singh JA, Upshur RE. The granting of emergency use designation to COVID-19 candidate vaccines: Implications for COVID-19 vaccine trials. Lancet Infectious Diseases. 2021;21:e103–9.
353. Ahirwar K, Rohila A, Shukla R. Regulatory consideration and pathways for vaccine development. In: Apostolopoulos V, Vora LK, Chavda VP, editors. Advanced Vaccination Technologies for Infectious and Chronic Diseases: A Guide to Vaccinology. London: Academic Press; 2024. p. 325–39.
354. Shah SS. Health Economics of Vaccine Development and Distribution: Lessons from the COVID-19 Pandemic. Public Health. 2024;1:100015.
355. Lin L, Liu Y, Tang X, He D. The disease severity and clinical outcomes of the SARS-CoV-2 variants of concern. Frontiers in Public Health. 2021;9:775224.
356. Charitos IA, Ballini A, Lovero R, Castellaneta F, Colella M, Scacco S, et al. Update on COVID-19 and Effectiveness of a Vaccination Campaign in a Global Context. International Journal of Environmental Research and Public Health. 2022;19:10712.
357. McLean G, Kamil J, Lee B, Moore P, Schulz TF, Muik A, et al. The impact of evolving SARS-CoV-2 mutations and variants on COVID-19 vaccines. mBio. 2022;13(2):e0297921.
358. Focosi D, Quiroga R, McConnell S, Johnson MC, Casadevall A. Convergent evolution in SARS-CoV-2 spike creates a variant soup from which new COVID-19 waves emerge. International Journal of Molecular Sciences. 2023;24:2264.
359. Callaway E. The next generation of coronavirus vaccines. Nature. 2023;614: 22–5.
360. Sarker R, Roknuzzaman A, Nazmunnahar, Shahriar M, Hossain MJ, Islam MR. The WHO has declared the end of pandemic phase of COVID-19: Way to come back in the normal life. Health Science Reports. 2023;6:e1544.
361. Mambelli F, de Araujo ACV, Farias JP, de Andrade KQ, Ferreira LC, Minoprio P, et al. An Update on Anti-COVID-19 Vaccines and the Challenges to Protect Against New SARS-CoV-2 Variants. Pathogens. 2025;14(1):23.
362. Rathore AP, John ALS. Promises and challenges of mucosal COVID-19 vaccines. Vaccine. 2023;41:4042–9.
363. Alqahtani SAM. Mucosal immunity in COVID-19: A comprehensive review. Frontiers in Immunology. 2024;15:1433452.

364. Borenfreund E, Puerner JA. A simple quantitative procedure using monolayer cultures for cytotoxicity assays (HTD/NR-90). Journal of Tissue Culture Methods. 1985;9(1):7–9.
365. Manenti A, Maggetti M, Casa E, Martinuzzi D, Torelli A, Trombetta CM, et al. Evaluation of SARS-CoV-2 neutralizing antibodies using a CPE-based colorimetric live virus micro-neutralization assay in human serum samples. Journal of Medical Virology. 2020;92(10):2096–104.
366. Yang Y, Peng F, Wang R, Guan K, Jiang T, Xu G, et al. The deadly coronaviruses: The 2003 SARS pandemic and the 2020 novel coronavirus epidemic in China. Journal of Autoimmunity. 2020;109:102434.
367. Wang Y, Wang Y, Chen Y, Qin Q. Unique epidemiological and clinical features of the emerging 2019 novel coronavirus pneumonia (COVID-19) implicate special control measures. Journal of Medical Virology. 2020;92(6):568–76.
368. World Health Organization. Weekly Epidemiological Update on COVID-19 [Internet]. Geneva, Switzerland: World Health Organization; 2025 Feb 11 [cited 2025 Feb 11]. Available from: https://data.who.int/dashboards/covid19.
369. Fenner R, Cernev T. The implications of the COVID-19 pandemic for delivering the Sustainable Development Goals. Futures. 2021;128:102726.
370. World Health Organization. COVID-19–Landscape of Novel Coronavirus Candidate Vaccine Development Worldwide [Internet]. Geneva, Switzerland: World Health Organization; 2023 Mar 30 [cited 2025 Feb 11]. Available from: https://www.who.int/teams/blueprint/covid-19/covid-19-vaccine-tracker-and-landscape.
371. Hossain MK, Hassanzadeganroudsari M, Feehan J, Apostolopoulos V. The race for a COVID-19 vaccine: where are we up to? Expert Review of Vaccines. 2022; 21(3):355–76.
372. World Health Organization. Summary Status of COVID-19 Vaccines Within WHO EUL/PQ Evaluation Process [Internet]. Geneva, Switzerland: World Health Organization; 2024 Dec 9 [cited 2025 Feb 11]. Available from: https://extranet.who.int/prequal/sites/default/files/document_files/summary-status-of-covid-19-vaccines-within-who-eul-pq-evaluation-process-09-december-2024.pdf.
373. Christensen D, Polacek C, Sheward DJ, Hanke L, Moliner-Morro A, McInerney G, et al. Protection against SARS-CoV-2 transmission by a parenteral prime–intranasal boost vaccine strategy. EBioMedicine. 2022;84:104248.
374. Wagstaffe HR, Thwaites RS, Reynaldi A, Sidhu JK, McKendry R, Ascough S, et al. Mucosal and systemic immune correlates of viral control after SARS-CoV-2 infection challenge in seronegative adults. Science Immunology. 2024;9: eadj9285.
375. Leñini C, Rodríguez Ayala F, Goñi AJ, Rateni L, Nakamura A, Grau RR. Probiotic properties of *Bacillus subtilis* DG101 isolated from the traditional Japanese fermented food nattō. Frontiers in Microbiology. 2023;14:1253480.
376. Fricke C, Pfaff F, Ulrich L, Halwe NJ, Schön J, Timm L, et al. SARS-CoV-2 variants of concern elicit divergent early immune responses in hACE2 transgenic mice. European Journal of Immunology. 2023;53:e2250332.

377. Ayala F, Cardinali N, Grau R. Effectiveness of the probiotic *Bacillus subtilis* DG101 to treat type 2 diabetes mellitus triggered by SARS-CoV-2 infection. Journal of Clinical Images and Medical Case Reports. 2022;3:1847.
378. Cardinali N, Ayala F, Leñini C, Perez O, Grau R. Efficacy of The Probiotic *Bacillus subtilis* DG101 Against Intestinal Discomfort and Constipation in Healthy Adults: A Double-Blind, Placebo-Controlled Study. American Journal of Clinical Medicine Research. 2024;4:129.
379. Rosales-Mendoza S, Angulo C. *Bacillus subtilis* comes of age as a vaccine production host and delivery vehicle. Expert Review of Vaccines. 2015;14: 1135–48.
380. Amuguni H, Tzipori S. *Bacillus subtilis*: A temperature resistant and needle free delivery system of immunogens. Human Vaccines & Immunotherapeutics. 2012;8:979–86.
381. Arnaouteli S, Bamford NC, Stanley-Wall NR, Kovács ÁT. *Bacillus subtilis* biofilm formation and social interactions. Nature Reviews Microbiology. 2021;19:600–14.
382. Afzaal M, Saeed F, Islam F, Ateeq H, Asghar A, Shah YA, et al. Nutritional health perspective of natto: A critical review. Biochemistry Research International. 2022;2022:5863887.
383. Khodavirdipour A, Chamanrokh P, Alikhani MY, Alikhani MS. Potential of *Bacillus subtilis* Against SARS-CoV-2—A Sustainable Drug Development Perspective. Frontiers in Microbiology. 2022;13:718786.
384. Xu R, Hong HA, Khandaker S, Baltazar M, Allehyani N, Beentjes D, et al. Nasal delivery of killed *Bacillus subtilis* spores protects against influenza, RSV and SARS-CoV-2. Frontiers in Immunology. 2025;16:1501907.
385. Setlow P. Spores of *Bacillus subtilis*: Their resistance to and killing by radiation, heat and chemicals. Journal of Applied Microbiology. 2006;101:514–25.
386. Yuan M, Liu H, Wu NC, Wilson IA. Recognition of the SARS-CoV-2 receptor binding domain by neutralizing antibodies. Biochemical and Biophysical Research Communications. 2021;538:192–203.
387. Min L, Sun Q. Antibodies and vaccines target RBD of SARS-CoV-2. Frontiers in Molecular Biosciences. 2021;8:671633.
388. Kleanthous H, Silverman JM, Makar KW, Yoon IK, Jackson N, Vaughn DW. Scientific rationale for developing potent RBD-based vaccines targeting COVID-19. NPJ Vaccines. 2021;6:128.
389. Valdés-Balbín Y, Santana-Mederos D, Quintero L, Fernández S, Rodríguez L, Sánchez Ramírez B, et al. SARS-CoV-2 RBD-tetanus toxoid conjugate vaccine induces a strong neutralizing immunity in preclinical studies. ACS Chemical Biology. 2021;16:1223–33.
390. Zang J, Zhu Y, Zhou Y, Gu C, Yi Y, Wang S, et al. Yeast-produced RBD-based recombinant protein vaccines elicit broadly neutralizing antibodies and durable protective immunity against SARS-CoV-2 infection. Cell Discovery. 2021;7:71.
391. Dashti N, Golsaz-Shirazi F, Soltanghoraee H, Zarnani A-H, Mohammadi M, Imani D, et al. Preclinical assessment of a recombinant RBD-Fc fusion protein

as SARS-CoV-2 candidate vaccine. European Journal of Microbiology & Immunology. 2024;14:228–42.
392. Pollet J, Strych U, Chen WH, Versteeg L, Keegan B, Zhan B, et al. Receptor-binding domain recombinant protein on alum-CpG induces broad protection against SARS-CoV-2 variants of concern. Vaccine. 2022;40:3655–63.
393. Law JLM, Logan M, Joyce MA, Landi A, Hockman D, Crawford K, et al. SARS-CoV-2 recombinant receptor-binding-domain (RBD) induces neutralizing antibodies against variant strains of SARS-CoV-2 and SARS-CoV-1. Vaccine. 2021;39:5769–79.
394. Cho W-I, Chung M-S. Bacillus spores: A review of their properties and inactivation processing technologies. Food Science and Biotechnology. 2020;29:1447–61.
395. Ahimou F, Paquot M, Jacques P, Thonart P, Rouxhet PG. Influence of electrical properties on the evaluation of the surface hydrophobicity of *Bacillus subtilis*. Journal of Microbiological Methods. 2001;45:119–26.
396. Boggiano-Ayo T, Palacios-Oliva J, Lozada-Chang S, Relova-Hernández E, Gómez-Pérez J, Oliva G, et al. Development of a scalable single process for producing SARS-CoV-2 RBD monomer and dimer vaccine antigens. Frontiers in Bioengineering and Biotechnology. 2023;11:1287551.
397. Kehagia E, Papakyriakopoulou P, Valsami G. Advances in intranasal vaccine delivery: A promising non-invasive route of immunization. Vaccine. 2023;41: 3589–603.
398. Ramvikas M, Arumugam M, Chakrabarti SR, Jaganathan KS. Nasal Vaccine Delivery. In: Skwarczynski M, Toth I, editors. Micro- and Nanotechnology in Vaccine Development. Amsterdam: Elsevier; 2017. p. 279–301.
399. Tub-Chafer F, Reyes-Díaz LM, Vega-García IG, González-Aznar E, Otero-Alfaro O, Lumpuy-Castillo J, et al. Acción adyuvante de esporas de *Bacillus subtilis* por vía mucosa. VacciMonitor. 2016;25:19–29.
400. Song M, Hong HA, Huang J-M, Colenutt C, Khang DD, Van Anh Nguyen T, et al. Killed *Bacillus subtilis* spores as a mucosal adjuvant for an H5N1 vaccine. Vaccine. 2012;30:3266–77.
401. Ricca E, Baccigalupi L, Cangiano G, De Felice M, Isticato R. Mucosal vaccine delivery by non-recombinant spores of *Bacillus subtilis*. Microbial Cell Factories. 2014;13:115.
402. Isticato R, Ricca E, Baccigalupi L. Spore adsorption as a nonrecombinant display system for enzymes and antigens. Journal of Visualized Experiments. 2019:e59102.
403. Ricca E, Baccigalupi L, Isticato R. Spore-adsorption: Mechanism and applications of a non-recombinant display system. Biotechnology Advances. 2020;47:107693.
404. George AJ, Harmsen BJ, Ford JA, Tadepalli SR, Horton ND. Evaluation of submental blood collection in mice (*Mus musculus*). Journal of the American Association for Laboratory Animal Science. 2023;62:92–8.
405. Parasuraman S, Raveendran R. Biological Sample Collection from Experimental Animals. In: Lakshmanan M, Shewade DG, Raj GM, editors. Introduction to

Basics of Pharmacology and Toxicology: Volume 3: Experimental Pharmacology: Research Methodology and Biostatistics. Singapore: Springer; 2022. p. 45–63.
406. Henderson M. Transcardial Perfusion in Mouse [Internet]. Protocols.io; 2023 Oct 20 [cited 2025 Feb 11]. Available from: https://dx.doi.org/10.17504/protocols.io.dm6gpbrw1lzp/v1.
407. Sam-Yellowe TY. Immunology: Overview and Laboratory Manual. Cham: Springer; 2021. p. 255–65.
408. Vanlandewijck M, Andrae J, Gouveia L, Betsholtz C. Preparation of single cell suspensions from the adult mouse lung [Internet]. Protocols.io; 2018 Feb 26 [cited 2025 Feb 11]. Available from: https://dx.doi.org/10.1038/protex.2018.006.
409. Daubeuf F, Frossard N. Performing bronchoalveolar lavage in the mouse. Current Protocols in Mouse Biology. 2012;2:167–75.
410. Cisney ED, Fernandez S, Hall SI, Krietz GA, Ulrich RG. Examining the role of nasopharyngeal-associated lymphoreticular tissue (NALT) in mouse responses to vaccines. Journal of Visualized Experiments. 2012;(66):3960.
411. Oluka GK, Namubiru P, Kato L, Ankunda V, Gombe B, Cotten M, et al. Optimisation and Validation of a conventional ELISA and cut-offs for detecting and quantifying anti-SARS-CoV-2 antibodies in Uganda. Frontiers in Immunology. 2023;14:1113194.
412. Santana-Mederos D, Pérez-Nicado R, Climent Y, Rodríguez L, Ramírez BS, Pérez-Rodríguez S, et al. A COVID-19 vaccine candidate composed of the SARS-CoV-2 RBD dimer and *Neisseria meningitidis* outer membrane vesicles. RSC Chemical Biology. 2021;3:242–9.
413. Manuylov V, Dolzhikova I, Kudryashova A, Cherepovich B, Kovyrshina A, Iliukhina A, et al. Simple ELISA methods to estimate neutralizing antibody titers to SARS-CoV-2. Archives of Microbiology and Immunology. 2022;6:213–20.
414. Pi-Estopiñan F, Pérez MT, Fraga A, Bergado G, Díaz GD, Orosa I, et al. A cell-based ELISA as surrogate of virus neutralization assay for RBD SARS-CoV-2 specific antibodies. Vaccine. 2022;40:1958–67.
415. Muul LM, Heine G, Silvin C, James SP, Candotti F, Radbruch A, et al. Measurement of proliferative responses of cultured lymphocytes. Current Protocols in Immunology. 2011;94:7.10.1–26
416. Foster B, Prussin C, Liu F, Whitmire JK, Whitton JL. Detection of intracellular cytokines by flow cytometry. Current Protocols in Immunology. 2007;78:6.24.1–21.
417. Rybkina K, Davis-Porada J, Farber DL. Tissue immunity to SARS-CoV-2: Role in protection and immunopathology. Immunological Reviews. 2022;309:25–39.
418. Allie SR, Bradley JE, Mudunuru U, Schultz MD, Graf BA, Lund FE, et al. The establishment of resident memory B cells in the lung requires local antigen encounter. Nature Immunology. 2019;20:97–108.

419. Hassan AO, Case JB, Winkler ES, Thackray LB, Kafai NM, Bailey AL, et al. A SARS-CoV-2 infection model in mice demonstrates protection by neutralizing antibodies. Cell. 2020;182:744–53.
420. Rogers TF, Zhao F, Huang D, Beutler N, Burns A, He W, et al. Isolation of potent SARS-CoV-2 neutralizing antibodies and protection from disease in a small animal model. Science. 2020;369:956–63.
421. Trichel AM. Overview of Nonhuman Primate Models of SARS-CoV-2 Infection. Comparative Medicine. 2021;71:411–32.
422. Chen Z, Yuan Y, Hu Q, Zhu A, Chen F, Li S, et al. SARS-CoV-2 immunity in animal models. Cellular & Molecular Immunology. 2024;21:119–33.
423. Koch T, Mellinghoff SC, Shamsrizi P, Addo MM, Dahlke C. Correlates of vaccine-induced protection against SARS-CoV-2. Vaccines. 2021;9(3):238.
424. Khoury DS, Cromer D, Reynaldi A, Schlub TE, Wheatley AK, Juno JA, et al. Neutralizing antibody levels are highly predictive of immune protection from symptomatic SARS-CoV-2 infection. Nature Medicine. 2021;27:1205–11.
425. Cromer D, Steain M, Reynaldi A, Schlub TE, Wheatley AK, Juno JA, et al. Neutralising antibody titres as predictors of protection against SARS-CoV-2 variants and the impact of boosting: A meta-analysis. Lancet Microbe. 2022; 3:e52–61.
426. Pilapitiya D, Wheatley AK, Tan HX. Mucosal vaccines for SARS-CoV-2: Triumph of hope over experience. EBioMedicine. 2023;92:104585.
427. Yahyaei S, Abdoli A, Jamali A, Teimoori A, Arefian E, Eftekhari Z, et al. Targeting respiratory viruses: Intranasal mRNA vaccination generates protective mucosal and systemic immunity against influenza A (H1N1). Influenza and Other Respiratory Viruses. 2025;19:e70093.
428. Anthi AK, Kolderup A, Vaage EB, Bern M, Benjakul S, Tjärnhage E, et al. An intranasal subunit vaccine induces protective systemic and mucosal antibody immunity against respiratory viruses in mouse models. Nature Communications. 2025;16:3999.
429. Hassan AO, Shrihari S, Gorman MJ, Ying B, Yuan D, Raju S, et al. An intranasal vaccine durably protects against SARS-CoV-2 variants in mice. Cell Reports. 2021;36:109452.
430. Gallo O, Locatello LG, Mazzoni A, Novelli L, Annunziato F. The central role of the nasal microenvironment in the transmission, modulation, and clinical progression of SARS-CoV-2 infection. Mucosal Immunology. 2020;14:305–16.
431. Mahla RS, Reddy MC, Prasad DVR, Kumar H. Sweeten PAMPs: Role of sugar complexed PAMPs in innate immunity and vaccine biology. Frontiers in Immunology. 2013;4:248.
432. Sterlin D, Mathian A, Miyara M, Mohr A, Anna F, Claër L, et al. IgA dominates the early neutralizing antibody response to SARS-CoV-2. Science Translational Medicine. 2021;13:eabd2223.
433. Kurano M, Morita Y, Nakano Y, Yokoyama R, Shimura T, Qian C, et al. Response kinetics of different classes of antibodies to SARS-CoV-2 infection in the Japanese population. International Immunopharmacology. 2022;103:108491.

434. Takamatsu Y, Omata K, Shimizu Y, Kinoshita-Iwamoto N, Terada M, Suzuki T, et al. SARS-CoV-2-neutralizing humoral IgA response occurs earlier but is modest and diminishes faster than IgG response. Microbiology Spectrum. 2022;10:e02716–22.
435. Yaugel-Novoa M, Noailly B, Jospin F, Pizzorno A, Traversier A, Pozzetto B, et al. Impaired mucosal IgA response in patients with severe COVID-19. Emerging Microbes & Infections. 2024;13:2401940.
436. Stacey HD, Golubeva D, Posca A, Ang JC, Novakowski KE, Zahoor MA, et al. IgA potentiates NETosis in response to viral infection. Proceedings of the National Academy of Sciences USA. 2021;118:e2101497118.
437. Yaugel-Novoa M, Bourlet T, Paul S. Role of the humoral immune response during COVID-19: Guilty or not guilty? Mucosal Immunology. 2022;15:1170–80.
438. Di Stefano M, Mirabella L, Cotoia A, Faleo G, Rauseo M, Rizzo AC, et al. A Possible Protective Effect of IgA Against Severe Acute Respiratory Syndrome Coronavirus 2 (SARS-CoV-2) in Bronchoalveolar Lavage in COVID-19 Patients Admitted to Intensive Care Unit. Viruses. 2024;16:1851.
439. Tyagi R, Basu S, Dhar A, Gupta S, Gupta SL, Jaiswal RK. Role of Immunoglobulin A in COVID-19 and Influenza Infections. Vaccines. 2023;11: 1647.
440. Noh HE, Rha MS. Mucosal Immunity against SARS-CoV-2 in the Respiratory Tract. Pathogens. 2024;13:113.
441. Lee CM, Oh JE. Resident memory B cells in barrier tissues. Frontiers in Immunology. 2022;13:953088.
442. Longet S, Paul S. Pivotal role of tissue-resident memory lymphocytes in the control of mucosal infections. Frontiers in Immunology. 2023;14:1216402.
443. Poon MM, Rybkina K, Kato Y, Kubota M, Matsumoto R, Bloom NI, et al. SARS-CoV-2 infection generates tissue-localized immunological memory in humans. Science Immunology. 2021;6:eabl9105.
444. Rha MS, Kim AR, Shin EC. SARS-CoV-2-specific T cell responses in patients with COVID-19 and unexposed individuals. Immune Network. 2021;21:e2.
445. Pavel AB, Glickman JW, Michels JR, Kim-Schulze S, Miller RL, Guttman-Yassky E. Th2/Th1 cytokine imbalance is associated with higher COVID-19 risk mortality. Frontiers in Genetics. 2021;12:706902.
446. Yang Y, Miller H, Byazrova MG, Candotti F, Benlagha K, Camara NOS, et al. The characterization of $CD8^+$ T-cell responses in COVID-19. Emerging Microbes & Infections. 2024;13:2287118.
447. Heitmann JS, Bilich T, Tandler C, Nelde A, Maringer Y, Marconato M, et al. A COVID-19 peptide vaccine for the induction of SARS-CoV-2 T cell immunity. Nature. 2022;601:617–22.
448. Gartlan C, Tipton T, Salguero FJ, Sattentau Q, Gorringe A, Carroll MW. Vaccine-associated enhanced disease and pathogenic human coronaviruses. Frontiers in Immunology. 2022;13:882972.
449. Zheng MZ, Wakim LM. Tissue resident memory T cells in the respiratory tract. Mucosal Immunology. 2022;15:379–88.

450. Cheon IS, Son YM, Sun J. Tissue-resident memory T cells and lung immunopathology. Immunological Reviews. 2023;316:63–83.
451. Carbone FR. Unique properties of tissue-resident memory T cells in the lungs: Implications for COVID-19 and other respiratory diseases. Nature Reviews Immunology. 2023;23:329–35.
452. Mitsi E, Diniz MO, Reiné J, Collins AM, Robinson RE, Hyder-Wright A, et al. Respiratory mucosal immune memory to SARS-CoV-2 after infection and vaccination. Nature Communications. 2023;14:6815.
453. Isticato R. Bacterial spore-based delivery system: 20 years of a versatile approach for innovative vaccines. Biomolecules. 2023;13:947.
454. Cutting SM. *Bacillus* probiotics. Food Microbiology. 2011;28:214–20.
455. Hong HA, Khaneja R, Tam NM, Cazzato A, Tan S, Urdaci M, et al. *Bacillus subtilis* isolated from the human gastrointestinal tract. Research in Microbiology. 2009;160:134–43.
456. Zhou M, Xiao H, Yang X, Cheng T, Yuan L, Xia N. Novel vaccine strategies to induce respiratory mucosal immunity: Advances and implications. MedComm. 2025;6:e70056.
457. So YJ, Park O-J, Kwon Y, Im J, Lee D, Yun S-H, et al. *Bacillus subtilis* induces human beta defensin-2 through its lipoproteins in human intestinal epithelial cells. Probiotics and Antimicrobial Proteins. 2024;17:1648–62.
458. Saggese A, Baccigalupi L, Donadio G, Ricca E, Isticato R. The bacterial spore as a mucosal vaccine delivery system. International Journal of Molecular Sciences. 2023;24:10880.
459. Roos TB, de Moraes CM, Sturbelle RT, Dummer LA, Fischer G, Leite FPL. Probiotics *Bacillus toyonensis* and *Saccharomyces boulardii* improve vaccine immune response in sheep. Research in Veterinary Science. 2018;117:260–5.
460. Santos FDS, Maubrigades LR, Gonçalves VS, Ferreira MRA, Brasil CL, Cunha RC, et al. Immunomodulatory effect of *Bacillus toyonensis* and *Saccharomyces boulardii* in sheep vaccinated with *Clostridium chauvoei*. Veterinary Immunology and Immunopathology. 2021;237:110272.
461. Sung JC-C, Lai NC-Y, Wu K-C, Choi M-C, Ho-Yi CMA, Lin J, et al. Safety and Immunogenicity of Inactivated *Bacillus subtilis* Spores as a Heterologous Antibody Booster for COVID-19 Vaccines. Vaccines. 2022;10:1014.
462. Lei H, Alu A, Yang J, Ren W, He C, Lan T, et al. Intranasal administration of a recombinant RBD vaccine induces long-term immunity against Omicron-included SARS-CoV-2 variants. Signal Transduction and Targeted Therapy. 2022;7:159.
463. Huang C, Wang Y, Li X, Ren L, Zhao J, Hu Y. Clinical features of patients infected with 2019 novel coronavirus in Wuhan, China. The Lancet. 2020;395:497–506.
464. Chan JFW, Kok KH, Zhu Z, Chu H, To KKW, Yuan S. Genomic characterization of the 2019 novel human-pathogenic coronavirus isolated from a patient with atypical pneumonia after visiting Wuhan. Emerging Microbes & Infections. 2020;9(1):221–36.

465. Rota PA, Oberste MS, Monroe SS, Nix WA. Characterization of a novel coronavirus associated with severe acute respiratory syndrome. Science. 2003;300:1394–9.
466. Lu R, Zhao X, Li J, Niu P, Yang B, Wu H. Genomic characterisation and epidemiology of 2019 novel coronavirus: implications for virus origins and receptor binding. The Lancet. 2020;395:565–74.
467. Wu C, Liu Y, Yang Y, Zhang P, Zhong W, Wang Y. Analysis of therapeutic targets for SARS-CoV-2 and discovery of potential drugs by computational methods. Acta Pharmaceutica Sinica B. 2020;10:766–88.
468. Carlson CR, Asfaha JB, Ghent CM, Howard CJ, Hartooni N, Safari M. Phosphoregulation of phase separation by the SARS-CoV-2 N protein suggests a biophysical basis for its dual functions. Molecular Cell. 2020;80:1092–103.
469. Perdikari TM, Murthy AC, Ryan VH, Watters S, Naik MT, Fawzi NL. SARS-CoV-2 nucleocapsid protein phase-separates with RNA and with human hnRNPs. The EMBO Journal. 2020;39:e106478.
470. Chang C-K, Hou M-H, Chang C-F, Hsiao C-D, Huang T-H. The SARS coronavirus nucleocapsid protein – forms and functions. Antiviral Research. 2014;103:39–50.
471. Wu CH, Chen PJ, Yeh SH. Nucleocapsid phosphorylation and RNA helicase DDX1 recruitment enable coronavirus transition from discontinuous to continuous transcription. Cell Host & Microbe. 2014;16(4):462–72.
472. Kaidanovich-Beilin O, Woodgett JR. GSK-3: functional insights from cell biology and animal models. Frontiers in Molecular Neuroscience. 2011;4:40.
473. Beurel E, Grieco SF, Jope R. Glycogen synthase kinase-3 (GSK3): regulation, actions, and diseases. Pharmacology & Therapeutics. 2015;148:114–31.
474. Taylor A, Harker JA, Chanthong K, Stevenson PG, Zuniga EI, Rudd CE. Glycogen synthase kinase 3 inactivation drives T-bet-mediated downregulation of co-receptor PD-1 to enhance $CD8^+$ cytolytic T cell responses. Immunity. 2016;44:274–86.
475. Agata Y, Kawasaki A, Nishimura H, Ishida Y, Tsubata T, Yagita H. Expression of the PD-1 antigen on the surface of stimulated mouse T and B lymphocytes. International Immunology. 1996;8:765–72.
476. Gordon S, Maute RL, Dulken BW, Hutter G, George BM, McCracken MN. PD-1 expression by tumor-associated macrophages inhibits phagocytosis and tumor immunity. Nature. 2017;545(7655):495–9.
477. Niu C, Li M, Zhu S, Chen Y, Zhou L, Xu D. PD-1-positive natural killer cells have a weaker antitumor function than that of PD-1-negative Natural Killer Cells in Lung Cancer. International Journal of Medical Sciences. 2020;17(13):1964–73.
478. Lim TS, Chew V, Sieow JL, Goh S, Yeong JP-S, Soon AL. PD-1 expression on dendritic cells suppresses $CD8^+$T cell function and antitumor immunity. OncoImmunology. 2016;5(3):e1085146.
479. Skalniak L, Zak KM, Guzik K, Magiera K, Musielak B, Pachota M. Small-molecule inhibitors of PD-1/PD-L1 immune checkpoint alleviate the PD-L1-induced exhaustion of T-cells. Oncotarget. 2017;8(42):72167–81.

480. Chowdhury PS, Chamoto K, Honjo T. Combination therapy strategies for improving PD-1 blockade efficacy: a new era in cancer immunotherapy. Journal of Internal Medicine. 2018;283(2):110–20.
481. Reck M, Rodriguez-Abreu D, Robinson AG. Pembrolizumab versus chemotherapy for PD-L1-positive non-small-cell lung cancer. The New England Journal of Medicine. 2016;375(19):1823–33.
482. Rudd CE, Chanthong K, Taylor A. Small molecule inhibition of GSK-3 specifically inhibits the transcription of inhibitory co-receptor LAG-3 for enhanced anti-tumor immunity. Cell Reports. 2020;30(7):2075–82.
483. Maruhashi T, Sugiura D, Okazaki I-m, Okazaki T. LAG-3: from molecular functions to clinical applications. Journal for Immunotherapy of Cancer. 2020;8(2):e001014.
484. Klein PS, Melton DA. A molecular mechanism for the effect of lithium on development. Proceedings of the National Academy of Sciences of the United States of America. 1996;93(16):8455–9.
485. López-Muñoz F, Shen W, D'Ocon P. A history of the pharmacological treatment of bipolar disorder. International Journal of Molecular Sciences. 2018;19:2143.
486. Skinner GR, Hartley C, Buchan A, Harper L, Gallimore P. The effect of lithium chloride on the replication of herpes simplex virus. Medical Microbiology and Immunology. 1980;168(2):139–48.
487. Murru A, Manchia M, Hajek T, Nielsen RE, Rybakowski JK, Sani G. Lithium's antiviral effects: a potential drug for CoViD-19 disease? International Journal of Bipolar Disorders. 2020;8(1):21.
488. Harrison SM, Tarpey I, Rothwell L, Kaiser P, Hiscox JA. Lithium chloride inhibits the coronavirus infectious bronchitis virus in cell culture. Avian Pathology. 2007;36(2):109–14.
489. Zhao FR, Xie YL, Liu ZZ. Lithium chloride inhibits early stages of foot-and-mouth disease virus (FMDV) replication *in vitro*. Journal of Medical Virology. 2017;89(11):2041–6.
490. Zhao Y, Yan K, Wang Y, Cai J, Wei L, Li S. Lithium chloride confers protection against viral myocarditis via suppression of coxsackievirus B3 virus replication. Microbial Pathogenesis. 2020;144:104169.
491. Sarhan MA, Abdel-Hakeem MS, Mason AL. Glycogen synthase kinase 3beta inhibitors prevent hepatitis C virus release/assembly through perturbation of lipid metabolism. Scientific Reports. 2017;7(1):2495.
492. Li H-j, Gao D-s, Li Y-t, Wang Y-s, Liu H-y, Zhao J. Antiviral effect of lithium chloride on porcine epidemic diarrhea virus *in vitro*. Research in Veterinary Science. 2018;118:288–94.
493. Nowak JK, Walkoviak J. Lithium and coronaviral infections. A scoping review. F1000Research. 2020;9:93.
494. Medic B, Stojanovic M, Stimec BV, Divac N, Vujovic KS, Stojanovic R. Lithium - pharmacological and toxicological aspects: the current state of the art. Current Medicinal Chemistry. 2020;27(3):337–51.
495. Yang C, Wang W, Zh K, Liu W, Luo Y, Yuan X. Lithium chloride with immunomodulatory function for regulating titanium nanoparticle-stimulated

inflammatory response and accelerating osteogenesis through suppression of MAPK signaling pathway. International Journal of Nanomedicine. 2019;14: 7475–88.
496. Soares Fernandes M, Barbisan F, Farina Azzolin V, Schmidt do Prado-Lima PA, Ferreira Teixeira C, da Cruz Jung IE. Lithium is able to minimize olanzapine oxidative-inflammatory induction on macrophage cells. PLoS One. 2019;14(1): e0209223.
497. Albayrak A, Halici Z, Polat B, Karakus E, Cadirci E, Bayir Y. Protective effects of lithium: a new look at an old drug with potential antioxidative and anti-inflammatory effects in an animal model of sepsis. International Immunopharmacology. 2013;16:35–40.
498. Kwon YJ, Yoon CH, Lee SW, Park YB, Lee SK, Park MC. Inhibition of glycogen synthase kinase-3β suppresses inflammatory responses in rheumatoid arthritis fibroblast-like synoviocytes and collagen-induced arthritis. Joint Bone Spine. 2014;81(3):240-6.
499. Knijff EM, Breunis MN, Kupka RW, de Wit HJ, Ruwhof C, Akkerhuis GW. An imbalance in the production of IL-1b and IL-6 by monocytes of bipolar patients: restoration by lithium treatment. Bipolar Disorders. 2007;9:743–53.
500. Spuch C, López-García M, Rivera-Baltanás T, Rodrígues-Amorím D, Olivares JM. Does lithium deserve a place in the treatment against COVID-19? A preliminary observational study in six patients, case report. Frontiers in Pharmacology. 2020;11:557629.
501. Ogando NS, Dalebout TJ, Zevenhoven-Dobbe JC, Limpens RWAL, van der Meer Y, Caly L. SARS-CoV-2 replication in Vero E6 cells: replication kinetics, rapid adaptation and cytopathology. Journal of General Virology. 2020;101:925–40.
502. Mossel EC, Huang C, Narayanan K, Makino S, Tesh RB, Peters J. Exogenous ACE2 expression allows refractory cell lines to support severe acute respiratory syndrome coronavirus replication. Journal of Virology. 2005;79(6):3846–50.
503. Barreto-Vieira DF, Nunes da Silva MA, Couto Garcia C, Dias Miranda M, da Rocha Matos A, Costa Caetano B. Morphology and morphogenesis of SARS-CoV-2 in Vero-E6 cells. Memórias do Instituto Oswaldo Cruz. 2021;116: e200443.
504. Gong SR, Bao LL. The battle against SARS and MERS coronaviruses: reservoirs and animal models. Animal Model and Experimental Medicine. 2018;1(2):125–33.
505. Roberts A, Vogel L, Guarner J, Hayes N, Murphy B, Zaki S. Severe acute respiratory syndrome coronavirus infection of golden Syrian hamsters. Journal of Virology. 2005;79(1):503–11.
506. Rosenke K, Meade-White K, Letko M, Clancy C, Hansen F, Liu Y. Defining the Syrian hamster as a highly susceptible preclinical model for SARS-CoV-2 infection. Emerging Microbes & Infections. 2020;9(1):2673–84.
507. Imai M, Iwatsuki-Horimoto K, Hatta M, Loeber S, Halfmann PJ, Nakajima N. Syrian hamsters as a small animal model for SARS-CoV-2 infection and countermeasure development. Proceedings of the National Academy of Sciences of the United States of America. 2020;117:16587–95.

508. Chan JF, Zhang AJ, Yuan S, Poon VK, Chan CC-S, Lee AC-Y. Simulation of the clinical and pathological manifestations of Coronavirus Disease 2019 (COVID-19) in golden Syrian hamster model: implications for disease pathogenesis and transmissibility. Clinical Infectious Diseases. 2020;71(9):2428–46.
509. Sia SF, Yan LM, Chin AWH, Fung K, Choy K-T, Wong AYL. Pathogenesis and transmission of SARS-CoV-2 in golden hamsters. Nature. 2020;583(7818): 834–8.
510. Lee AC-Y, Zhang AJ, Chan JF-W, Zhou J, Chu H, Yuen K-Y. Oral SARS-CoV-2 inoculation establishes subclinical respiratory infection with virus shedding in golden Syrian hamsters. Cell Reports Medicine. 2020;1(7):100121.
511. Reed LJ, Muench H. A simple method of estimating fifty percent endpoints. American Journal of Hygiene. 1938;27(3):493–7.
512. Álvarez G, Dubed M, Noa E, Navea LM, Pérez MT, Rodríguez A. Validación del método de titulación del virus de la inmunodeficiencia humana tipo 1. Revista Cubana de Medicina Tropical. 2009;61(2):112–9.
513. Festing MF, Altman DG. Guidelines for the design and statistical analysis of experiments using laboratory animals. ILAR Journal. 2002;43(4):244–58.
514. Borenfreund E, Puerner J. A simple quantitative procedure using monolayer cultures for cytotoxicity assays (HTD/NR90). Journal of Tissue Culture Methods. 1984;9(1):7–9.
515. Manenti A, Maggetti M, Casa E, Martinuzzi D, Torelli A, Trombetta CM. Evaluation of SARS-CoV-2 neutralizing antibodies using a CPE-based colorimetric live virus micro-neutralization assay in human serum samples. Journal of Medical Virology. 2020;92(10):2096–104.
516. Sebaugh J. Guidelines for accurate EC_{50}/IC_{50} estimation. Pharmaceutical Statistics. 2011;10(2):128–34.
517. Jing L, Jiechao Y, Xiuwen S, Guangxing L, Xiaofeng R. Comparative analysis of the effect of glycyrrhizin diammonium and lithium chloride on infectious bronchitis virus infection *in vitro*. Avian Pathology. 2009;38(3):215–21.
518. Ren X, Meng F, Yin J, Li G, Li X, Wang C. Action mechanisms of lithium chloride on cell infection by transmissible gastroenteritis coronavirus. PLoS One. 2011; 6(5):e18669.
519. Bosetti F, Rintala J, Seemann R, Rosenberger TA, Contreras MA, Rapoport SI. Chronic lithium downregulates cyclooxygenase-2 activity and prostaglandin E2 concentration in rat brain. Molecular Psychiatry. 2002;7:845–50.
520. Li B, Zhang C, He F, Liu W, Yang Y, Liu H. GSK-3β inhibition attenuates LPS-induced death but aggravates radiation-induced death via down-regulation of IL-6. Cellular Physiology and Biochemistry. 2013;32:1720–8.
521. Kaptein SJ, Jacobs S, Langendries L, Seldeslachts L, ter Horst S, Liesenborghs L, et al. Favipiravir at high doses has potent antiviral activity in SARS-CoV-2-infected hamsters, whereas hydroxychloroquine lacks activity. Proceedings of the National Academy of Sciences of the USA. 2020;117(43):26955-65.
522. Rosenke K, Jarvis MA, Feldmann F, Schwarz B, Okumura A, Lovaglio J, et al. Hydroxychloroquine prophylaxis and treatment is ineffective in macaque and hamster SARS-CoV-2 disease models. JCI Insight. 2020;5(23):e143174.

523. van der Lubbe JEM, Rosendahl Huber SK, Vijayan A, Dekking L, van Huizen E, Vreugdenhil J. Ad26.COV2.S protects Syrian hamsters against G614 spike variant SARS-CoV-2 and does not enhance respiratory disease. NPJ Vaccines. 2021;6:39.
524. Petersen KP. Effect of age and route of administration on LD_{50} of lithium chloride in the rat. Acta Pharmacologica et Toxicologica. 1980;47(5):351–4.
525. Abdel Hamid OI, Ibrahim EM, Hussien MH, ElKhateeb SA. The molecular mechanisms of lithium-induced cardiotoxicity in male rats and its amelioration by N-acetyl cysteine. Human & Experimental Toxicology. 2020;39(5):696–711.
526. Strbe S, Gojkovic S, Krezic I, Zizek H, Vranes H, Barisic I. Overdose lithium toxicity as an occlusive-like syndrome in rats and gastric pentadecapeptide BPC 157. Biomedicines. 2021;9(11):1506.
527. Rudd CE. GSK-3 inhibition as a therapeutic approach against SARs CoV2: dual benefit of inhibiting viral replication while potentiating the immune response. Frontiers in Immunology. 2020;11:1638.
528. Pai NM, Malyam V, Murugesan M, Ganjekar S, Moirangthem S, Desai G. Lithium toxicity at therapeutic doses as a fallout of COVID-19 infection: a case series and possible mechanisms. International Clinical Psychopharmacology. 2022;37 (1):25–8.
529. Suwanwongse K, Shabarek N. Lithium toxicity in two coronavirus disease 2019 (COVID-19) patients. Cureus. 2020;12(5):e8384.
530. Ott M, Stegmayr B, Salander Renberg E, Werneke U. Lithium intoxication: incidence, clinical course and renal function–a population-based retrospective cohort study. Journal of Psychopharmacology. 2016;30(10):1008–19.
531. Manzoni GC, Bono G, Lanfranchi M, Micieli G, Terzano MG, Nappi G. Lithium carbonate in cluster headache: assessment of its short- and long-term therapeutic efficacy. Cephalalgia. 1983;3(2):109–14.
532. Dong W, Mead H, Tian L, Park J-G, Garcia JI, Jaramillo S, et al. The K18-human ACE2 transgenic mouse model recapitulates non-severe and severe COVID-19 in response to an infectious dose of SARS-CoV-2. Journal of Virology. 2022;96 (1):e00964–21.
533. Gruber AD, Firsching TC, Trimpert J, Dietert K. Hamster models of COVID-19 pneumonia reviewed: How human can they be? Veterinary Pathology. 2022; 59(4):528–45.
534. Shou S, Liu M, Yang Y, Kang N, Song Y, Tan D, et al. Animal models for COVID-19: hamsters, mice, ferrets, minks, tree shrew, and non-human primates. Frontiers in Microbiology. 2021;12:626553.
535. Avni C, Blasbalg U, Toren P. Reduced risk of severe COVID-19 with lithium use: a large-scale comparison with valproate users and other COVID-19 patients. Frontiers in Psychiatry. 2025;16:1702189.
536. Nilsson NH, Bendix M, Öhlund L, Gibbs A, Widerström M, Werneke U, et al. Lithium and the risk of severe COVID-19 infection: A retrospective population-based register study. Journal of Psychosomatic Research. 2025;190:112053.

Curriculum Vitae

Raúl Ramos Pupo was born in Havana, Cuba, in 1988. He obtained his Medical Degree in 2013 from Holguín Medical University in Cuba, after completing six years of medical training. Motivated by a strong interest in Biomedical Sciences and Immunology, he pursued postgraduate specialization in Immunology at Havana Medical University, completing the four-year residency program in 2017.

Following his specialization, he joined the Department of Immunology at the *Instituto de Ciencias Básicas y Preclínicas "Victoria de Girón"* of Havana Medical University, where he combined academic, clinical, and research activities. During this period, he became Associate Professor of Immunology and later served as Head of the Department of Immunology. His research work focused on Immunology, Vaccinology, and Translational Biomedicine, while also contributing to the education and supervision of medical students and residents.

He subsequently joined the Biomedical Research Institute (BIOMED) at Hasselt University, Belgium, as a doctoral researcher in 2019. His PhD research focused on novel vaccination and antiviral approaches for the prevention and treatment of COVID-19.

His scientific interests include, not limited to, Clinical and Fundamental Immunology, Mucosal Immunity, Vaccine Development, Infectious Diseases, and Translational Biomedical Research. Throughout his academic career, he has participated in international collaborative projects between Cuba and Belgium and contributed to scientific publications and presentations in the fields of Immunology and Vaccinology.

Below are his latest peer-reviewed publications and international presentations detailing clinical and preclinical evaluations of novel vaccine adjuvants, therapeutic agents, and immunomodulators.

Publications:

- Reyes Díaz LM, Lastre González MDSJ, Cuello M, Sierra-González VG, **Ramos Pupo R**, Lantero MI, Harandi AM, Black S, Pérez O. VA-MENGOC-BC vaccination induces serum and mucosal anti-Neisseria gonorrhoeae immune responses and reduces the incidence of gonorrhea. The Pediatric Infectious Disease Journal. 2021;40(4):375-81. IF = 2.1
- Suárez GM, Catalá M, Peña Y, Portela S, Añé-Kourí AL, González A, Lorenzo-Luaces P, Díaz M, Molina M_A, Pereira K, Hernández JDCCC, **Ramos Pupo R**, Reyes MC, Ledón N, Mazorra Z, Crombet T, Lage A, Saavedra D. Thymic polypeptide fraction Biomodulina T decreases exhausted and terminally differentiated EMRA T cells in advanced lung cancer patients treated with platinum-based chemotherapy. Frontiers in Oncology. 2022;12:823287. IF = 4.7
- Soriano-Torres O, Noa Romero E, González Sosa NL, Enríquez Puertas JM, Fragas Quintero A, García Montero M, Martín Alfonso D, Infante Hernández Y, Lastre M, Rodríguez-Pérez L, Borrego Y, González VE, Vega IG, **Ramos Pupo R**, Reyes LM, Zumeta Dubé MT, Amaro Hernández I, García de la Rosa I, Mínguez Suárez A, Alarcón Camejo LA, Pérez O. Lithium salts as a treatment for COVID-19: Pre-clinical outcomes. Biomedicine & Pharmacotherapy. 2022;150:112952. IF = 7.5
- **Ramos Pupo R**, Reyes Díaz LM, Suárez Formigo GM, Borrego González Y, Lastre González M, Saavedra Hernández D, Crombet Ramos T, Sánchez Ramírez B, Grau R, Hellings N, Stinissen P, Pérez O, Bogie JFJ. Mucosal vaccination against SARS-CoV-2 using human probiotic Bacillus subtilis spores as an adjuvant induces potent systemic and mucosal immunity. Vaccines. 2025;13(7):772. IF = 3.4

Presentations:

- **Ramos Pupo R**, Lastre M., Reyes L., Tub F., Robles L., Borrego Y., Pérez Y., Avila L., Ramírez W., Labrada A., Romeu B., González E., Bogie J., Hellings N., Stinissen P., Pérez O. SinTimVaS as a novel effective vaccination strategy. In: 17th International Congress of Immunology (IUIS 2019); 2019 Oct 19-23; Beijing, China.
- **Ramos Pupo R**, Reyes L., Borrego Y., Suárez G., Pérez O., Bogie J., Hellings N., Stinissen P. Challenges and opportunities improving COVID-19 vaccination. In: 13th Latin American and Caribbean Congress of Immunology (ALACI 2022); 2022 May 9-13; Varadero, Cuba.
- **Ramos Pupo R**, Reyes L., Borrego Y., Suárez G., Saavedra D., Sánchez B., Pérez O., Bogie J., Hellings N., Stinissen P. A COVID-19 mucosal vaccine formulation adjuvanted with Bacillus subtilis spores. In: Vaccine Delivery and Immune Response Symposium, Flanders Vaccine; 2024 Sep 17; Antwerp, Belgium.

Acknowledgments

The completion of this doctoral thesis would not have been possible without the support, guidance, and encouragement of many individuals and institutions to whom I would like to express my deepest gratitude.

First and foremost, I would like to sincerely thank my promoter, Prof. Dr. Piet Stinissen, my co-promoter, Prof. Dr. Niels Hellings, and doctoral committee member Prof. Dr. Jeroen Bogie from Hasselt University for their continuous supervision, mentorship, scientific guidance, constructive feedback, and encouragement throughout my doctoral journey. Their expertise, critical insight, and commitment to academic excellence greatly contributed to the development of this research and to my professional growth. I am deeply grateful for the trust they placed in me and for the opportunity to carry out this PhD project within such an international and collaborative environment.

I would especially like to express my profound gratitude to my external tutor, Prof. Dr. Oliver Pérez from Havana Medical University, for his constant support, mentorship, and invaluable scientific guidance, particularly during the research activities conducted in Cuba. This thesis represents the continuation of a longstanding collaborative scientific effort initiated by the research team he led at the Department of Immunology of the *Instituto de Ciencias Básicas y Preclínicas "Victoria de Girón"*. It was within this academic and scientific environment that I completed my specialization in Immunology under his supervision and later had the privilege of working alongside him for five years. His scientific rigor, dedication to research, extensive experience, and continuous encouragement profoundly shaped my academic and professional development and were fundamental to the successful completion of this thesis.

I would also like to express my sincere gratitude to all my colleagues from the Department of Immunology at the *Instituto de Ciencias Básicas y Preclínicas "Victoria de Girón"*, as well as to the institution itself, for their collaboration and support. I would particularly like to thank Laura Reyez, Miriam Lastre, and Yusnaby Borrego for generously sharing their expertise regarding the adjuvant used in this research. Special thanks are also due to the Immunology resident, Ormany Soriano, for his extraordinary dedication and tireless efforts in bringing an important part of this research to fruition. Conducting this work during the unprecedented challenges of the COVID-19 pandemic required exceptional resilience, adaptability, and commitment from everyone involved. Working alongside such dedicated professionals greatly enriched both my scientific and personal growth.

I am deeply grateful to the Center of Molecular Immunology in Havana for providing institutional support and essential logistical resources throughout this research, including the specialized immunogen critical to this work. I also sincerely thank the colleagues and staff for their technical expertise, valuable insights, and warm collaboration, all of which greatly enriched this project.

I would also like to acknowledge the Biomedical Research Institute (BIOMED), the Doctoral School of Health & Life Sciences, and the Faculty of Medicine & Life Sciences of Hasselt University, my home doctoral institution, for providing outstanding institutional support and access to state-of-the-art technology, which were instrumental in broadening the scope of this research. My sincere thanks go to my colleagues and the staff at BIOMED for their expertise, support, and collaborative spirit. I am especially grateful to Kristina and Veronique for their

exceptional administrative assistance, constant helpfulness, daily support, and most importantly: their friendship.

I would like to gratefully acknowledge the Special Research Fund (BOF) of Hasselt University and VLIR-UOS for awarding me a doctoral scholarship that made this research possible. Their support was essential for the successful completion of this doctoral journey.

I also wish to thank all institutions, collaborators, researchers, technicians, laboratory staff, students, and colleagues in both Belgium and Cuba who contributed, directly or indirectly, to this work.

On a personal level, I would like to express my heartfelt gratitude to my friends for their encouragement, companionship, and unwavering support throughout both the challenging and rewarding moments of this journey. Their presence made these years truly unforgettable.

Finally, and most importantly, I would like to thank my whole family, especially my wife, children, parents, sister, and nieces, for their unconditional love, patience, sacrifices, and constant encouragement throughout all these years. Their support gave me the strength and motivation to continue pursuing my goals despite every challenge encountered along the way. This achievement would not have been possible without them, and I dedicate this thesis to them and my friends with all my love and gratitude.

A mi familia, gracias por acompañarme siempre, incluso en la distancia.

Raúl, May 2026

www.uhasselt.be
Hasselt University
Martelarenlaan 42 | BE-3500 Hasselt

Stichting transnationale Universiteit Limburg (tUL) is a cooperation between Hasselt University (Belgium) and Maastricht University (the Netherlands) and can be considered as one university with a home base in each country.